

## **New Strategies for Bone Graft Materials**

A dissertation submitted to the department of mechanical engineering  
in partial fulfillment of the requirements for the degree of Master

Field of mechanical engineering

Submitted in August, 2015

By

Sacha Cavelier, Department of Mechanical Engineering, McGill University,  
Montreal

© Sacha Cavelier 2015

## **Abstract**

Millions of people worldwide suffer from pathologies associated with bone loss and bone defects, and the treatment of bone loss remains a major challenge in orthopedic surgery because of the limitations including donor site morbidity, viral transmission, immunologic incompatibility, long rehabilitation time and structural failure. The need for new strategies for the treatment of bone defects is therefore urgent. The ideal bone graft material must: (i) match the mechanical properties of healthy bone; (ii) be biocompatible and promote healing and (iii) degrade and resorb over time so healthy bone can take over. To this day, there is no synthetic material that can fulfill these three requirements simultaneously. The purpose of this project is to create a new toughened multilayered bone graft material consisting of calcium sulfate and gelatin that is assembled layer-by layer. All components of this material are fully biocompatible, resorbable. The high mineral content provides stiffness, while the weaker protein layers can deflect incoming cracks, a powerful toughening mechanism exploited in advanced engineering ceramics. As a result, this multilayered bone graft material is sixty times tougher than pure calcium sulfate. The proposed technology thus overcomes the limitations of current bone graft materials. The implication is that this material can be used to fabricate load-carrying grafts, as opposed to traditional calcium phosphates/sulfates which are too brittle. This proposed bone graft will therefore have significant impact on restoring functionality and quality of life in patients.

Des millions de personnes dans le monde souffrent de pathologies associées avec les pertes osseuses et les défauts osseux, dont les traitements demeurent un défi majeur en chirurgie orthopédique à cause des limitations comme la morbidité de la région donneuse, la transmission de virus, l'incompatibilité immunologique, le temps de réhabilitation et la fracture structurelle. Le besoin de nouvelles stratégies pour le traitement des défauts osseux est donc urgent. Le matériau idéal de greffe osseuse doit : (i) Avoir les mêmes propriétés mécaniques que l'os sain ; (ii) Etre biocompatible et promouvoir la guérison et (iii) se dégrader et se résorber au cours du temps afin d'être remplacé par de l'os sain. A ce jour, il n'y a pas de matériau synthétique remplissant ces trois critères de façon simultanée. L'objectif de ce projet est de créer un nouveau matériau de greffe osseuse tenace dont la structure est composée de couches de sulfate de calcium et de gélatine. Tous les composants de ce matériau sont biocompatibles et résorbables. La haute teneur en minéral procure la rigidité, pendant que les couches de protéines souples permettent de dévier les fractures, un mécanisme de renforcement utilisé dans les céramiques d'ingénierie. Ainsi, ce matériau de greffe osseuse multicouche est soixante fois plus tenace que le sulfate de calcium pur. La technologie proposée dépasse de ce fait les limitations des matériaux de greffes osseuses couramment utilisées. Cela implique que ce matériau pourrait être utilisé pour fabriquer des greffes destinées à supporter une charge, s'opposant ainsi au sulfate de calcium ou phosphate de calcium traditionnels qui sont trop cassants. La greffe osseuse proposée aurait par conséquent un impact significatif sur la restauration des fonctionnalités, et sur la qualité de vie des patients.

## **Acknowledgements**

I would like to express my gratitude to my supervisor François Barthelat for the useful comments, patience, engagement and continuous support during my Master. Furthermore, I would like to thank my fellow labmates in the laboratory for advanced materials and bioinspiration for the stimulating discussions, help, support and all the fun we have had. The years spent in the laboratory and in the office were greatly appreciated. Besides the member of the laboratory, my sincere thanks also go to the Luc Mongeau's group and Chris Barrett's group. They were available for all AFM related or chemistry related issues and even more. Finally, I would like to thank my loved ones: my family in France for supporting me spiritually through this master thesis and my life in general; and Gwendoline for her love and encouragements.

## Table of Contents

Abstract .....	ii
Acknowledgements .....	iv
List of figures .....	vii
List of tables .....	ix
1. Chapter I: Introduction .....	1
1.1 The Material Bone: Structure, Properties and Functions .....	1
1.2 Large Segmental Bone Defects .....	5
1.3 Overview of Bone Grafts Materials .....	6
1.3.1 Autografts, Allografts and Xenografts .....	8
1.3.2 Titanium .....	10
1.3.3 Calcium based materials.....	11
1.3.4 Bioglass .....	13
1.3.5 Polymers.....	14
1.3.6 Biogenic materials.....	15
1.3.7 Comparison of existing bone graft materials.....	15
2. Chapter II: Mechanics of Multilayered Materials .....	18
2.1 Multilayered design to dissipate energy with brittle materials.....	19
2.2 Crack deflection and energy dissipated.....	21
2.3 Conditions for crack deflection .....	24
2.4 Maximal interface thickness.....	28
3. Chapter III: Biocompatible Materials: Biopolymers and Minerals .....	30
3.1 Mineral .....	30
3.1.1 Gypsum – dihydrate calcium sulfate .....	32
3.1.2 Impression plaster – hemihydrate calcium sulfate $\beta$ -form – type I .....	32
3.1.3 Plaster of paris – hemihydrate calcium sulfate $\beta$ -form – type II .....	33
3.1.4 Dental stone - hemihydrate calcium sulfate $\alpha$ -form - type III .....	34
3.1.5 High strength dental stone - hemihydrate calcium sulfate $\alpha$ -form - type IV .....	34
3.1.6 Ultra high strength dental stone - hemihydrate calcium sulfate $\alpha$ -form - type V .....	35
3.2 Biopolymers .....	36
3.2.1 Cellulose.....	37
3.2.2 Chitosan.....	38

3.2.3 Starch.....	40
3.2.4 Glucomannan extracted from the Konjac plant.....	41
3.2.5 Collagen and gelatin.....	42
3.2.6 Alginate from kelps.....	45
3.2.7 Shellac from insects.....	46
3.2.8 Pullulan.....	47
3.2.9 Polyhydroxybutyrate (PHB) from microorganisms .....	48
3.2.10 Polylactide acid .....	49
3.2.11 Comparison of selected biopolymers .....	50
4. Chapter IV: Gelatin and Calcium Sulfate: Preparation Protocol and Mechanical Properties .....	52
4.1 Gelatin .....	52
4.1.1 Tensile properties and effect of hydration.....	52
4.1.2 Energy release rate .....	54
4.2 Mechanical properties of Suprastone .....	59
4.2.1 Fabrication and testing protocol .....	59
4.2.2 Properties of Suprastone.....	60
5. Chapter V: The Multilayered Bone Graft.....	71
5.1 Samples preparation and geometry of the bone graft.....	71
5.2 Crack deflection in a multilayered sample .....	74
5.2.1 Crack deflection in the case of calcium sulfate and gelatin.....	74
5.2.2 Crack deflection observations .....	76
5.2.3 Stress – strain curves .....	77
5.3 Flexural strength results .....	78
5.4 Toughness and energy results.....	80
6. Chapter VI: Conclusion.....	83
6.1 Accomplishments .....	83
6.1.1 An efficient design in terms of energy .....	83
6.1.2 A bone graft at reduced cost.....	84
6.1.3 Limitations.....	85
6.2 Future work .....	86
6.2.1 Improvement of the mechanical performances of the mineral .....	86
6.2.2 Large scale production .....	89
6.2.3 Complex shapes.....	90
6.2.4 Cylindrical implants .....	91
References .....	93

## List of figures

Figure 1.1: (a) Macroscopic view of natural bone with its trabeculae; (b) Scheme of an osteon; (c) Microscopic view of a mineralized collagen fibril; (d) Scheme of the collagen molecules linked to the mineral crystal. Adapted from [1, 3-5].	2
Figure 1.2: Toughness versus modulus material property chart for natural materials. Guidelines to identify materials best able to resist fracture under various loading conditions [7].	4
Figure 1.3: Open fracture of the tibial region on a 11-years-old patient due to a bike wreck [10].	6
Figure 1.4: Characteristics of an ideal bone graft.	7
Figure 2.1: Microscopic view of microtablets arrangements in nacre [71].	18
Figure 2.2: (a) Crack propagation and bifurcation in a multilayered ceramic material [72]; (b) load displacement curve of a multilayered ceramic material [74].	21
Figure 2.3: (a) Schematic illustration defining the deflection length $\delta$ ; (b) Cumulative distribution plot of delamination crack [76].	22
Figure 2.4: SEM micrographs of the side surface of broken flexural specimens containing (a) 10, (b) 25, (c) 50, and (d) 80 vol.% $\text{Si}_3\text{N}_4$ in the interphase; (e) strength and work-of-fracture (WOF) plotted versus the $\text{Si}_3\text{N}_4$ content in the interphase [76].	23
Figure 2.5: Energy dissipated in the case of Kovar et al.'s multilayered material with adjustable interfacial properties plotted versus (a) normalized stiffness ( $E_i/E_c$ , with $E_i$ the stiffness of the interface in Pa and $E_c$ the stiffness of the layers in Pa) and (b) normalized toughness ( $\Gamma_i/\Gamma_c$ , with $\Gamma_i$ the toughness of the interface in $\text{J.m}^{-2}$ and $\Gamma_c$ the toughness of the layers in $\text{J.m}^{-2}$ ), adapted from [76].	25
Figure 2.6: Critical length of the dominant defect susceptible to kink the interface out of the interface plotted versus the normalized toughness ( $\Gamma_i/\Gamma_c$ ), of a silicon nitride-boron nitride multilayered composite [76].	26
Figure 2.7: Diagram of possible deflections as a function of the elastic mismatch parameter $\alpha$ , toughness ratio and normalized residual stress parameter $\eta$ [78].	27
Figure 2.8: Effect of interface thickness on the fracture toughness of a graphite (interface) – silicon (layer) carbide multilayer composite [73].	29
Figure 3.1: Plaster particles (top left), dental stone particles (top middle), high strength dental stone particles (top right) [81]. Crystals of plaster (bottom left) to be compared with the typical crystal structure of dental stone (bottom right). Adapted from [84].	31
Figure 3.2: Comparison of the compressive strengths of various types of calcium sulfates [41, 81-83].	35
Figure 3.3: Hierarchical schematic representation of the collagen structure in a tendon: (a) tendon is divided in primary fibers, collagen fibers, and collagen fibrils [123]; (b) junction of two tropocollagen molecules in a collagen fibril [124]; (c) molecular structure of a mer in tropocollagen [125].	43
Figure 4.1: (a) Dog bone shape obtained from a film of gelatin after laser cutting; (b) Typical stress-strain curve of dry gelatin in tension; (c) Typical stress-strain curve of hydrated gelatin in tension.	53
Figure 4.2: Three different modes of fracture characterizes the failure of interfacial materials [170].	55
Figure 4.3: Geometry of the ENF test which consists in a three points bending test of a beam ( $2L \times b \times 2h$ ) with a notch of length $a$ . [171].	55
Figure 4.4: Energy release rate in mode II of hydrated gelatin and effect of the thickness (100 and 10 $\mu\text{m}$ ).	58

Figure 4.5: Three points bending tests and its geometrical parameters: a force $F$ is applied on the center of a beam (width $b$ , thickness $d$ ) supported by two points separated by a distance $L$ . ....	60
Figure 4.6: Effect of powder – water ratio on the flexural strength of the Suprastone. ....	61
Figure 4.7: (a) SEM view of doctor bladed Suprastone; (b) SEM view of standard Suprastone; (c) SEM view of compressed Suprastone; (d) density measured for the three different samples of Suprastone; (e) flexural strength measured for the three different samples of Suprastone. ....	63
Figure 4.8: Typical stress-strain curves for the three different processed Suprastone. ....	64
Figure 4.9: Effect of hydration on standard and compressed Suprastone. ....	66
Figure 4.10: Effect of calcium ion content on compressed Suprastone. ....	68
Figure 4.11: Mode I fracture toughness testing for a 20 mm Suprastone beam. ....	68
Figure 4.12: Effect of hydration on the fracture toughness of Suprastone and comparison with concrete. ....	70
Figure 5.1: Fabrication steps of the multilayered samples. ....	73
Figure 5.2: Two optical microscopic views of: (a) dry multilayered sample; (b) hydrated multilayered sample. ....	74
Figure 5.3: Comparison of the fracture toughnesses of Suprastone and gelatin for two different thicknesses. ....	76
Figure 5.4: (a) Microscopy of the failure of the thin gelatin multilayered samples; (b) microscopy of the failure of the thick gelatin multilayered samples. ....	77
Figure 5.5: Stress – strain curve of a multilayered gelatin – Suprastone composite. ....	78
Figure 5.6: Flexural strength of the multilayered gelatin – Suprastone composite, compared to the flexural strength of pure compressed Suprastone, and tensile strength of pure gelatin, in hydrated conditions. ....	79
Figure 5.7: (a) Fracture toughness of the multilayered gelatin – Suprastone composite, compared to the fracture toughness of pure Suprastone, and fracture toughness of pure gelatin, in hydrated conditions; (b) energy release rate of the multilayered gelatin – Suprastone composite, compared to the energy release rate of pure Suprastone, and energy release rate of pure gelatin, in hydrated conditions. ....	81
Figure 6.1: Example of doctor blading machine (MSK-AFA-L800, MTI Corporation, Richmond, CA, USA) for large scale doctor bladed film production and high accuracy [190]. ....	89
Figure 6.2: Step by step fabrication of a complexly shaped multilayered bone graft. ....	90
Figure 6.3: Osteon-like multilayered bone graft for cylindrical bone replacement on rabbits. ....	92



## List of tables

Table 1.1: Comparison of current and past bone graft materials.....	17
Table 3.1: Comparison of previous biopolymers through their mechanical data [52, 94, 95, 99-101, 110, 120, 133, 136, 142, 151, 158, 159, 163].....	50
Table 4.1: Solubility of Suprastone, sugar and HA at 20°C in water [178, 179]. .....	65

## **1. Chapter I: Introduction**

### **1.1 The Material Bone: Structure, Properties and Functions**

There are various mechanical or non-mechanical roles assigned to the bones. Bones are used in the organism for protection and storage of healing cells, mineral ion homeostasis, major reservoir of calcium and phosphate for various metabolic functions, facilitating blood production or even sound transduction to the ear [1-3]. The skeleton has also the primary function of structural support and protection of the organism [1, 2]. To play these roles, bones are exceptional natural material in terms of mechanics and more especially to absorb energy from impacts. During a shock, natural bone is subjected to an amount of stress which is much larger than the stress implicated by normal locomotion. Natural bone can resist shocks by absorbing a large amount of energy. This property is due to the particularly complex structure of bones. Bones are hierarchical materials with no less than seven levels of hierarchy [1]. Overall, bones can be described as an organic matrix of collagen fibers (20-30 wt.%) which is combined with an inorganic mineral part made of calcium phosphate cement (60-70 wt.%). Therefore, the mineral part contributes to the stiffness of the tissue [2] while the collagen part adds toughness [4].

The composition of natural bone is not the only reason to its mechanical performances. Its structure is also of primary importance. Especially, bone is a hierarchical material: Weiner and Wagner [3] described the seven levels of hierarchy as: (1) the whole bone; (2) the cancellous and cortical bone; (3) microstructural motifs (osteons); (4) fibrils array patterns; (5) fibrils array; (6) mineralized collagen fibril and (7) major components (collagen molecule and mineral crystal). The second level where bone is separated between cancellous bone and cortical bone is depicted on figure 1.1a. Cancellous bone is highly porous and composes the inner part of the bone, while the cortical bone is dense and found on the outside. Cancellous bone is made of interconnected struts called trabeculae that follow the lines of principal stress (figure 1.1a). Cortical bone is composed of small units parallel to the bone axis, called osteons (diameter 200-300  $\mu\text{m}$ ) which are the level three of the hierarchy. These units are made of lamella, or in other words concentric layers made of mineralized collagen, around a Haversian canal on the center (figure 1.1b). This microscopic configuration prevents crack propagation

and provide tensile and compressive mechanical properties [4]. In fact, the lamellae are made of fibrils arranged in various directions thus making complex and efficient patterns. These fibrils are the level six of the hierarchical structure and are the building blocks of the bone family of materials (figure 1.1c). To finish, the fibrils can be described by collagen molecules with mineral crystal growing within the spaces between the molecules (figure 1.1d). The mineral is carbonated apatite ( $\text{Ca}_5(\text{PO}_4, \text{CO}_3)_3(\text{OH})$ ) and is plate-shaped and oriented in a specific crystalline direction [1].

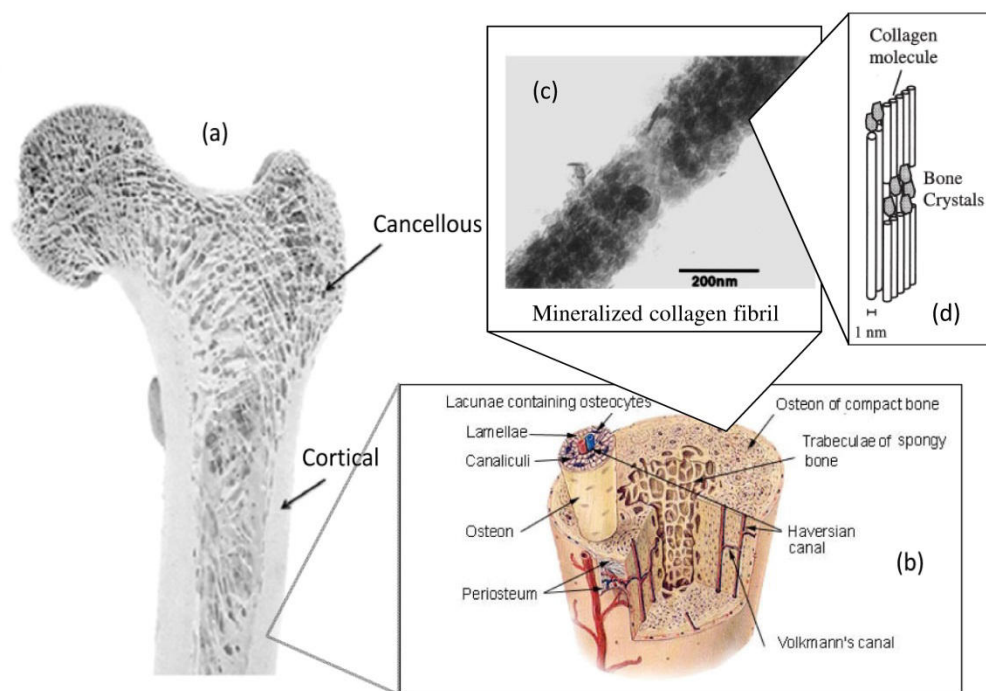


**Figure 1.1: (a) Macroscopic view of natural bone with its trabeculae; (b) Scheme of an osteon; (c) Microscopic view of a mineralized collagen fibril; (d) Scheme of the collagen molecules linked to the mineral crystal. Adapted from [1, 3-5].**

Bones are capable adapting their local density to the level of mechanical stress applied, by a continuous remodeling process which occurs thanks to three types of bone cells called osteoblasts, osteocytes and osteoclasts. Osteoblasts construct and reinforce new sections of bone where the amount of stress is increasing cyclically over time while osteoclasts degrade the parts of bones that are not fatigued sufficiently [3]. Osteoblasts thus secrete the primary component of the matrix which is type I collagen [1]. Osteocytes are derived from osteoclasts and maintain the surrounding tissue [4]. This aspect has to be taken into account in the choice of materials of the bone graft: these materials must be biocompatible (accepted by the cells without provoking inflammation) and biodegradable (digested by the bone cells). Finally,

these materials must be osteoconductive: they must promote bone formation and attract bone cells so as to be colonized and replaced by natural bone as fast as they are digested.

Because of its composition and structure, natural bone exhibits remarkable mechanical performances. It combines high strength and large elongation at strain. Considering that the energy dissipated is the product of strain and stress applied to the bone during the shock, bones can absorb large amounts of energy. This quantity of energy strongly depend on various parameters (variation in mineralization, porosity, location in the skeleton [3], age, sex, connection with the vascular network, health, cortical or spongy bone [2]) and the direction since bone is anisotropic because of the orientation of the components [1]. Bones however exhibit less and less anisotropy at the highest hierarchical level, suggesting that bones are designed to resist to various types of stresses in various directions [3]. Typically the tensile strength of natural cortical bone is reported to be between 50 and 350MPa, 150 MPa being the most common value [3], for an elongation of 1.5% while its Young's modulus is between 7 and 26 GPa (10 GPa being the most commonly reported modulus) [3]. But one of the most important properties is the fracture toughness (in  $\text{Pa}\cdot\text{m}^{1/2}$ ) that can be defined as the resistance to crack propagation. Fracture toughness is intimately linked to the dissipated energy rate (in  $\text{J}/\text{m}^2$ ). Since these two parameters are equivalent (formula (4.1) in chapter IV gives the relationship between them), the energy rate is often called toughness in literature. In this work, fracture toughness indicates the resistance to fracture while toughness (or energy release rate or dissipated energy) indicates an energy, but both terms are used to describe the ability of a material to resist to crack propagation and thus absorb energy. The fracture toughness of natural bones is among the highest for a natural material as depicted in figure 1.1 [6]. Depending on the factors previously listed, fracture toughness can vary from 3 to 10  $\text{MPa}\cdot\text{m}^{1/2}$  which is three to ten times higher than the fracture toughness of silicon [2]. These values are considered as ultimate objectives to evaluate the mechanical performances of a bone replacement material.

Ritchie et al. [2] discussed several mechanisms responsible of the high strength of bones: intermolecular slip of mineralized collagen fibers, resistance in that slip at the interface between collagen and hydroxyapatite minerals, collagen fibers stretching, hydrogen bonds breaking, continuous resistance to fracture by hydrogen bonds reforming or the role of the strong biological glues (osteopontin, sialoprotein) that adhere to the negatively charged phosphate groups of the mineral. Ritchie et al. also described powerful toughening mechanisms that increase the fracture toughness of bones: unbroken collagen fibrils can

bridge crack faces and resist its propagation, resulting in fracture toughness increase of  $0.1 \text{ MPa}\cdot\text{m}^{1/2}$ . The same phenomenon occurs with the uncracked bone ligaments that can act as bridges and add  $1\text{-}2 \text{ MPa}\cdot\text{m}^{1/2}$  to the fracture toughness. The most powerful effect however comes from the crack deflection which occurs when a crack meets weak interfaces (osteon boundaries) and is deviated from the line of maximal stress. This effect can contribute as much as  $3\text{-}20 \text{ MPa}\cdot\text{m}^{1/2}$  to the fracture toughness [2]. Bones are located at the top right of the modulus versus toughness chart as shown on figure 1.2, meaning it is among the most mechanically efficient natural materials.

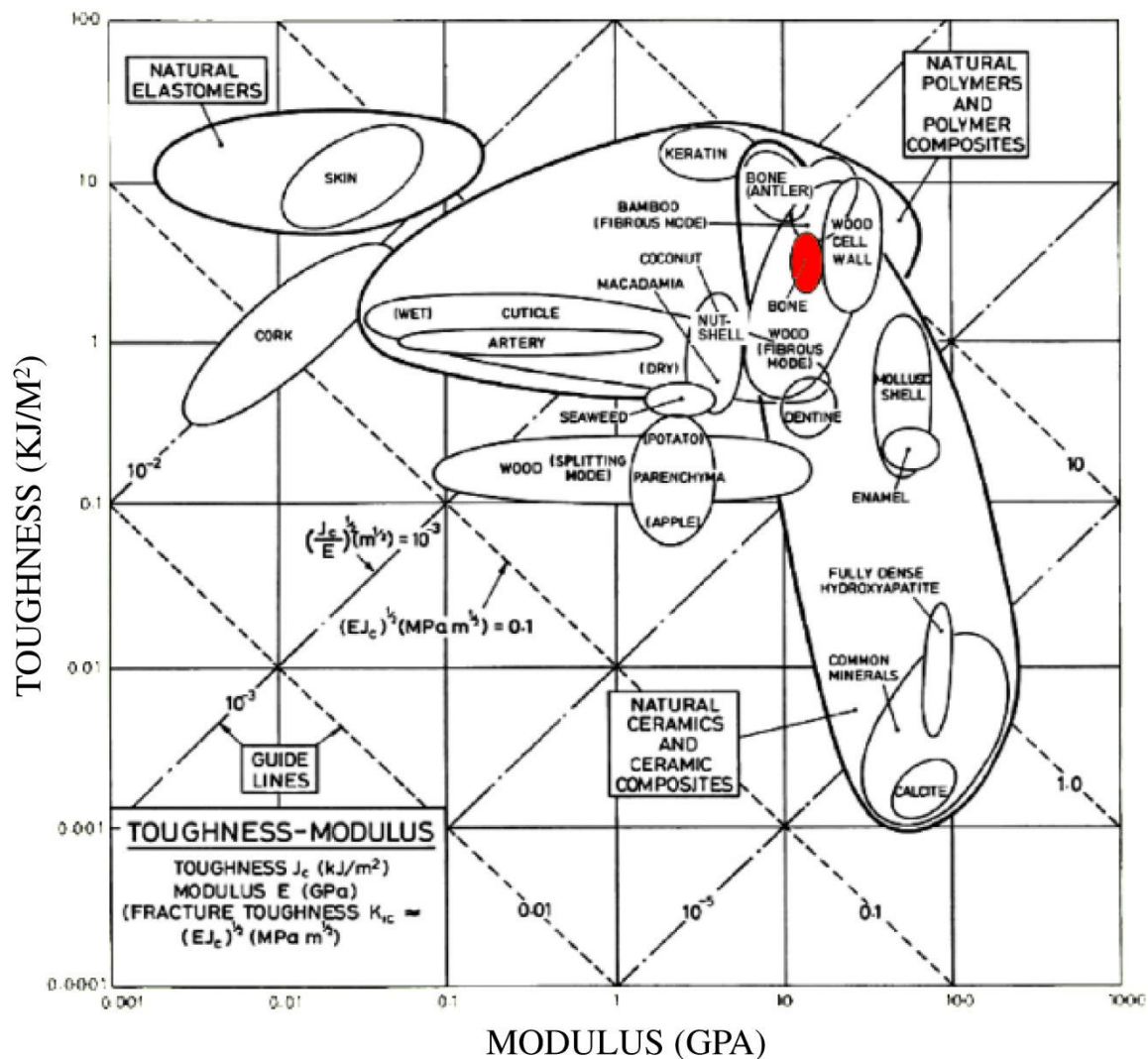


**Figure 1.2: Toughness versus modulus material property chart for natural materials. Guidelines to identify materials best able to resist fracture under various loading conditions [7].**

The bone composition and these toughening mechanisms highlight two important things that will be used in the bone graft design. First, the composition shows that the combination of

two dissimilar components and their volume fraction are important keys to optimize mechanical properties such as strength or toughness. Then, crack deflection is a very important mechanism to dissipate energy, and it occurs when weak interfaces exist in a brittle material. This study will therefore focus on duplicating this mechanism in order to develop new bone graft materials which can carry mechanical loads and absorb impact energy.

## **1.2 Large Segmental Bone Defects**

According to Pneumatics [8], a large segmental bone defect is a bone defect larger than the critical size at which the bone cannot heal by itself, or a bone defect with less than 10% of regeneration during the lifetime of the patient. As a result, a large segmental bone defect requires a bone grafting procedure to heal properly. Typically, the critical size defect is a length that exceeds 2-3 times the diameter of the damaged bone [9].

Replacing bones has a long history in medicine starting with first attempts in 19<sup>th</sup> century with pure wood. The field of bone tissue engineering greatly accelerated during World War II. Before this period, the only remediation to large bone loss was amputation. To face to the large number of wounded soldier, bone graft materials started to emerge [10]. High energy traumas remain the primary cause of large segmental bone defects [8, 10]. In his review, Decoster [10] explains that in the case of post traumatic bone losses, the most common clinical case is the tibial shaft. In this area, the bone is not protected by soft tissues such as muscles, and is directly exposed to shocks, which explains the large part of tibial open fractures among open fractures cases. In the case of tibial trauma, the critical bone loss length is 2 cm. Bone defect in the tibial area can be healed by using the adjacent bone (fibula) to fill the gap, thus making a one-bone leg [11]. However this technique leaves patients with many problems such as prolonged time of treatment, refracture (the fibula can transmit only 15% of the load of the leg and thus cannot replicate the tibial mechanical functions [12]), poor mechanical results or infections [13, 14]. Moreover this technique is not applicable to other part of the skeleton. In more general terms, Decoster describes open fractures even without bone loss as a serious cause for large bone defect. Depending on the degree of damage, the surgeon has to decide how much bone to remove. Removing large part of damaged bone reduces considerably the risk of infection, and an open fracture with no bone loss but high fragmentation can turn into a large bone loss problem. Figure 1.3 shows a X-ray image showing multiple fractures of the tibial region which resulted in a 20 cm bone loss during the

surgery. Even if no bone material was lost, the reconstruction required removing 20 cm of bone fragments which required bone grafting procedure. According to the American Academy of Orthopaedic Surgeons, 6.3 million fractures occur each year in the United States, and 500 000 of them require a surgery and in some cases a bone graft treatment. The total cost is estimated at 2.5 billion \$ [15].



**Figure 1.3: Open fracture of the tibial region on a 11-years-old patient due to a bike wreck [10].**

Open fractures and/or bone surgeries increase the risk of infection which might require another bone surgery if the infection occurs on a large segment. Infection is thus another important cause of large bone defects [8, 10, 16]. As explained above, open fractures without segmental bone loss can complicate because of chronic infections and in some cases bone fragments removing is the most efficient way to control the infection [10]. Another important cause is bone tumor resection [8] since new surgical techniques considerably reduced the number of amputations on patient with bone cancer. Rare genetic or developmental abnormalities can also occur because of a disruption of the system that maintains growth and maintenance of the skeleton [17]. Such deformities are rare causes of large segmental bone defect, as well as failed or revised arthroplasty [8, 16].

### **1.3 Overview of Bone Grafts Materials**

According to Böhner [18], the ideal bone graft material must meet three major requirements, which represent the main challenges in the field of bone tissue engineering (Figure 1.4): (i)

load-bearing property: mechanical properties of these materials should be better than or at least as high as those of cortical bone. Therefore the bone graft must comply with the stiffness, strength and toughness of natural bone; (ii) degradability: materials should degrade overtime and thus be resorbable to prevent fractures due to long term use; (iii) osteoconductivity: bone formation should be promoted by the surface of the material (which also includes biocompatibility; the material should not produce undesirable effect while contacting with bone cells). Osteoconductivity can be combined with osteoinductivity (Bone formation should be chemically promoted by the material) and osteointegration (stable anchorage of the whole implant in the bone). Currently all of the materials destined to be used as bone graft have only one or two of these three characteristics. Examples of such limitations are presented in this section.

Two other practical parameters must be taken into account. The human skeleton is made of very complex shapes, which are hard to duplicate. However, if a bone graft must reproduce the functionality of the missing bone, it has to replicate its shape with sufficient fidelity. The ease to replicate this three-dimensional geometry is thus an important parameter. Figure 1.4 summarizes the four mentioned requirements for an ideal bone graft. Finally, bone grafts must not be too expensive. The direct biomedical applications for bone graft materials require a production at an acceptable cost.

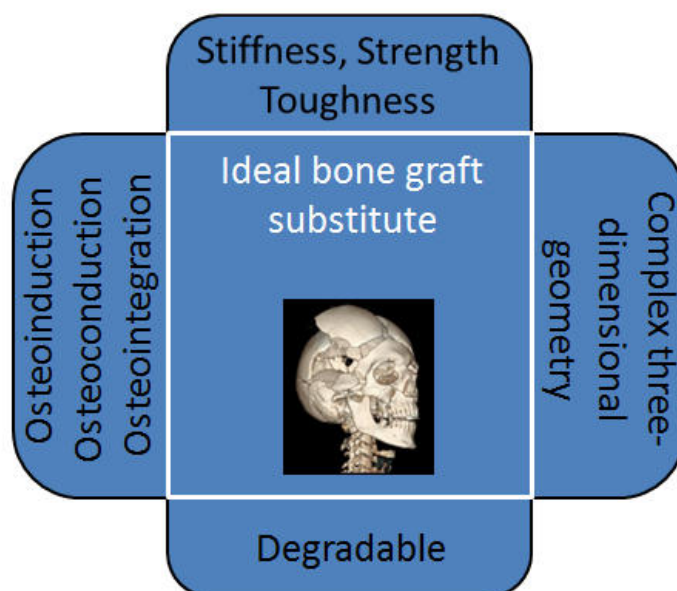


**Figure 1.4: Characteristics of an ideal bone graft.**



From 1992 to 2007, 2 000 000 bone graft procedures were operated in the US only, which represents 0,67 % of the population [19]. Bone grafting is thus a common surgery and the number of types of bone graft has increased in the last decades. Synthetic bone grafts can be classified according to their chemical composition: glass, polymers, metals, biological materials and mineral based materials [8, 16]. These materials are reviewed and their properties discussed below. The breakthroughs that have been made in the bone grafting history are highlighted, and the current limitations in bone grafts that prevent the existence of the ideal bone graft are listed.

### **1.3.1 Autografts, Allografts and Xenografts**

The best material to replace bone is natural bone itself. Therefore attempts to implant natural bones from the body of the patient (autograft), from a donor (allograft) or from an animal (xenograft) started to develop 50 years ago [16].

First allografts were performed with cortical bone since the bony support was immediate and superior when compared to cancellous bone. However, vascularization and union were very slow with cortical bone and even never occurred in some cases while fatigue fractures were common. Therefore cancellous bone was then preferred and provided a better osteoinductivity and vascularization and a faster remodeling [20]. Nowadays, three procedures of cancellous autograft are commonly used in reconstructive surgery: open cancellous grafting, closed cancellous grafting and autoclaved grafting [16]. In the open technique, after excision of the necrotic bone, a bed of granulation forms on the excised bone, and receives the cancellous graft. The bed of granulation then vascularizes the bone graft and the bone starts to repair. This technique is very successful for infected segmental bone defects [21] but is not suitable for defects larger than 9 cm because of the limited volume of bone graft available [22]. Even for defects larger than 4 cm, results are poor in region with no surrounding muscles, and bone strength is slow to develop [16]. In the closed cancellous grafting technique, a stable soft tissue covers the bed of granulation before receiving the cancellous graft. This technique is more efficient in the case of large bone defect but increases the risk of morbidity of the donor site and the healing rate is only of 1 cm per month. Moreover three to five operative procedures are required [16]. Another important problem for both open and closed cancellous autografts is the very limited capability to make complex shapes [23]. The third technique (autoclaved allograft) is used in the case of bone tumor. It

consists in the excision of the bone defect and debridement of the tumor. The remaining bone is then autoclaved for five minute to kill the remaining tumor deposits before being reimplanted with prosthetic fixations. However, this technique is applicable only for certain types of low grade tumors, and the healing time is longer than the healing time of the other autografts [24].

Allografts appeared to be a better option than autografts because of the limitations mentioned before. The first allografts were reported in 1908 and later in the 1960s, it was discovered that the immunogenicity decreases by freezing, which relaunched the interest for this type of bone graft [23]. A human bone bank was even created in the USA in the 1970s, where FDBA (Freeze Dried Bone Allograft) and DFDBA (Demineralized Freeze Dried Bone Allograft) are stored and used for large bone defect cases. Allografts allowed solving many issues: complex shape and various size of bone are in unlimited supply, no donor site morbidity, and even entire joints can be preserved through cryopreservation techniques (for future osteoarticular allografts) [16]. However, many risks are possible in the cases of allografts: transmission of viral or bacterial pathologies, immune response of the host versus graft even if the graft is irradiated, nonunion, fractures, slower revascularization than autografts, and contraindication in the case of infected patients [8, 25]. Also, the elevated costs related to the maintenance of human bone banks trends to make this procedure more expensive than the others bone graft techniques [8].

Xenografting is a recent and less popular technique. It consists in grating a bone tissue taken from a donor of a different species. The poor tolerance of bovine bone material by the human body is the cause of its lack of interest [16] but recently, freeze dried baboon bone combined with autogenous cancellous bone successfully reconstructed large segmental defects caused by traumas and tumors [26]. The advantages and disadvantages of xenografts are the same than allografts: there are a variety of sizes and complex shapes possible and an unlimited supply, but also a risk of disease transmission, immune response, or slow revascularization [16].

The price for an autograft for a segmental tibial defect is estimated at 113 000 US\$ [27] which is among the most expensive bone grafts but 2 to 10 times less expensive than amputations because of the elevated cost of the lifetime prosthesis of amputees [10]. In 2007, 75,000 autogenous bone grafts were operated in the US which represents 25 bone grafting procedures for 100,000 inhabitants. This is also 82.4 % of the bone grafting procedures operated the same year. However autografts are very successful in the treatment of intervertebral or lumbar disk,

but not necessarily in large segmental bone defects. Displacement or degeneration of intervertebral disk is ranked first cause (28 % of cases) of bone grafting procedures while traumatic large bone defect is ranked second with 9.4 % of cases. Concerning the rest of bone grafting procedures (allografts, xenografts or artificial grafts), they represented 5 procedures for 100,000 inhabitants in 2007 in the US, or 15,000 procedures [19].

### 1.3.2 Titanium

Titanium is one of the rare biomaterials that exceeds the mechanical properties of bones: it has a tensile strength, Young's modulus and fracture toughness of respectively 345 MPa, 103 GPa and  $60 \text{ MPa.m}^{1/2}$  [28]. For proper comparison, the corresponding values for cortical bone are respectively 150 MPa, 10 GPa [3] and  $10 \text{ MPa.m}^{1/2}$  [6]. Titanium is also biocompatible (which is not the case for other metals) and osteointegrative, which helps the bone cells to colonize the implant and improve the anchorage of small titanium medical devices such as screws [29]. However, a good bone graft material should not have mechanical properties lower nor higher than those of bones. In the case of titanium, the dissimilar mechanical properties with natural bone increase the stress shielding phenomenon in the case of larger implants: because of the high modulus of titanium, more stress is transmitted to the implant which results in bone resorption due to the lack of stress in bone and consequent failure of titanium implant [30]. Moreover titanium is not degradable which limits its use as an implant for large segmental bone defects. Using titanium also requires a second surgery to remove the implant once the bone is healed which increases the recovery time [31]. Therefore, titanium is commonly used as screws in reconstructive surgery, since its lifetime of 20 to 30 years is adapted for a long term use implant [29]. Concerning large segmental bone defects, titanium was successfully used as wires to support another type of bone graft implant [32] but titanium alone was never used to replace a segmental bone loss. Another important use of titanium in bone defects that deserves to be mentioned is the replacement of joints like shoulders, hips or knees. The fact that titanium does not degrade and is stable over time makes it interesting for artificial joint systems destined to be implanted for the rest of the patient's lifetime: knee replacement arthroplasty consists in the implantation of a titanium – polymer joint system [33, 34] while hip or shoulder arthroplasty consists in the implantation of a titanium – polyethylene – ceramic joint system [34]. In these cases, the grafts are abandoned in the body for the rest of the patient's life. It is not the case of reconstructive surgery that requires a second surgery to remove the titanium implants which does not fully comply with all the

requirements of an ideal bone graft (biodegradability of the implant). Titanium is thus perfect for joint replacement but not for large segmental defect replacements, and moreover titanium is not a material easy to shape; making complex shapes requires to make a specific metallic mold for each shape which is not practical.

### 1.3.3 Calcium based materials

Calcium based cements such as hydroxyapatite (HA), calcium sulfate (CS) or calcium phosphate (CP) exhibit promising properties for bone tissue engineering. Each of them have been used in the treatment segmental bone defect [18, 35, 36] but have a wide range of properties concerning their osteoconductivity and degradability. Calcium cements have the form of a powder that has to be mixed with water. Hence they can be easily shaped with the help of a specific mold. Since they comply with most of the requirements for an ideal bone graft, they are good candidates in the making of complexly shaped bone grafts. Because of the non-degradability of HA, CS and CP cements [18] are also potential candidates for bone graft materials.

HA has the chemical formula  $\text{Ca}_{10}(\text{PO}_4)_6(\text{OH})_2$  which is very close to the mineral part of bones [37]. HA can be produced in two different ways: it can be extracted from a biological material such as purified bovine or porcine bones, and in this case, the bone graft is a xenograft. Or HA can be synthesized and in this case, the sintering temperature during the fabrication process is a very important parameter that will impact the size of the pores and the osteoconductivity. There are various types of HA with different pore sizes, which can promote bone cell ingrowth, or act as a biocompatible filler or a mineral reservoir for bone cells [38]. In any cases, HA is biocompatible and osteoconductive but has poor (or non-existent) degradability [18]. This material has also poor mechanical properties in comparison to natural bone [39]. It remains however one of the most used bone graft materials through its numerous brands of synthetic or biological grafts: Cerapatite® (synthetic, Ceraver, Roissy, FRA), Trans-Ossatite® (synthetic, Transysteme JMT implant, Nimes, FRA), Endobon® (biological, Biomet, Valence, FRA), Bio-Oss® (biological, Geistlich, Wolhusen, SUI), Surgibone® (biological, Unilab, Coppet, SUI) or Osteograft® (biological, Osteomed, Addison, TX, USA).

CS is one of the oldest bone graft materials still in use [40]. CS has formula  $\text{CaSO}_4$  and is also used in masonry under the form of plaster (plaster of Paris) [41]. CS is biodegradable, biocompatible and osteoconductive [35, 36, 40]. Studies even reported the ability of CS to regenerate bone [42, 43]. CS is easy to prepare, and the various types of existing CS have a wide range of mechanical properties as it will be described in chapter III. CS bone grafts are used in the biomedical industry under the brands Capset® (Lifecore Biomedicals, Chaska, MN, USA) and Osteoset® (Wright, Memphis, TN, USA).

CP degrades faster than CS in the human body, and sometimes too fast since new bone has not completely invaded the graft. For this reason various types of CP cement have been investigated as bone grafts (phosphate mixtures, tricalcium phosphate, octacalcium phosphate, anhydrous dicalcium phosphate and dicalcium phosphate dihydrate) to try to slow degradation time [18]. Since CP and CS are both cements prepared from powder and water, mixing a certain amount of CP in CS can be a way to adjust the degradation rate. CP is osteoinductive because of its phosphate ions [44], but it does not stimulate bone growth. Hence CP is osteoinductive but not osteoconductive [18]. Osteoconductivity is a more powerful characteristic for the development of natural bone on the implant. The process to prepare CP is also longer than the one of CS, since CP must be mixed with a binder such as polyvinyl alcohol followed by a sintering step ( $1000^\circ\text{C}$ ) to remove the binder and strengthen the CP [45]. CP is used under various brands like Biosorb® (SBM Science for BioMaterials, Winchester, MA USA), Ceros® (Thommen Medical, Grenchen, SUI), Cerasorb® (Curasan, Kleinostheim, GER). Some grafts proposed in the industry mix CP and HA in various proportions to adjust the properties of the minerals and are known as Ceraform® (Teknimed, Vic En Bigorre, FRA), MBCP® (Biomatlante, Vigneux De Bretagne, FRA) or Calciorsorb 35® (CeraVer, Roissy, FRA), to name just a few.

The weakness of these materials is their poor mechanical properties. Calcium cements have poor mechanical properties when compared to natural bone [18, 41]. Various studies tried to address this problem by integrating various types of inclusions in calcium cements, making calcium based composite materials. While it is hard to embed inclusions in HA, it is relatively easy to integrate inclusions in CS or CP powder prior to mix with water: Gerhart [46] was able to improve the properties of CP by adding gelatin, and other studies successfully embedded biocompatible fibers in CP such as poly(lactide-co-glycolide) [47], collagen [48], HA whiskers [49] or chitosan [50] to name just a few. With CS, wood fibers [51], gelatin [52], viscous polymeric (carboxymethylcellulose and hyaluronan) [53], or cellulose fibers

[54] have also been investigated. In all of these studies, the fibers successfully improved the strength and/or the toughness of the bone graft material. Chemical ways also exist to improve the strength of CS such as mixing with potassium sulfate ( $K_2SO_4$ ), with a saturated solution of CS [55], calcium oxide (CaO) or calcium hydroxide (CaOH) [40]. Sanad [56] was able to double the strength (tensile and compressive) of CS by mixing arabic gum and calcium oxide or hydroxide. However the properties of the resulting material remain lower than natural bone. According to Kruger [57], the first objective of fibers-calcium cement composites is to overcome the brittle fracture behavior of CP and CS by ductilization with fiber reinforcements and the second objective is to reach the natural bone strength and modulus. Although the first goal is partially solved, the application of fiber reinforcements to calcium based bone grafts is still a young field and many questions have to be resolved to reach the performances of natural bone. Because there are still limitations in terms of mechanical performance, calcium based cements are used only as non-weight bearing structures, to fill defects, or to coat hip implants [16].

#### 1.3.4 Bioglass

Bioglasses are made of bioactive components CaO,  $Na_2O$ ,  $SiO_2$ , or  $P_2O_5$ . *Bioactive* refers to the unique phenomenon that occurs when these bioglasses are in contact with body fluids: a double layer composed of a silica gel layer and a calcium-phosphorous layer appears and covers the surface of the bioglass after 16 weeks [58]. The CP layer resembles the bone mineral phase and adsorbs proteins utilized by osteoblasts to form a mineralized extracellular matrix. Bioglass bone grafts therefore promote cell growth and are highly osteoinductive, but also osteoconductive and osteointegrative [8]. This property occurs at the surface of the implant (bone–implant interface) but also within the implant (away from the bone–implant interface) [59]. Clinical studies showed that bone formation is enhanced in the case of bioglass and even occurs at a faster rate than calcium based cement [60, 61]. Bioglasses have also improved mechanical properties compared to other bone grafts, but the disadvantage of this type of graft is its brittleness [59]. Finally, the major problem is that only the bilayer silica gel – CP resorbs over time, and not the entire graft [38]. To summarize, bioglass is both highly osteoinductive, osteoconductive and osteointegrative [59] (which is a main advantage on all calcium cements) and is more mechanically interesting than cements (but has yet an undesirable brittleness), but does not resorb. However, recent studies showed that borate-

based bioactive glasses are resorbable and non-toxic for the bone cells [62]. Bioglass could thus become a promising material for bone tissue engineering, but the problem of its brittleness remains, and also the fact that bioglasses are not easy to shape in complex forms limits its use in bone defects. Bioglass bone grafts are used in the biomedical industry under the brands Perioglass® (NovaBone, Jacksonville, FL, USA) or Biogran® (Atek Medical Group, Grand Rapids, MI, USA).

### 1.3.5 Polymers

In the case of the treatment of large segmental bone defects, the most widely used polymers are Polylactic acid (PLA), polyglycolic acid (PGA) and their co-polymer PLGA [8]. These polymers are also used in the making of sutures, screws and rods [63]. They are biodegradable and degrade into lactic acid (a muscular waste produced and recycled naturally in the body), glycolic acid, water and carbon dioxide with a controllable degradation rate [8]. The main problem for polymeric bone grafts is the mechanical properties which are too weak and compliant when compared to those of natural bone. PLA can be mixed with a calcium cement in order to increase the tensile property. For example Kasuga [64] mixed PLA with 30wt% of calcium carbonate and improved the tensile modulus by a factor of two. In vivo studies are still required to determine the biocompatibility of the composite material.

Another type of polymer-calcium cement composite used in biomedical industry combines a biocompatible polymer such as polymethylmethacrylate (PMMA), or polyhydroxyethylmethacrylate (PHEMA) with a mineral cement (calcium hydroxide,  $\text{Ca}(\text{OH})_2$ ). These polymers have a negatively charged surface that provide adherence to bone cells, resulting in a biocompatible scaffold that promotes bone formation. This type of graft is therefore very osteoconductive [38]. Consequently, polymeric bone grafts are interesting to promote bone formation, and some of them can fill bone defects up to 70% according to clinical studies made on polymeric graft HTR® [65]. The main problem for such polymeric scaffolds is that they do not resorb over time and hence the patient has to live with the polymeric scaffold for the rest of his life. Another disadvantage is its poor tensile and shear properties, and poor adhesion properties which increases the risk of debonding in the defect zone before the ingrowth of the new bone [4].

Polymeric bone grafts have disadvantages (lack of osteoconductivity and low tensile properties) which can be partially solved by the incorporation of a calcium phase. This young

field has promising perspectives of development especially PLA which is already used to make complex shapes such as screws and could be used to replace bones with complex shapes.

### 1.3.6 Biogenic materials

Biogenic materials (i.e. produced by natural organisms) have a long history as bone graft materials. For example wood is known to have been used as bone graft in the 19<sup>th</sup> century, albeit with many problems associated with low biocompatibility and poor resorbability. Highly mineralized biological materials offer interesting perspectives as bone graft materials because of their composition similar –or close– to the composition of natural bones. The high mineral content of these materials make them osteoconductive and osteoinductive in the presence of human bone [66, 67]. An example of mineralized biomaterial is coral. After its purification (i.e. removal of the organic content), the remaining skeleton of the animal (calcium carbonate  $\text{CaCO}_3$ ) has a composition which is close to the mineral part of the human bone. It is resorbable, with mechanical properties close to those of bones. The material is however not osteoconductive [6] but can be combined with osteoinductive factors. This material is already used in biomedical industry: Biocoral is a company specialized in the fabrication of bone graft products extracted from the natural coral *porites lutea*. The porosity of this coral is close to the porosity of bone, and it has impressive compressive strength, but the limitation of this product is its brittleness and the low tensile strength. Paradoxically, calcium carbonate also resorbs too fast and the healed bone has more risks to break again. In the same idea, Duplat [66] tried to use nacre from mollusk shells because of its mechanical properties and osteoconductivity, but the graft did not exhibit enough signs of resorbability. Natural nacre combines good mechanical properties and osteoconductivity because of its structure and composition, but does not degrade well: Lopez [67] showed that only 20 % of the nacre implanted into the human body degrades very fast, and the 80 % remaining for a long time in the body with no significant changes.

### 1.3.7 Comparison of existing bone graft materials

Table 1.1 below summarizes the advantages and drawbacks for each of the bone graft materials discussed above, in the context of the three main requirements for an ideal bone



graft, which are biocompatibility-osteoconductivity, resorbability and mechanical properties. It appears that biocompatibility is not a major issue: except for wood (one of the first grafts tested more than a century ago) and some allografts and xenografts. All the other materials are sufficiently biocompatible to be accepted by the host body. However biocompatible does not mean osteoconductive and this properties is much more complicated to obtain. If some biological materials already have this property, synthetic bone grafts must be chemically modified (negatively charged surface of polymeric grafts or appearance of a silica gel – CP bilayer at the surface of the bioglasses) to be osteoconductive. Some chemical techniques might be needed in the future design of bone graft to make them osteoconductive. In terms of mechanical properties, biological materials are more interesting than synthetic materials. As previously mentioned, the improvement of the mechanical properties of a new bone graft is the main challenge to overcome and will also be the main challenge in this work. Finally, the resorbability of the current bone graft is also a challenging property, but it appears than calcium base cements have the best results.

Table 1.1 also shows that autografts have all the requirements needed for an ideal bone graft. It thus remains the preferred type of bone graft and represents 83 % of the 2,000,000 bone grafting procedures operated in the US between 1992 and 2002 [19]. Autografts have however several other major problems that make them not suitable to the treatment of large defect: very limited bone supply, morbidity of the donor site. Xenografts and allografts have unlimited supply but have a limited biocompatibility because of the enhanced risks of infection and diseases transmissions. Because of the presence of foreign bodies, even after purification, a dislocation can appear at the graft – host bone interface which reduces the mechanical efficiency of the graft [8].

It appears from this review that among the variety of materials used for bone graft purpose, CS might be the most promising material. CS has excellent biodegradability and osteoconductivity but poor mechanical properties in tension which satisfies two of the three requirements previously mentioned for an ideal bone graft. Most of the studies on CS reported good compression strength. Tensile and flexural strength are low compared to bone. But there are several strategies to improve these properties [41, 68]. CS is under the form of a cement powder which can be processed into complex shapes relatively easily. CS exists under different forms (types I to V, type V being the strongest) which provide dissimilar mechanical properties. CS will thus be considered as one of the components of the bone graft of this

work. CS exists under various forms and a selection has still to be done. An overview of the different chemical forms of CS will take place in chapter III.

<b>Material</b>	<b>Osteoconductivity</b>	<b>Biocompatibility</b>	<b>Resorbability</b>	<b>Good strength and toughness</b>
<b>Titanium</b>	No	Yes	No	Yes
<b>Autografts</b>	Yes	Yes	Yes	Yes
<b>Allografts, Xenografts</b>	Yes	No	Yes	No
<b>HA</b>	Yes	Yes	No	No
<b>CP</b>	No	Yes	Yes	No
<b>CS</b>	Yes	Yes	Yes	No
<b>Glass</b>	Yes	Yes	No	Yes
<b>Polymers</b>	Yes	Yes	No	No
<b>Wood</b>	No	No	No	Yes
<b>Coral</b>	No	Yes	Yes	Yes
<b>Nacre</b>	Yes	Yes	No	Yes

**Table 1.1: Comparison of current and past bone graft materials.**

## 2. Chapter II: Mechanics of Multilayered Materials

Nature has been producing high performance green materials for millions of years, and these materials can therefore serve as models for the design of new engineering materials. Biological materials such as bones, teeth or mollusk shells boast unique properties: one of the best examples of a natural high-performance composite material is nacre, also known as mother-of-pearl. Nacre is made of thousands of inorganic wavy microtablets that can slide over each other. Under impact, this layered structure plays a critical role by absorbing energy. 95% of this material is composed by inorganic microtablets made of aragonite and 5% is an organic network. The contrast between the stiff and brittle inorganic part with the soft and ductile organic one makes this composite material highly efficient [69]. Nacre thus associates the stiffness and strength of calcium carbonate and the toughness of the organic material in order to make a composite 3000 times tougher than the elements it is made with [70]. Figure 2.1 is a microscopic view of this natural structure found in mollusk seashells.



**Figure 2.1: Microscopic view of microtablets arrangements in nacre [71].**

Bones are also good examples of composite materials designed by Nature because of their structure made with embedded reinforcing mineral elements while the collagen serves as a matrix [53]. At some levels of its hierarchy, bone can also be viewed as a multilayered material. As explained in the first chapter, the osteons are made of lamella, or concentric layers made of mineralized collagen, around a Haversian canal in the center. This multilayered structure is capable of deflecting cracks into the interface between the lamellae. This powerful phenomenon is one of the reasons of the high fracture toughness of natural bones. The osteons themselves are also weak interfaces that deflect incoming cracks [2].

These examples demonstrate the structures that can improve the toughness of a material, and can inspire artificial materials.

Nature thus teaches us interesting things that have to be taken into account in the design of high performing materials:

- (i) Combining two dissimilar materials (a brittle inclusion inside a soft matrix of interface) leads to superior material properties (as the example of nacre shows).
- (ii) The volume fraction of the two materials is an important parameter. Depending on the type of material, the volume fraction can be very different: nacre shows remarkable mechanical results with 95 vol.% of inorganic inclusion [70] which is challenging to reach experimentally and requires a perfectly regular structure. Natural bone exhibits around 50 vol.% of mineral part [1]. The volume fraction has hence to be optimized.
- (iii) Natural materials exhibit different types of inclusions: particles, fibers, or micro-platelets [53]. The type of mineral inclusions is another parameter. Additionally, the secret of the performance of natural materials resides in the perfect arrangement of the structure. This point might be challenging depending on the type of inclusions selected.
- (iv) Crack deflection is a critical mechanism in nacre and bone. This mechanism requires interfaces which are weaker than the rest of the material: organic mortar in nacre, cement lines in bone.

## **2.1 Multilayered design to dissipate energy with brittle materials**

Among the variety of possible designs and configurations for a composite material, multilayered materials appear to be one of the most efficient in terms of toughening mechanisms. Clegg [72] was able to increase the toughness of silicon carbide from  $28 \text{ J.m}^{-2}$  (bulk material) to  $4625 \text{ J.m}^{-2}$  (multilayered material) by incorporating weak interfaces to deflect cracks, multiplying by more than 160 the amount of energy dissipated. The samples were made of two materials mechanically dissimilar and the phenomenon involved in this increasing of energy dissipated is the crack bifurcation. While in a bulk ceramic a crack propagates suddenly and through the whole thickness of the ceramic because of its brittleness, in a multilayer material, the crack propagates only until the next ceramic/ceramic border. The

idea is to fill the very small space between the ceramics with a weaker material which acts as a weak interface and is able to deflect the crack. After the crack is deflected, two powerful phenomena contribute to increase the toughness of the material. First, there is balance between the straight propagation in the weak material and the defect at the surface of the ceramics that can make the crack kinks out of the interface. When a crack propagates straight in a material, the effective crack length extends perpendicularly to the applied stress, so that the stress intensity factor increases, leading to unstable fracture. In contrast, a crack which is deflected at the interface propagates with a stress intensity factor that decreases, so that additional force and energy are required. The complete fracture of the material is therefore delayed and more energy is dissipated [73, 74]. Because of this multilayered structure, the ceramic is completely notch insensitive: a notch weakens only the first layer in a multilayered ceramic since the propagating crack will be deflected at the first interface it meets. For a monolithic sample, the notch weakens the whole sample in provoking straight crack propagation through the whole thickness. A notched multilayered ceramics therefore reaches the stress of an unnotched multilayered sample [73]. Additionally, other toughening mechanisms such as frictional work of the layers in the crack wake can occur [74]. Figure 2.2a shows a typical crack propagation in the silicon carbide/graphite multilayered composite tested by Clegg. The crack was deflected at each weaker interface and the resulting load-displacement curve (figure 2.2b) suggests a work of fracture superior than the monolithic material because of the increased stress and strain. If most of the time there is no change in the strength [75], figure 2.2b exhibits an important increase in strength. According to Clegg, when the stress in the multilayered ceramic sample reaches the strength of the monolithic ceramic, the crack is deflected in the interface instead of breaking the sample. The load continues rising while the cross section of the sample is constant hence the increase in strength [73].

Multilayering and embedding weak interfaces in a brittle material clearly introduces toughening and strengthening mechanisms when a crack propagates into the composite. In some cases, even stiffening mechanisms occur because of the progressive compression of the weak interfaces [75]. The interest of such architecture is thus multiple.

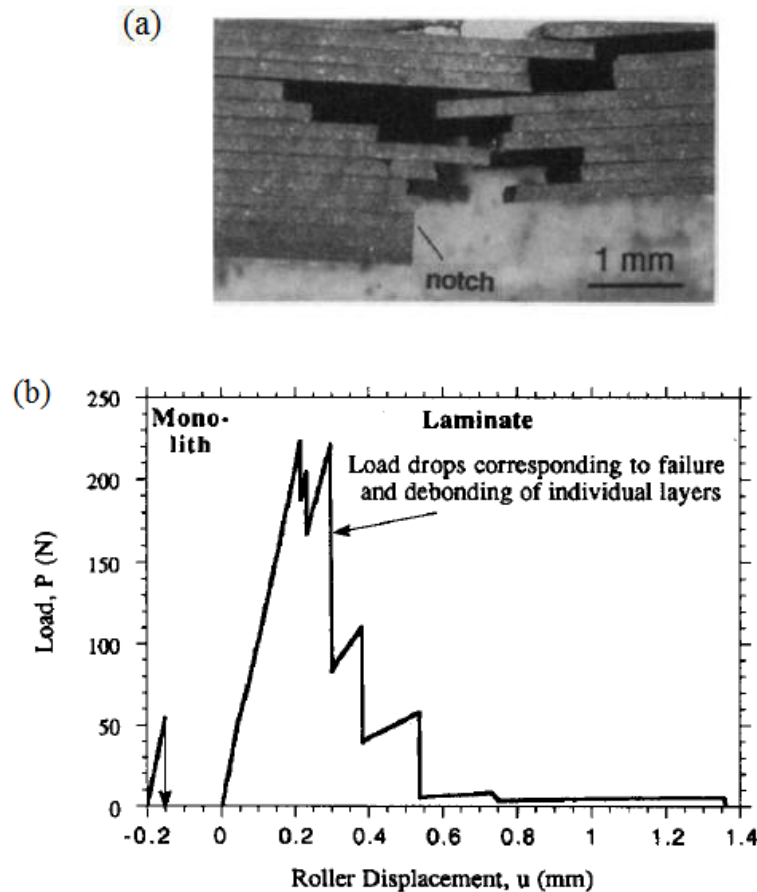


**Figure 2.2: (a) Crack propagation and bifurcation in a multilayered ceramic material [72]; (b) load displacement curve of a multilayered ceramic material [74].**

Increasing by 160 the amount of energy dissipated could be a critical point in the case of artificial bones. Additionally, more precise relationships between the size of the deflections and the increasing in the toughness of the material have been experimentally done as it is described in the next section.

## 2.2 Crack deflection and energy dissipated

In their work, Kovar et al. [76] created a multilayered material made of silicon nitride ( $\text{Si}_3\text{N}_4$ ) ceramic plates assembled with a weak interface made of boron nitride. Kovar et al. also demonstrated in this study that the ratio of the Young's moduli (interface and ceramic) and the ratio of the toughnesses (interface and ceramic) are important parameters to predict crack deflection. Kovar et al. mixed the boron nitride interface with silicon nitride (the same component than the ceramic plate) to modify the modulus and toughness of the interface and

obtained different propagation lengths. The modulus linearly varied with the volume fraction of silicon nitride from 250 GPa (0 vol.% silicon nitride, pure boron nitride) to 320 GPa (100 vol.% silicon nitride, pure silicon nitride). The toughness also linearly varied with the volume fraction of silicon nitride from 40 J.m<sup>-2</sup> (0 vol.% silicon nitride, pure boron nitride) to 120 J.m<sup>-2</sup> (100 vol.% silicon nitride, pure silicon nitride). Clearly, for low contents of silicon nitride (and so weaker interfaces), more crack deflections are visible and measurable. Kovar et al. defined the deflection length  $\delta$  as depicted on figure 2.3a.  $\delta$  is the highest in the materials that contain 0 vol.% and 10 vol.% of silicon nitride in the interface (figure 2.3b). The deflection length dramatically decreases for tougher and stiffer interfaces. Kovar et al. were able to describe quantitatively instead of qualitatively the amount of deflection in their multilayered material.

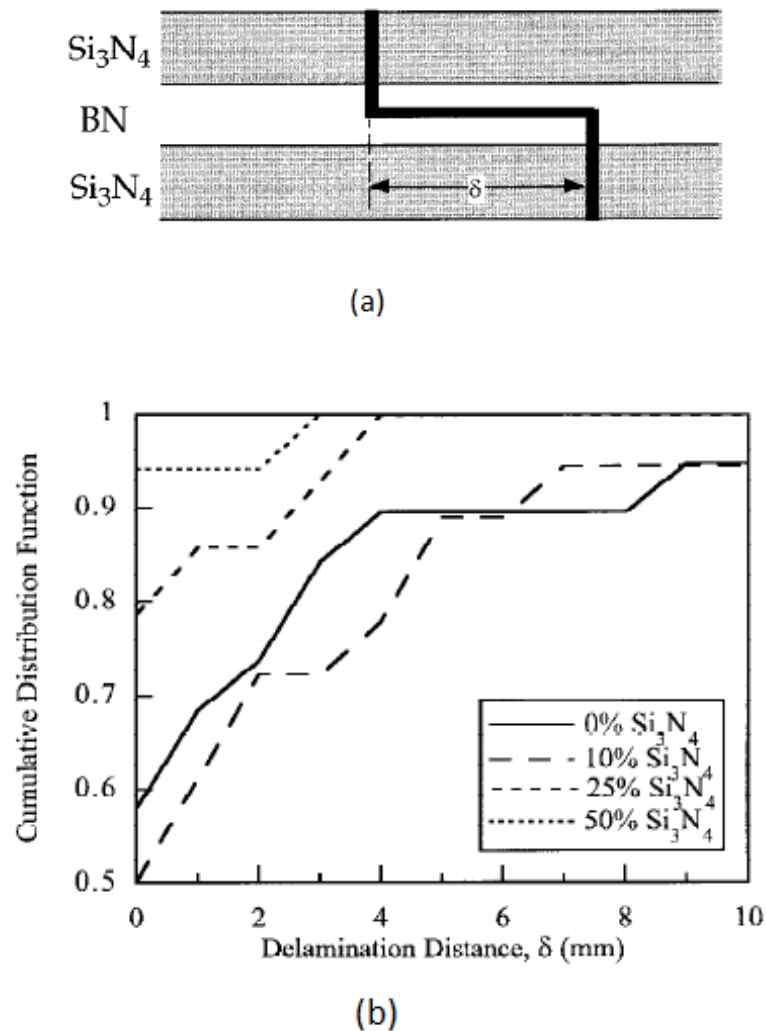


**Figure 2.3: (a) Schematic illustration defining the deflection length  $\delta$ ; (b) Cumulative distribution plot of delamination crack [76].**

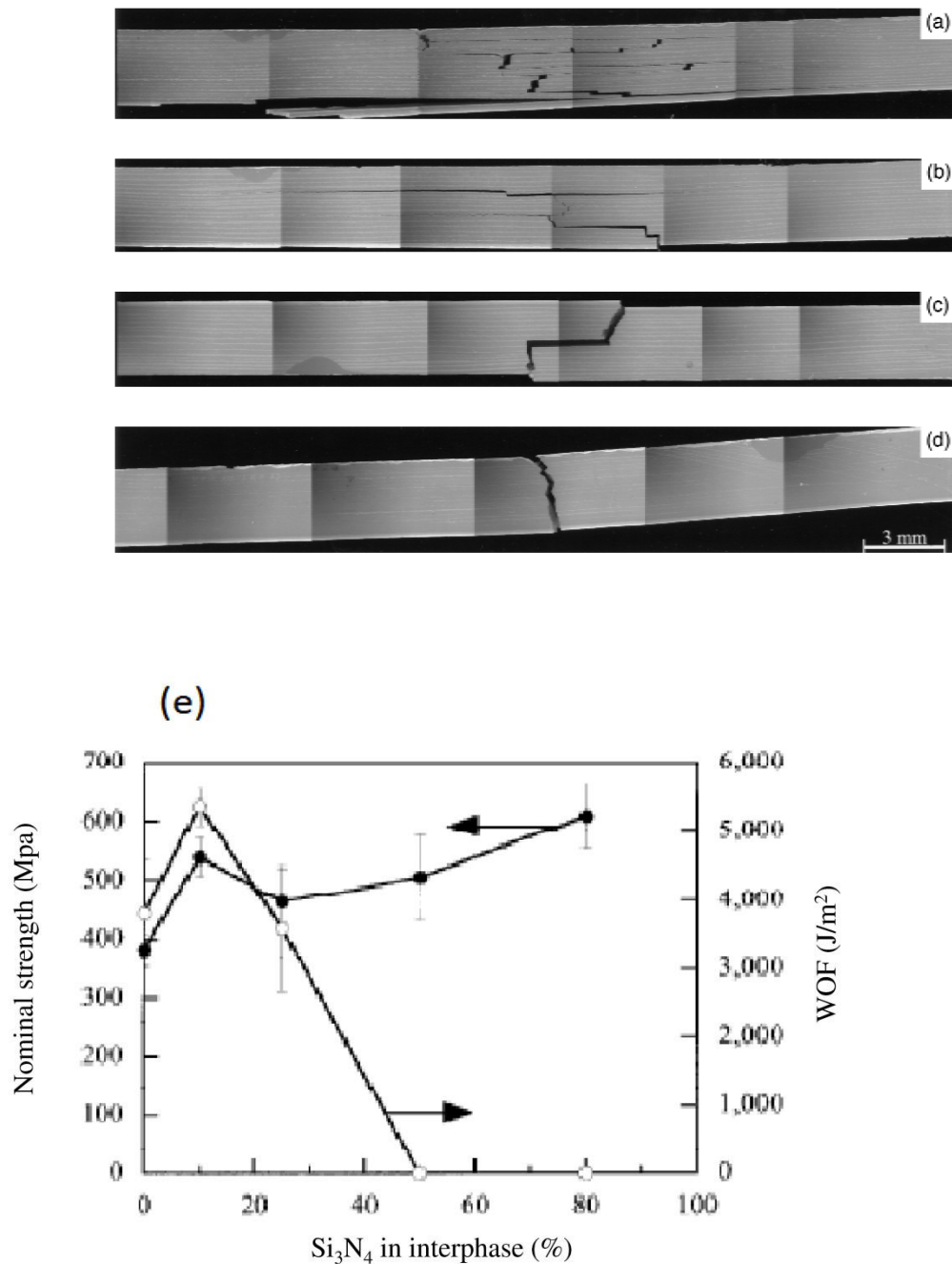


**Figure 2.4: SEM micrographs of the side surface of broken flexural specimens containing (a) 10, (b) 25, (c) 50, and (d) 80 vol.%  $\text{Si}_3\text{N}_4$  in the interphase; (e) strength and work-of-fracture (WOF) plotted versus the  $\text{Si}_3\text{N}_4$  content in the interphase [76].**

Figure 2.4 describes the patterns of crack deflection obtained with various compositions of the weak interfaces. The most interesting part of Kovar et al.'s work is the comparison of the strength and toughness of the samples, where they showed that the samples with the longest deflection were the weakest in terms of strength but the highest in terms of toughness and



energy dissipation. Along the same idea, samples with stiffer and tougher interfaces exhibit less deflection, more strength but less fracture toughness as summarized by figure 2.4e. All samples with more than 50 vol.% of silicon nitride (tough interfaces) did not exhibit deflection (figure 2.4d) and the resulting toughness was 5,000 times lower than the toughness with low concentration of silicon nitride (weak interface).

Kovar et al. thus showed the strong relationship between the deflection length and the amount of energy dissipated. They also demonstrated that strength and toughness of the multilayered material cannot be obtained simultaneously since one can increase while the other decreases. Even if Kovar et al. described quantitatively this relationship, a theoretical model is needed to understand better the mechanisms occurring during crack deflection. More detailed theories of the conditions for crack deflection are the topic of the next section.

### 2.3 Conditions for crack deflection

Additionally to the relationship between the sizes of crack deflections and the energy dissipated, Kovar et al. [76] related in their work the relationship between the stiffness and the toughness of the interface and the length of the crack deflections at the interfaces. By adjusting the volume fraction of  $\text{Si}_3\text{N}_4$  in the interface, Kovar et al. could increase the stiffness and the toughness of the interface. From Kovar et al.'s data and from figure 2.4e, a new plot can be produced in order to identify the effect of the toughness and the stiffness of the interface on the energy dissipated. The toughness and the stiffness of the interface has to be compared with those of the layers and that is why figures 2.5a and 2.5b show the impact of normalized toughness ( $\Gamma_i/\Gamma_c$ , with  $\Gamma_i$  the toughness of the interface in  $\text{J.m}^{-2}$  and  $\Gamma_c$  the toughness of the layers in  $\text{J.m}^{-2}$ ) and normalized stiffness ( $E_i/E_c$ , with  $E_i$  the stiffness of the interface in Pa and  $E_c$  the stiffness of the layers in Pa) on the energy dissipated by the multilayered sample. It appears that the stiffer (or tougher) the interfaces, the shorter the crack deflection and thus the lower the energy dissipated. If interfaces and layers are mechanically dissimilar, the crack is more likely to deflect when arriving at the border layer/interface, and then to propagate into the interface before kinking out of the interface and propagating through the next layer. It will make a longer way to completely break the sample and more energy is dissipated. On the other hand, for interfaces mechanically closer to the layer properties, there is no crack deflection, and much less energy is dissipated.

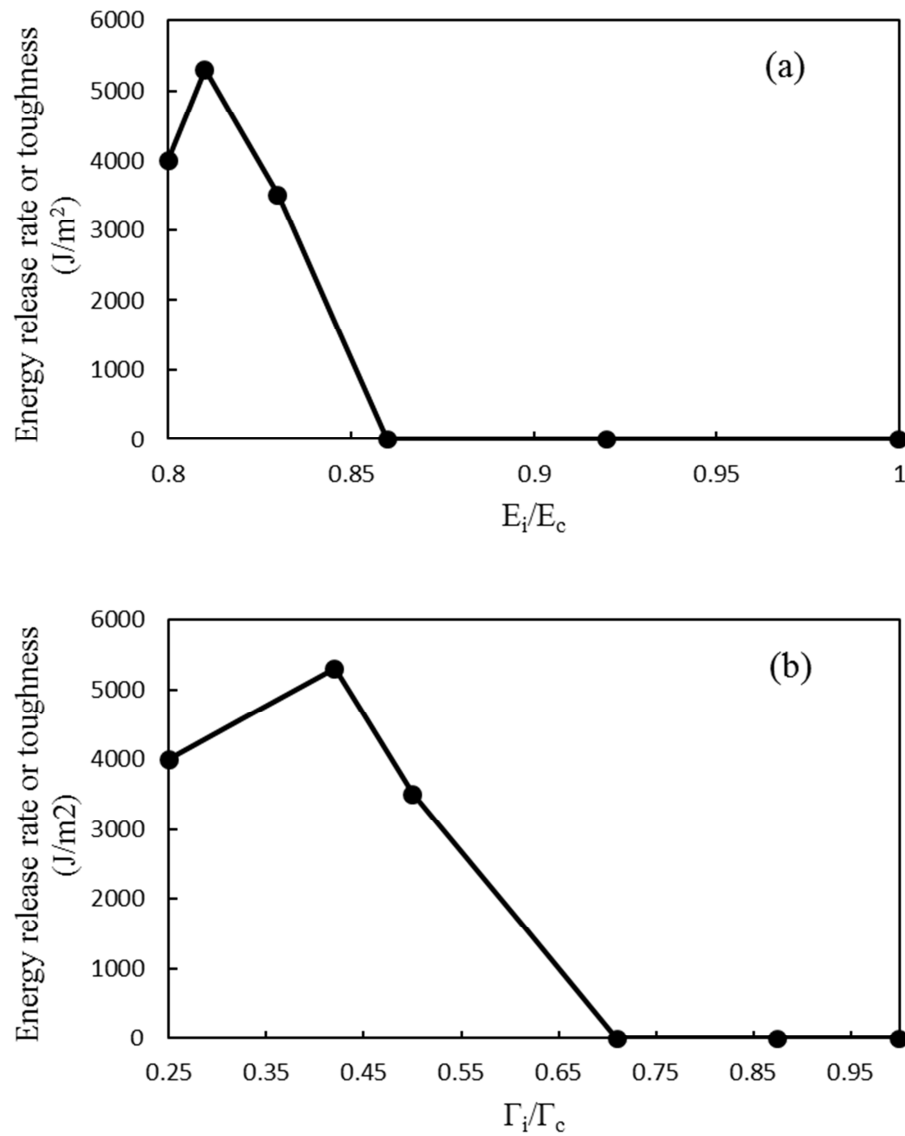


**Figure 2.5: Energy dissipated in the case of Kovar et al.'s multilayered material with adjustable interfacial properties plotted versus (a) normalized stiffness ( $E_i/E_c$ , with  $E_i$  the stiffness of the interface in Pa and  $E_c$  the stiffness of the layers in Pa) and (b) normalized toughness ( $\Gamma_i/\Gamma_c$ , with  $\Gamma_i$  the toughness of the interface in  $\text{J.m}^{-2}$  and  $\Gamma_c$  the toughness of the layers in  $\text{J.m}^{-2}$ ), adapted from [76].**

The condition for initial crack deflection is not sufficient to ensure high toughness. In addition, one must ensure that cracks deflected by the weak interfaces stay on these interfaces as much as possible. Kovar et al. suggested two possible reasons for a crack to deviate from the weak interface: first, the interfacial resistance increases due to the delamination length. Secondly, the presence of defects at the surface of the layer attracts the delamination crack out of the interface. The lower the number of defects in the layer, the longer the deflection, the higher the energy dissipated. Kovar et al. also described this problem as statistical, since

“crack kinking is controlled by the probability of encountering a suitable interfacial defect” [76]. The critical flaw size necessary to induce crack kinking was also plotted in function of the normalized toughness ( $\Gamma_i/\Gamma_c$ ) as shown on figure 2.6. The plot of this figure is not useful for other type of multilayered materials since it is specific to the material used in Kovar et al.’s work. It nonetheless illustrates the existence of two failure mechanisms for crack deflection: if all the flaws have a size below the critical one, large deflections and delamination are expected. On the other side, if some of the defects are bigger than the critical size, the crack will be deflected but will go back earlier in the layers, and overall it will propagate straighter in the sample.

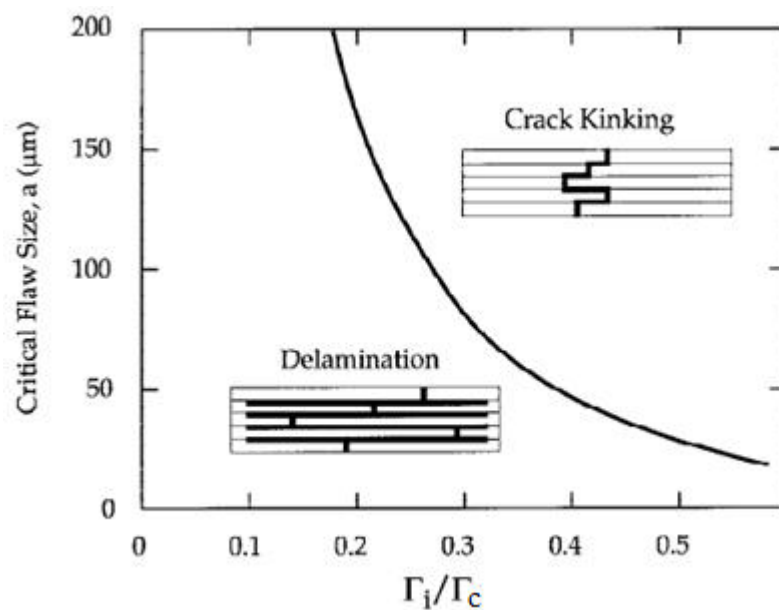


**Figure 2.6: Critical length of the dominant defect susceptible to kink the interface out of the interface plotted versus the normalized toughness ( $\Gamma_i/\Gamma_c$ ), of a silicon nitride-boron nitride multilayered composite [76].**

Although Kovar et al. highlighted the evidence of the relationships between toughness, stiffness, crack deflection and dissipated energy, other studies developed models capable of predicting better these failure mechanisms.

Some studies demonstrated that it is not sufficient to have two materials (layer and interface) significantly dissimilar to optimize the composite. This dissimilarity is a necessary condition to deflect the crack, but not to prevent sliding since an interface too weak will allow the layers to separate easily. Thus the toughness of the interface must respect a compromise. According to these models, to allow crack deflection, the ratio of the interface toughness,  $\Gamma_i$ , and the

toughness of the ceramic,  $\Gamma_c$ , must be less than 25%. Additionally, to prevent sliding, the aspect ratio of the beam must be increased, and the previous ratio should not be too small. Thus the optimal toughness ratio is in the range of 25% [77, 78].

However He and Hutchinson [78] demonstrated that the previous ratio is not enough to completely predict crack deflection. The normalized residual stress parameter  $\eta$  defined as  $\sigma_R a^{1/2}/K$  ( $\sigma_R$  being the residual stress in Pa,  $a$  the size of crack in m and  $K$  the stress intensity factor for the incident crack in  $\text{Pa}\cdot\text{m}^{1/2}$ ) as well as the elastic mismatch parameter,  $\alpha=(E_c-E_i)/(E_c+E_i)$  must also be considered. There are now three parameters describing the growth of the crack in the interface or its penetration into the layers. The competition between these two modes can be modelled by the comparison of the ratio of the toughnesses with the elastic mismatch parameter as described on figure 2.7. In this diagram, the maximal possible ratio of toughnesses at which the crack is deflected is plotted versus the alpha parameter. The diagram shows that this plot has a minimum in case of equal moduli ( $\alpha=0$ ), where the ratio of toughnesses is 0.25. This ratio must therefore be less than 0.25 to allow deflection in any cases, which also agrees with the Folsom's criterion described before and leads to the formula:

$$\Gamma_i < \frac{1}{4} \Gamma_c \quad (2.1)$$

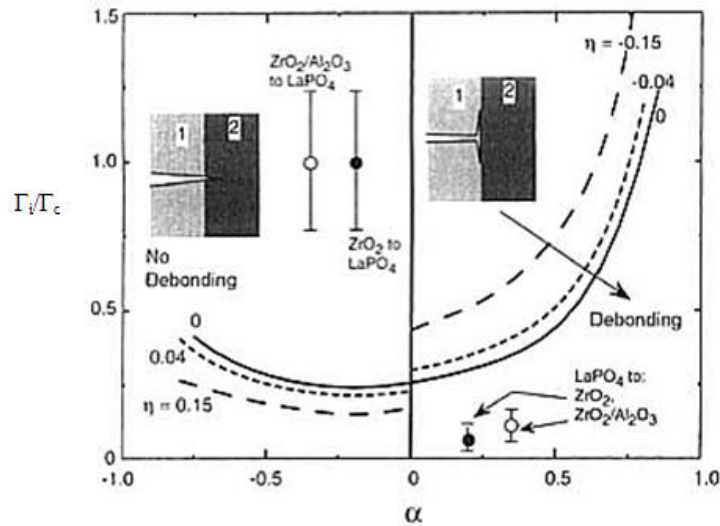


**Figure 2.7: Diagram of possible deflections as a function of the elastic mismatch parameter  $\alpha$ , toughness ratio and normalized residual stress parameter  $\eta$  [78].**

This case occurs most of the time, since the interface acts as an adhesive layer of negligible thickness, and because of its thickness, it does not have to be taken into account in the calculation of  $\alpha$ . In other words, materials 1 and 2 in figure 2.7 are the same, and the interface is a line between these two materials and consequently,  $\alpha=0$ . This model is thus more general but brings the same conclusions in the case of interfacial multilayered material. This criterion should thus be seen as a guideline in the design of these materials.

More practically, these models show that the toughness of the selected mineral must be four times higher than the toughness of the weak polymer in order to allow crack deflection and thus increase the amount of dissipated energy. The difficulty resides in the choice of the mineral and polymer since their mechanical properties must match this rule. However, we will take into account different other parameters (price, ease to work with, ...) since different techniques exist to change the properties of a given material: hydration can decrease the toughness of a material, fiber reinforcement can improve the toughness of a brittle material or crosslinking can improve all the properties of a weak polymer, as it will be discussed in chapters III and IV.

## 2.4 Maximal interface thickness

In the previous paragraph, an important geometrical parameter has been evoked in the optimization of the composite material: the thickness of the interface. Clegg [73] examined the problem in 1992 and he showed experimentally the existence of an optimal interface thickness that maximizes the fracture toughness of the sample. The results of the experiments are depicted in figure 2.8. The reason of the effect of the interface thickness is the discontinuity of the interface which is more likely to occur in for small thicknesses and which kinks the crack out of the interface. This reason explains why a small interface thickness implies less deflection and thus dramatically decreases the fracture toughness as shown on figure 2.8. On the other hand, a too thick interface implies a too large volume fraction of the weak material in the composite, decreasing properties such as strength. An optimal value exists as depicted on figure 2.8, where the interface is sufficiently thin to do not reduce the properties of the sample, but sufficiently thick to allow the crack to undulate without kinking out of the interface.

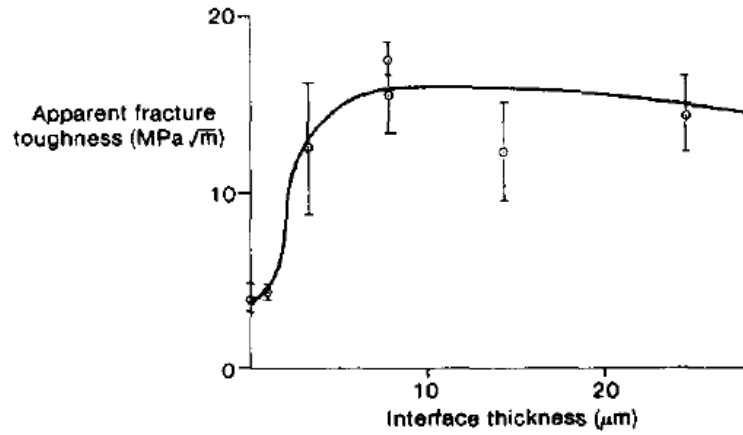


**Figure 2.8: Effect of interface thickness on the fracture toughness of a graphite (interface) – silicon (layer) carbide multilayer composite [73].**

In a different study, Phillipps et al. [74] developed a theoretical model to predict the optimal interface thickness based on the geometry and the properties of the materials used in the composite. They considered a crack that propagates while a critical stress is applied. The distance of propagation of the crack in the interface is dictated by the available energy. In this model, the maximal thickness  $\delta_m$  is:

$$\delta_m = \frac{6E_c G_{IIc}}{\sigma_c^2} \quad (2.2)$$

Where  $E_c$  is the Young's modulus of the layers in Pa,  $\sigma_c$  their strength in Pa and  $G_{IIc}$  the interfacial critical strain energy release rate in  $\text{J.m}^{-2}$ . These three parameters can be measured from several different tests. It will be the purpose of the chapter IV, and these parameters will serve to compute a value from (2.2) at the beginning of chapter V.

### 3. Chapter III: Biocompatible Materials: Biopolymers and Minerals

This chapter is a review of the potential materials for an ideal bone graft. Many biopolymers exist in Nature and are used in industry, and the first section is a non-exhaustive list of the most widely used. Chapter I discussed the potential of calcium sulfate (CS) cements. Here a review on the different types of CS will be presented. Chapter II gave rules and guidelines on the desired properties of the two materials which will be considered to select a polymer and a CS cement, and combine them into a multilayered bone graft composite.

#### 3.1 Mineral

Different mineral are used for bone graft substitute purposes, such as hydroxyapatite (HA) or calcium phosphate (CP). They however present issues that make them difficult to use. As described in chapter I, HA is the most widely used of the calcium based materials but it has poor (or even non-existent) degradability while CP is resorbable but has poor mechanical properties in comparison to other minerals [18]. On the other hand, CS is the mineral that presents the most interesting properties for biomedical application because it is completely degradable, osteoconductive [40] and promotes bone regeneration [42, 43]. Its mechanical properties are lower than those of bones but they can be improved with fiber reinforcements [51, 54] or chemically using additives to decrease the water needs of the CS powder (lignosulfonate and arabic gum) [40, 56, 79] or a water saturated in  $\text{Ca}^{2+}$  ions to limit the dissolution of the formed CaS [55].

The natural forms of CS are the anhydre form which is a solid and hard mineral ( $\text{CaSO}_4$ ), and the CS dihydrate also called gypsum with the formula ( $\text{CaSO}_4 \cdot 2\text{H}_2\text{O}$ ) [80]. This gypsum can be transformed by calcination into various other types of CS hemihydrate ( $\text{CaSO}_4 \cdot 0.5\text{H}_2\text{O}$ ) [41, 81-83]: CS type I (impression plaster), type II (plaster of Paris), type III (dental stone), type IV (high strength dental stone) and type V (ultra-high strength dental stone). The differences between those types reside at the crystalline level and are due to the preparation mode: calcination of gypsum at air produces the type I and II while calcination under steam pressure in an autoclave produces the type III, IV and V [40]. The size, shape and uniformity of the crystals of hemihydrate CS affect the density, porosity and mechanical properties of the solidified CS after setting. Figure 3.1 shows that the difference between the different types is

visible at the grain level. It also clearly shows how much dissimilar are the crystals of dental stone and those of plaster.

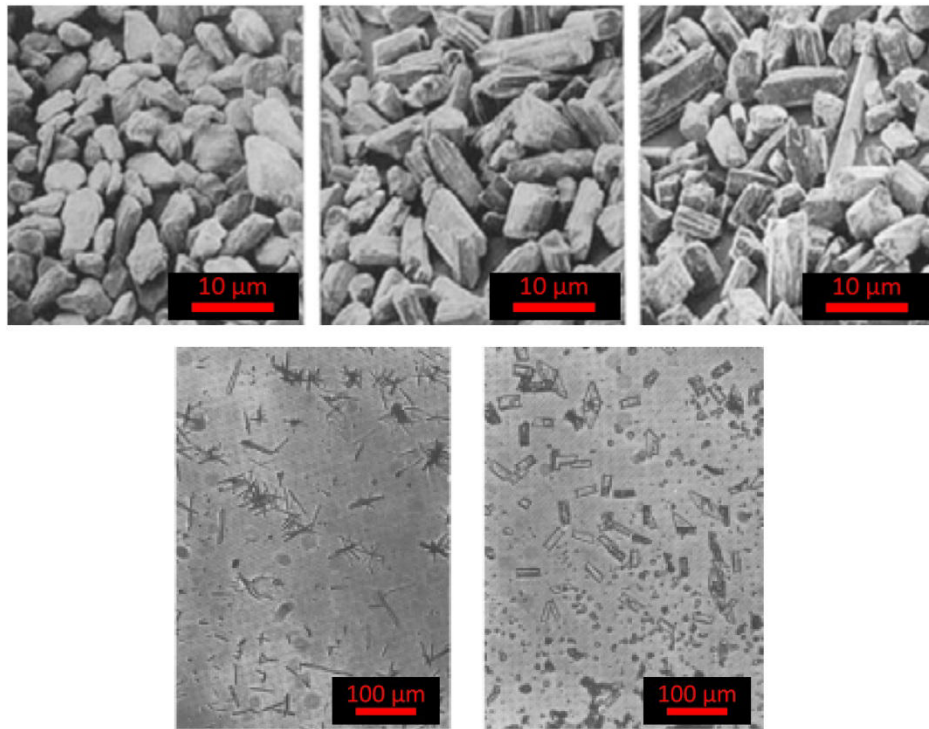
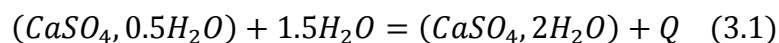


**Figure 3.1: Plaster particles (top left), dental stone particles (top middle), high strength dental stone particles (top right) [81]. Crystals of plaster (bottom left) to be compared with the typical crystal structure of dental stone (bottom right). Adapted from [84].**

The general solidification reaction for all the type of CS hemihydrate is the following:



Where  $Q$  is heat produced by the reaction. The result of the reaction is a highly crystalline gypsum with a very rigid structure because of the intermeshing of the crystals. The reaction can also be reversed by calcination at a temperature of 100-120 °C. The setting time of the reaction varies from 8 to 15 min depending on the type of CS but mixing techniques can reduce or increase this time. Finally the expansion of the material varies from 0.08 % to 0.20 % at air during the setting [40].



### 3.1.1 Gypsum – dihydrate calcium sulfate

During calcination, molecules of water are removed through the absorption of heat. Hemihydrate CS of various types are then obtained. When mixed to water, CS turns back into gypsum in an exothermic chemical reaction called setting, which then results in a cohesive and hard gypsum material. Three theories exist to explain the setting: first the colloidal theory proposes that the CS enters the colloidal state through solid-gel mechanism. In the solid state, hemihydrate CS particles are hydrated to form dihydrate CS and thereby enter in an active state. The entire mass consumes the water and converts into a solid gel. Another theory is the hydration theory where it is suggested that hydrogen bonds link sulfate groups together. To finish the dissolution-precipitation theory says that dissolution and instantaneous recrystallization of CS followed by interlocking of the crystals is the base of the setting [84].

Pure gypsum exhibits after setting a compressive strength between 2.3 MPa and 9.7 MPa depending on the mineral variety (selenite, alabaster, satin spar) [82]. Because of this low strength, Simple non-transformed gypsum has very poor use in dental applications and (mold and cast for dental diagnosis) but is commonly used for medical splints.

### 3.1.2 Impression plaster – hemihydrate calcium sulfate $\beta$ -form – type I

Impression plaster is the most porous and least dense of the hemihydrate CS. It is manufactured by addition of chemicals to gypsum [84]. At the crystalline level, non-uniform aggregates of crystals with capillarity are the origin of the weakness of the hard state of the material (after mixing with water and setting). The  $\beta$ -form indicates the non-uniformity of the crystal shape and size, to be opposed to the  $\alpha$ -form, more uniform. Moreover,  $\alpha$ -form crystals are smaller and stronger, and require less water to react leading to a less porous material. The  $\beta$ -form crystals are larger and less uniform, and their arrangement leaves more available space, leading to more porous mineral, and thus weaker. The difference between these two forms is due to the fabrication process as seen later. In dentistry, impression plaster, or hemihydrate calcium sulfate  $\beta$ -form is classified as calcium sulfate type I. There are 5 types of CS hemihydrate, with type V as the strongest material. Impression plaster has been used a few decades ago for preliminary impression of edentulous ridge in fabrication of dentures (mucostatic impression), but is now very rarely used since it does not resist to water at long term and has been replaced by stronger plasters or dental stones. A compressive strength of 4 MPa has been reported for impression plaster after setting [81].

### 3.1.3 Plaster of paris – hemihydrate calcium sulfate $\beta$ -form – type II

Plaster of Paris is also a  $\beta$ -form of hemihydrate CS and its powder consists of porous and irregular particles. It is stronger than impression plaster since it exhibits higher density and crystal uniformity due to its manufacturing process: calcination is performed by heating at 110-130 °C the gypsum powder in an open container [84]. Thus plaster of Paris is classified as type II in dentistry and is the least expensive CS.

Because of its low cost, its osteoconductivity and its resorbability, CS is preferred to design bone grafts and has a 100 year long history in bone grafting [40]. Since it is not water resistant, it has to be combined with another material that can resist to water. For example Gao [85] used crosslinked gelatin as a polymeric matrix to enhance the mechanical properties of the CS and make it resistant to water. Plaster of Paris is also used for preliminary mold in denture construction.

A compressive strength of 9 to 14.6 MPa [81], and a tensile strength of 3.2 MPa [41] have been reported in the literature. These relatively poor mechanical properties make the scientific and medical communities reluctant to use CS alone. To increase the properties, most of the studies report mixing the plaster with a biocompatible polymer like gelatin [85] which is a derivative of collagen. Other methods have also been investigated to increase the strength of plaster: Coutts [51] reinforced plaster with wood pulp fibres and was able to increase the toughness up to a factor 40. The strength was also 3 times higher through this method. Thomas [54] proposed to use cellulose-acetate glass fibres as reinforcement, and patents also mentioned the possibility to improve plaster by using magnesium sulfate [86] or cellulose with asbestos fibres [87]. From a more general point of view, any type of polymeric fibres (cellulose, collagen ...) could be able to reinforce both toughness and strength of plaster, especially the tensile or flexural strength. Gao [85] also improved the plaster by mixing it with gelatin: 10 % of gelatin increased by a factor of almost two the compressive strength, and the peak was reached for 60 % of gelatin – 40 % plaster of Paris, where the material exhibited a compressive strength of 80 MPa which is 5 times higher than pure plaster, and 1.4 times higher than pure gelatin. Sanad [56] also experimented with mixing plaster of Paris with Arabic gum, calcium oxide or calcium hydroxide and was able to improve the tensile strength by a factor 1.8, and the compressive strength by a factor 2.6 depending on the amounts of the different components in the mixture. Most of the investigations were conducted on plaster of

Paris but can also be applied to other stronger CS types (types III, IV, V), since Sanad repeated successfully his protocol on other types of plaster.

#### **3.1.4 Dental stone - hemihydrate calcium sulfate $\alpha$ -form - type III**

The differences between the  $\alpha$ -form and  $\beta$ -form of CS are the level of uniformity in crystal size, surface area and degree of lattice imperfection. Within type III we focus the discussion on  $\alpha$ -form of hemihydrate CS, or dental stone, since the method to manufacture this dental stone provides powder particles that are more uniform, in shape of rods and prisms, denser and less porous. Mixing this powder with water results in a harder dental stone even if this material still does not resist to water for long term. To manufacture it from gypsum, the calcination must be carefully controlled at 110-130 °C under steam pressure. The method releases the water of crystallization slower than for plaster of Paris manufacturing process hence the resultant crystals [84]. Dental stone type III dissolves in water too rapidly to be directly implanted in the human body but is used for dental cast and mold for diagnosis purpose.

Due to its crystalline properties, dental stone type III exhibits a compressive strength of 21 MPa [81]. Therefore, with the same chemical composition but an improved crystalline structure, the strength of the mineral is progressively increased.

#### **3.1.5 High strength dental stone - hemihydrate calcium sulfate $\alpha$ -form - type IV**

Hemihydrate CS type IV is an  $\alpha$ -form denser than the other types and so stronger once set. The shape of the crystal is also different (cuboidal shape). To manufacture it, the calcination of gypsum is at the same temperature, at 110-130 °C, but in calcium chloride solution so that a very dense particles powder with a reduced surface area is obtained [84]. While this dental stone is stronger, it is also more expensive. The main applications are still for casts and dies for denture crowns fabrication, but because of the increased strength and resistance to abrasion, type IV is also used for inlays, crowns and bridge casts. Type IV is thus resistant to water but have reduced mechanical properties in wet conditions.

Studies reported values for compressive strength from 35 MPa [81] to 45.5 MPa [83] which is stronger than the other types of CS with a crystalline structure less optimized.

### 3.1.6 Ultra high strength dental stone - hemihydrate calcium sulfate $\alpha$ -form - type V

Hemihydrate CS type V is the strongest of the dental stones and of the CS. To obtain such material, the manufacturing process of gypsum is the same than type IV but retardants and surface tension reducing agents such as lignosulfonate are used to decrease the porosity and increase the density and uniformity [84]. In dentistry, dental stone type V is the safest material to mold patient dentures and can then be used as mold for ceramic artificial dentures, or to be directly implanted as crowns.

The compressive strength of this material is between 49 and 90 MPa [81, 83] depending from the manufacturer and decreases by 40 % when hydrated which is high enough to biomedical purposes, especially in dentistry where the materials are submitted to compressive forces. In tension, progresses are still to be made because the strength values are far from those of bones (from 3.8 to 8.7 MPa [83]). Figure 3.2 below is a summary of the compressive strength values cited in this chapter and highlights how much the mechanical properties are improved from type I to type V by changing the microstructure of the mineral.

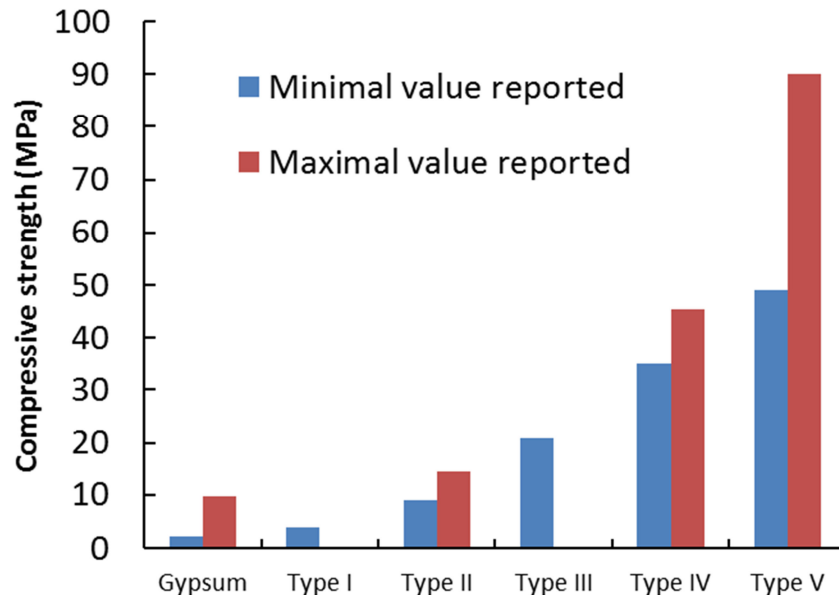


**Figure 3.2: Comparison of the compressive strengths of various types of calcium sulfates [41, 81-83].**

Mechanical data on the different types of CS are available in the literature and useful in the design and material selection for an ideal bone grafts. However, these data must be carefully

used. While strength values reported in literature are often compressive strengths, flexural or tensile strengths are much more relevant to bone tissue engineering applications. Moreover, implanting a material in human body implies that the material targets the desired properties in hydrated conditions, but most of the studies and values reported are in dry conditions. Some materials are already very close to bone in terms of compressive properties and dry conditions, but very far when considering flexural properties hydrated conditions. In most cases the dry compressive strength is more than double the wet compressive strength [40]. When considering compressive strength, figure 3.2 clearly shows that CS type V is the strongest of the CS forms. Even if in flexural testing and in hydrated conditions the measured values would be very different than the ones reported from the literature, it appears that CS type V has good chances to act as a hard and strong inclusion when combined with a soft polymer. The main criterion in terms of mechanics is still to have a mineral with a toughness at least four times higher than the toughness of the polymer. From literature, toughness considerations are scarce while strength and modulus description are widely reported. It is thus hard to predict the best mineral to be combined with gelatin, but for a bulk material, the fracture toughness is a function of the strength of the material, its geometry, and the size of its defects [88]. If we can control the defects and geometry of the material, the toughest of the materials described in this section will be the strongest. The strength will then be the properties that will be used to select the material for the hard layers. Moreover, there is still the option to improve the fracture toughness of the mineral with various techniques such as fiber reinforcement so has to reach the targeted toughness. We thus decided to select CS type V. A CS type V of the brand name *Suprastone* (Kerr Dental Laboratories, Orange, CA) was used to make the bone graft material developed in this work.

### 3.2 Biopolymers

This section focuses on the biopolymers available in Nature which could be used to increase the toughness and flexural strength of the minerals described above. Polymers that are produced in Nature tend to be more biocompatible than their synthetic counterparts. This principle has also been demonstrated in the long story of bone graft materials, where the most promising biocompatible materials have always been found in Nature: wood, corral, or nacre are good examples. In order to select the most promising of biopolymer for our bone graft, the non-exhaustive list below reflects the ones that are already used in actual applications.

Therefore their chemistry, structure and mechanical performances have been studied in details. The focus is placed on those which are biocompatible and FDA approved since these characteristics is primary for our purpose. Because the previous part described multilayered materials as efficient for our case, a particular attention will be put on the possibility of thin film making for each of the biopolymers below.

### 3.2.1 Cellulose

Cellulose is a polysaccharide and the most abundant natural polymer representing 50 % of the biomass on Earth [89]. Cellulose has the formula  $(C_6H_{10}O_5)_n$ , and exhibits a polymeric chain composed by glucose monomers. It can be extracted from various sources like cotton, wood or certain varieties of mushrooms even if it can be found in numerous plants as it constitutes the base of plants life. Cellulose has neither taste nor odor and is hydrophilic. This polymer is insoluble in water and in most of organic solvents. It also cannot be broken down chemically except by treating its glucose units with concentrated acid. Using it as a resin in a composite material would lead to a water-resistant material with potential application in biomedicine. Then the cellulose chain length or degree of polymerization varies between 300 and 1700 units [89]. Cellulose presents under both crystalline and amorphous form (semi-crystalline form). The cellulose polymeric molecules link thanks to their hydrogen bonds giving a fibrous structure. Studies already reported the use of cellulose in composite materials with cellulose fibres as reinforcements [90]. However it can also be treated to form plastic film hence showing the interest for this material as an interface in a multilayered material.

The most interesting point is that the hydroxyl bonding of cellulose provides sufficient strength to be used as a building material. Cellulose is an alternative to plastic and resins. The most known examples are biodegradable plastic bags and protective plastic films of cellophane. Ach [91] showed in 1993 a process to turn cellulose into plastic. The first step is to transform cellulose in its acetate ester, cellulose acetate. The powdered cellulose acetate is mixed at high-speed mixer with liquid additives and then granulated in a standard extruder at a temperature between 160 and 190 °C. The granular material can then be subjected to thermoplastic processing to make strands, sheets, and films

Cellulose acetate films present some limitations. Even if they are considered water resistant, the acetyl groups of the polymer break when exposed to moisture, heat, or acids for a long

time. Moreover acetic acid is released inside the plastic and then gradually diffuses to the surface. The acetic acid could interact with entities on the surface like cells for example which is a major problem for biomedical uses despite the remarkable mechanical properties. Bone grafts wrapped in oxidized cellulose have nonetheless proved efficient in craniomaxillofacial region surgeries [92] and allograft wrapped in cellulose successfully treated spinal disk degeneration [93]. Cellulose is hence biocompatible and cellulose based polymer sheets are available in medical industry under the brand Surgicel (Ethicon, Johnson & Johnson Medical Ltd, Somerville, NJ, USA). They are destined to wrap bone grafts and improve adaptation, to provide support to new tissues and to optimize tissue formation [92, 93]. Concerning the mechanical properties, firstly Stark [94] reported having tested fibers of cellulose with a Young's modulus of 3.5 GPa. However Sun [95] demonstrated that the mechanical properties of cellulose films are dependent on the water content. He showed that the Young's modulus is 3.5 GPa for 5 % water content in the film but it decreases down to 0.7 GPa when the water content increases to 25 %. He also found a maximal value of 110 MPa (5 % water content) and a minimal value of 50 MPa (25 % water content) for the tensile strength. The values for the elongation at break are ranged from 14 % to 26 %. This study also shows opportunities in the control of strength and tensile modulus of cellulose films since choosing the right part of water gives the desired mechanical properties, from 0 to 110 MPa for the strength and from 0 to 3.5 GPa for the modulus.

### 3.2.2 Chitosan

Chitosan is another polysaccharide produced from chitin which is a polymer made of acetylglucosamine units (a derivative of glucose). Chitin is extracted from crustacean skeletons (crabs, shrimps ...) and must be treated by deacetylation to give chitosan. This process is divided in four steps (demineralization, deproteinization, decoloration and deacetylation) [96]. Structurally, chitosan is composed of randomly distributed glucosamine units deacetylated or acetylated. Chitosan can crosslink with another polymer, between a structural unit of a chitosan chain and a structural unit of a polymeric chain or can crosslink with itself. The molecular weight or the concentration increases the crosslinking but the easiest way remains temperature treatment. After crosslinking, chitosan becomes resistant to water [97] which makes it suitable for tissue engineering [98]. Several studies already reported the use of chitosan to create chitosan thin films [99, 100]. Another study provided by

Bonderer [101] also reported using chitosan as a matrix to make composite materials with alumina tablets as stiff, inorganic inclusions. He also enhanced the interface between the alumina and chitosan by coating the surface of alumina tablets with chitosan which resulted in improved properties. This work represents an interesting start point for chitosan-based bio-composites and makes the chitosan a promising biopolymer.

Chitosan found many applications in agricultural and medicinal industry [102]. Chitin has also industrial applications: edible films in food processing, adhesives, separation membranes or ion-exchange media. A recent study also showed that chitosan can be used in the making of self-healing polymeric material: to obtain this high performance material, Ghosh [103] had to crosslink polyurethane and chitosan together. A scratch can heal in less than an hour under an ultraviolet light, because such light heals the chemical chains bonds. In the field of bone tissue engineering, chitosan possesses very useful properties: it has excellent biocompatibility, biodegradability, antibacterial Nature and can be easily shaped into various and complex geometries. It is among the best bioactive materials for bone regeneration and is thus an emerging polymer for bone tissue engineering [104] and more generally for tissue engineering because of its recent applications in 3D-scaffolds (gels, sponges) and 2D-scaffolds (films and fibers) [98].

Crosslinking is a required step to make a water-resistant film of chitosan. Two parameters have a strong influence on the crosslinking: time and temperature which leads to different crosslinking protocols. For instance Arvanitoyannis [99] found the best results when he evaporated the water at 22 °C (low temperature preparation) and then 60 °C for 6 h (high temperature preparation). Caner [100] prepared his films at lower temperature but with longer drying time: he let dry for 24 h at room temperature followed by 12 h at 50 °C. Bonderer [101] and Chen [105] also dried the material at 50 °C in air. Once crosslinked, the films were water resistant.

The different processes of chitosan films preparation described above produced materials with different mechanical properties. It first shows that these properties are dependent on the preparation since some protocols may not fully crosslink the chitosan polymer. Moreover Caner proved the storage time dependence of chitosan films [100] which could be a source of variations in the studies. Nonetheless the values are always in the same range: Arvanitoyannis provided value of 130 MPa for tensile strength, while Bonderer varied different acids, acid concentrations, plasticizer concentrations and finally found values between 25 and 50 MPa.



Concerning the elongation, Arvanitoyannis found 4.1 %, and Bonderer between 30 % and 40 %. Young's moduli are closer with a value of 2.5 GPa for Bonderer and 2.05 GPa for Arvanitoyannis.

### 3.2.3 Starch

Starch is a long polymer composed of glucose molecules and one of the primary sources of calories for humans. The only difference with cellulose is the glucose mers are oriented "upside-down" in cellulose while in starch all the mers are oriented in the same direction. Large polymers made of glucose like cellulose or starch are called carbohydrates and provides most of the calories in the normal human diet. Starch is extracted in large amounts in food as potatoes, wheat, corn, rice and others plants and is thus a biopolymer that can be found easily and in large quantities at low price, which is an important advantage. Starch is therefore widely used in industry: paper, corrugated board adhesives, clothing or even plastic films which represents an interesting point for our case. Starch has a semi-crystalline structure with a crystal size from 2  $\mu\text{m}$  (rice) to 100  $\mu\text{m}$  (potatoes). Like cellulose, starch is tasteless and odorless and insoluble in cold water or alcohol. However it can be dissolved in heated water since hot water breaks the semi-crystalline structure. Like chitosan, by crosslinking starch molecules, water resistant films can be created and starch thus finds interesting applications [106].

Most of the applications of starch are industrial because of the interesting mechanical properties of this natural polymer. Starch is often sold in powder to be diluted in water before being used for the following purposes: papermaking (a sheet of paper may content as high as 8 % of starch in order to make it more rigid); in clothing, liquid laundry starch is vaporized through a spray to stiffen clothes; since it is biodegradable and edible, starch is used in food industry to make plastic-like aspect for certain foods like edible packing peanuts; generally, corrugated boards are maintained together thanks to starch based adhesives; starch also shows a growing interest in bioplastics for packaging and wood glues [107]. This list demonstrates the interest to crosslink starch and to make it water resistant. Tomka [106] reported in a patent that starch can be melted. The melting of starch is possible by chemically lowering its melting point and/or by the application of heat and mechanical energy until it is homogeneous without the presence of water. This protocol produces granulates of starch that can be processed into complex shapes such as scaffolds. Starch-based scaffolds for bone tissue engineering already

proved they are biocompatible [108], osteoconductive and promote bone tissue regeneration [109].

Stark [94] measured a tensile strength at failure between 15 and 35 MPa for starch but reported a wider range for elongation at failure (10 to 150 %) and large variations in the Young's modulus, from 600 to 5000 MPa. On the other hand Piyada [110] more recently reported more accurate values: he measured tensile strength and elongation at break of rice starch films and found 7.0 MPa and 52 %. He also tried to reinforce the film with starch nanocrystal and improved the strength up to 16 MPa (20 % nanocrystal content) for an elongation at break of 8 %, hence making a stiffer material. The resulting Young's moduli were 13.5 MPa without nanocrystal and 200 MPa with 20 % nanocrystals content.

#### **3.2.4 Glucomannan extracted from the Konjac plant**

Glucomannan is another polysaccharide composed of two different sugars: glucose and mannose with 1.6 times more mannose [111]. As opposed to cellulose and chitosan, glucomannan is scarcer because it can be extracted only from the root of Konjac, a plant from subtropical to tropical eastern Asia, from Japan to Indonesia. Crosslinking this molecule is the easiest way to decrease the solubility in water, in and to obtain thermoplastic benzyl glucomannan films [112]. Thus, in addition to the various health benefits of glucomannan [113], interesting material applications like water resistant composite films are available [112].

Zhang [113] reported the use of glucomannan as a coating material to preserve the freshness of food, in biomedicine as biocompatible gel and in cosmetics. The most important use of glucomannan is due to its ability to form biodegradable resin compositions [114] which also demonstrates its very good film-forming ability. Chen [112] reported a precise procedure to obtain thin glucomannan films (5 to 10  $\mu\text{m}$ ), which could be useful for future bone designs. Concerning the use of glucomannan in bone tissue engineering, glucomannan is at its beginning and studies in this field are published since 2010 only: first, scaffolds made of chitosan, glucomannan and combined with HA have been found to be efficient to deliver anti-infection protein in infected regions of rabbit bones [115]. Another type of scaffolds made of chitosan and glucomannan only was found to be efficient to provide more suitable space rooms for bone cells and thus favor bone ingrowth [116]. Finally, scaffolds made of pure

glucomannan or scaffolds made of glucomannan and HA exhibited sufficiently good chemical properties (presence of functional groups of HA) and physical properties (microstructure, morphology, porosity) to be used as three-dimensional substrates in bone tissue engineering [117]. Even if patents of glucomannan scaffolds capable of promoting cell growth [118] have been published, further in vivo studies are still required to validate the effect of glucomannan on bone cells.

Studies on mechanical properties of pure glucomannan are very scarce in literature since most of the works relate the performances of composites materials made of glucomannan and another polymer like chitosan [119] or soy protein [112] for example. Enomoto-Rogers and Iwata [120] in a recent study used glucomannan acetate rather than glucomannan which is the corresponding anion of glucomannan. They preferred this molecule because of its better properties in tension than simple glucomannan and tested thin films. He found 76 MPa for tensile strength, 31 % for elongation at break and 0.98 GPa for Young's modulus.

### **3.2.5 Collagen and gelatin**

Collagen is the structural protein which serves as building block for most of the structural tissues of mammals. It is also the most abundant protein on Earth. This protein is relatively stiff and hard and it is used to transmit loads through tendon (figure 3.3a) and other tissues. Collagen also constitutes skin, muscles, vessels and other tissues in various percentages and orientations and provides different mechanical behaviors: stiffness (tendons) or deformability (skin). As a protein, collagen is composed by 18 different amino-acids. The part for each amino-acid can vary from an animal to another.

The molecular pattern shown on figure 3.3c is the monomer of collagen molecules and is repeated up to 300 times along the primary structure of this protein. These collagen molecules twist and assemble three by three in order to form tropocollagen in right handed triple helix shape (figure 3.3b). It uncoils under pressure, absorbing energy [121]. These tropocollagen molecules assemble via covalent crosslinking together and form collagen fibrils which are a polymers of tropocollagen also shown on figure 3.3b [122]. Since collagen is not fully crosslinked in animals, it can be extracted by heating and used to make strong glues as a primary application. Once crosslinked, collagen is insoluble in water. Given that collagen is

one the main origins of the mechanical properties of organic tissues (stiffness of tendons, strength of bones ...), this polymer represents a potential material for biocomposite purposes.

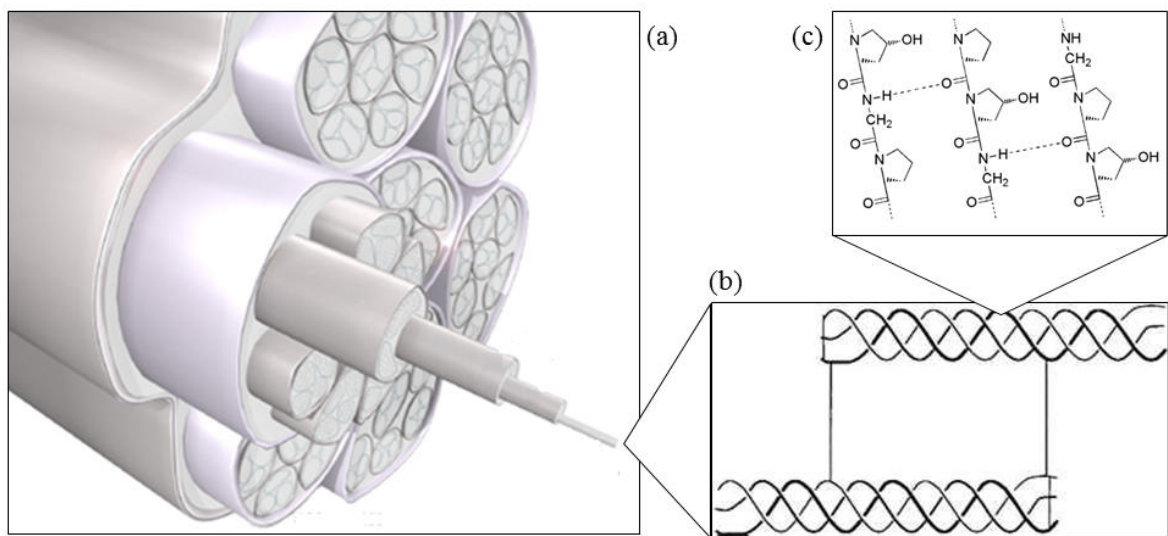


**Figure 3.3: Hierarchical schematic representation of the collagen structure in a tendon: (a) tendon is divided in primary fibers, collagen fibers, and collagen fibrils [123]; (b) junction of two tropocollagen molecules in a collagen fibril [124]; (c) molecular structure of a mer in tropocollagen [125].**

Collagen is the main component of human and animals tissues, and that is why it is biocompatible and finds many applications in the biomedical industry. When infiltrated in the cardiac muscle, collagen can restore the compliance needed by this muscle to move blood [126]. In surgery collagen is used for bone and skin reconstruction: the triple helical structure provides stiffness to the collagen molecule and moreover its adhesiveness for bone cells allows proper assembly of the extracellular matrix thus making the collagen an important material in bone grafts. Pure collagen has however dissimilar mechanical properties than natural bone, and that is why the introduction of a stiff mineral phase into collagen scaffold make them closer to the requirement of a bone graft material [126]. Hence, HA – collagen scaffolds provides adhesion for osteoblasts and both osteoconductivity and osteoinductivity [127], and even bone cells ingrowth and bone regeneration [128]. A study also reported the fabrication of a hierarchical scaffold made of collagen, polyvinyl alcohol and HA with a three dimensional structure that mimics cancellous bone. Such scaffolds were found resorbable overtime and efficient to heal large bone defects in rabbits [129], thus demonstrating the

potential of collagen in bone tissue engineering. Resorbable mineral – collagen composite scaffolds are sold under the brand Ossimend (Collagen Matrix, Inc., Oakland, NJ, USA).

Collagen also allows the manufacturing of thin films: Kotov [130] reported controlling the thickness of collagen biocompatible films by layer-by-layer assembly: films were fabricated with a mixed solution of collagen and polyelectrolyte and deposited on quartz or silica substrate. Positively charged molecules of poly(dimethyldiallyl-ammonium) were injected to the first film, thus forcing it to bond with another one once in contact. Although the polyelectrolytes used by Kotov are not biocompatible, the process could gain interest by using other polyelectrolytes that are biocompatible [131]. Therefore films of collagen can be manufactured with various thicknesses. Alternatively another simple way to produce films is to use gelatin: gelatin is a form of collagen that has been irreversibly transformed into smaller molecules. Bonds between individual collagen chains are broken down which gives a smaller structure that rearranges more easily. Effectively gelatin melts when heated and solidifies when cooled again. These two processes are reversible. Working with gelatin allows producing low cost films easily and quickly, providing thus interest for potential biocomposite applications. Although the produced gelatin films are sensitive to water and temperature, some studies solved this point by showing that gelatin could be chemically crosslinked in optimizing the ratio of crosslinkers dimethylaminopropyl-ethyl-carbodiimide hydrochloride and hydroxysuccinimide [132]. Pure type-I collagen films have already been crosslinked in the study of Koide [133] by ultraviolet radiation treatment and hence became water-resistant for biomedical purposes. Gelatin is a very inexpensive material which can be purchased in the form of a dehydrated powder. By mixing the powder with the right amount of water and then heating, the mixture becomes a workable viscous liquid, then a gel upon cooling down, and then a very strong solid after complete dehydration. The process is reversible and thus opens interesting opportunities for the fabrication process of multilayered bone grafts. In fact, the fabrication of scaffolds made of gelatin combined with a mineral was reported, with the same benefits than collagen-mineral scaffolds [134].

Koide also reported interesting mechanical properties thanks to his method to crosslink films of pure type-I collagen via ultraviolet radiation. He tested different crosslinking times from 5 min to 5 h and reported values for strength from 27.7 to 32.7 MPa (depending on the UV treatment time) while non-crosslinked collagen exhibited strength of 37.7 MPa). The different elongations at break were 2.4 to 4.6 % (6.8 % for non-crosslinked collagen) the different elastic moduli were in the range 1.4 to 1.8 GPa (1.1 GPa for non-crosslinked collagen) [133].

These results also show that, as expected, crosslinking collagen also makes it more brittle: the more the chemical bonds between the molecules, the less the mobility of these molecules, and the less ductile the material.

### **3.2.6 Alginate from kelps**

Alginate also known as alginic acid, is an anionic polysaccharide extracted from giant kelps in the Pacific Ocean, and more precisely by harvesting brown seaweeds. This molecule is a block copolymer which blends mers of mannuronic acid and guluronic acid. The length of the blocks varies depending on the natural source [135]. However alginate is not the best candidate since it presents only capabilities to gel forming. Some modifications have to be done in order to manufacture thin films as it is explained in Mollah's work [136].

Because alginate absorbs water very quickly and up to 300 times its dry weight [137], it is widely used as an additive in dehydrated products and also a thickening agent or a gelling agent in drinks. Alginate has good film-forming properties and gels of alginate have applications in biology for cell immobilization and encapsulation [135]. Alginate films have poor mechanical properties and to solve this, films of alginate mixed with another polymer like gelatin or chitosan [138] can be manufactured. Mollah [136] reported an interesting way to improve mechanical properties of pure alginate films; he used a solution of sodium alginate blended with ethylene glycol that he poured and photo-cured to make thin films with better properties. If alginate was at first view not relevant for bio-inspired composites, this recent study places alginate as a potential candidate. Moreover other recent studies proved that scaffolds made of pure alginate have mechanical properties, biocompatibility [139] and biodegradability [138] sufficiently good to be used in bone tissue engineering purposes.

Mollah [136] also reported the effect of UV intensity treatment on pure alginate films. He reported a maximal tensile strength of 35 MPa obtained for 20 passes of 3 minutes UV radiation. The corresponding elongation at break was 12 % but he also was able to reach a maximal value of 22 % with 15 passes of 1 minute UV radiation with almost the same strength (33 MPa). The highest Young's modulus recorded in the study was 170 MPa. Pure alginate films with no UV treatment exhibited a strength of 24 MPa and an elongation at break of 11.5 %. The lowest strength value of the analysis was 18 MPa (only one UV pass) but the elongation dramatically decreased to 7 % which is a value less interesting than the

previous since a soft polymer is required for an interface in a multilayered material. Although no clear relationships between the UV intensity and the effect on the mechanical performance was found, Mollah demonstrated that it was possible to modify (increase or decrease) the properties with UV treatment.

### 3.2.7 Shellac from insects

Shellac is a biopolymer secreted by an insect found in tropical Asia. This insect produces shellac in waxy resin for protection and increases its secretions when harvested. It is widely used as an adhesive polymer especially in cosmetics and moreover it is considered as a natural form of plastic due to its chemistry close to synthetic polymers: very first studies reported shellac as a polyester formed by the self-esterification of a mixture of hydroxy acids: different mers are present in the polymeric chains such as aleuritic acid, butolic acid, shellolic acid, jalaric acid [140]. When molded under heat and pressure, shellac can be turned into granulates. Hence it can potentially be processed and be an interface in composite materials.

Shellac has very few applications since it is produced in its acid form to be used as a protective coating material. However this process reduces the mechanical properties of shellac [141] which leads to decrease its use except for coating and protective layer (cosmetics, violins ...). These issues do not place shellac as the best material for multilayering purposes. Nevertheless aqueous ammoniacal solutions gave back to shellac some importance since they allow the production of films that lack the aging instability. Farag [141] explained in his protocol that once shellac is dissolved in ammonium bicarbonate solution, such films can be fabricated on Teflon plates through evaporation at 50 °C for 4 to 5 hours.

In a recent study of Arnautov and Faitelson [142], shellac films were prepared from simple solutions of shellac powder dissolved in ethanol and crosslinked through UV treatment. This process fully crosslinked the structure and exhibited interesting properties; even if the mechanical performances were far from those of other biopolymers, for the very first time water resistant films of pure shellac were fabricated and tensile properties such as elongation at break, tensile strength and Young's modulus were measured. They respectively reported 1.7 %, 5.7 MPa and 0.46 GPa. Shellac needs however to be more stable before being used in biomedical applications. More recently, a study showed that mixing gelatin with shellac

enhances significantly its stability [143] but further studies are still required before making bone grafts with shellac.

### 3.2.8 Pullulan

Pullulan ( $C_6H_{12}O_5$ )<sub>n</sub> is a polysaccharide polymer produced from starch by *Aureobasidium pullulans* through a fermentation process. This fungus grows on starch and glucose and gives pullulan when harvested. This polymer is structurally composed by mers of maltotriose. Maltotriose is another polysaccharide (trisaccharide) made of three glucose units. The glucose in maltotriose is linked with  $\alpha$ -1,4 glycosidic bonds while the maltotriose molecules in pullulan are linked together thanks to  $\alpha$ -1,6 glycosidic bonds. This unique type of bonding is the origin of the structural flexibility and solubility of pullulan giving a capability in film-forming and fiber-forming which does not exist in other polysaccharides [144].

The various interests of pullulan for industry (potential for price reduction when produced in mass, properties as a great oxygen barrier or chemical inactivity vis-à-vis other chemical products) led to numerous patents from 1976 to 2002 [144]. Moreover different patents showed that the problem of the water solubility of pullulan can be reduced by esterification [145] or etherification [146], or by crosslinking [147] which opened the door to water resistant films for biomedical applications. Among the various applications of pullulan in industry, some are related to the mechanical properties of this polymer especially in biomedical industry. Pullulan exhibits adhesive properties [145] that can be used in dental health care, as a binder and stabilizer, sustained-release formulations and other oral care products based on pullulan films. In food industry, edible films have already been manufactured [148]. Because of these interesting properties, pullulan is a candidate for bone graft substitutes. A very recent study in 2015 described a pullulan based scaffold coated with HA with improved osteoconductivity and mechanical properties for bone tissue engineering [149].

Yuen [150] showed that 5 to 60  $\mu$ m thick pullulan films with excellent mechanical properties can be formed just by drying a pullulan solution (5-10 %) on a smooth surface. Kawahara [151] explored the effect of temperature during the film preparation on the final mechanical properties of pullulan films. He demonstrated that around 60 °C the properties of the films decrease but around room temperature (between 10 °C and 30 °C) no significant changes have



been found: tensile strength was 65 MPa, the elongation at break was 5 % and the Young's modulus was 2.0 GPa were reported. Even when Kawahara explored other preparation temperatures, tensile properties did not change significantly which leads to conclude that pullulan is not the most extensible of the biopolymers.

### **3.2.9 Polyhydroxybutyrate (PHB) from microorganisms**

Polyhydroxybutyrate (PHB) is a polymer produced from microorganisms like fungus and bacteria and is classified as polyester [152]. It synthesizes from hydroxy fatty acids with short chain length (3 to 5 carbon atoms) and its chain grows up to 30,000 hydroxy fatty acid monomers. PHB has several interesting properties that make it a potential candidate for biocompatible composite material: water insoluble, biocompatible and suitable for medical applications.

PHB has better physical properties than other plastic like polypropylene and is nontoxic. It is thus used for food packaging applications. The low-impact strength of PHB has been solved with the incorporation of hydroxyvalerate monomers in the polymeric chain [153]. This protocol made PHB a mechanically interesting material. The resulting polymer is polyhydroxybutyrate-co-valerate (PHBV), which is also known under its trade name Biopol (Monsanto, St. Louis, MO, USA). PHB is also biodegradable and with excellent biocompatibility [154] which make it promising for biomedical scaffolds: for instance, Khorasani [155] fabricated PHB scaffolds for nerve tissue engineering. To finish, the remarkable mechanical properties of PHB already led to use this material in biodegradable composites made with layered silica inclusions [156], or to make medical devices such as sutures, screws, bone filling material, stents, bone marrow scaffolds, meniscus regeneration devices, ligament and tendon grafts, and even bone graft substitutes [157].

Aoyagi [158] reported the fabrication of PHB films with strong mechanical properties. His protocol consisted in using ultra-high-molecular-weight PHB swelled chloroform for 48 h, and then dissolved at 100 °C for 30 minutes. Films of PHB were prepared by a solvent-casting technique from chloroform solutions and dried in vacuum at room temperature. Aoyagi revealed the same mechanical properties than Stark [94]: 40 MPa for tensile strength, 3.0 GPa for Young's modulus and 4-10 % for elongation at failure which testified that PHB is a strong material. However Aoyagi used a two steps annealing procedure called two-step hot-

drawn procedure where films were annealed at various temperature (room temperature, 100 °C or 160 °C) and he defined the draw ratio as the ratio of time of annealing in these two steps. Depending on these temperatures Aoyagi was able to increase the mechanical performances: tensile strength and elongation at break reached up 277 MPa and 84 % and even beyond for ultra-high molecular weight PHB. The Young's modulus was also increased by 220 %. These values largely exceed all the previous values exhibited by other polymers. Aoyagi explained this phenomenon by the formation of lamellar crystals in "shishkebab" structure. These crystals play an important role in the final mechanical performances and their size and shape depend on the annealing temperature. These mechanical properties highlight the capabilities of PHB to absorb large quantities of energy and explain the interest in PHB films.

### **3.2.10 Polylactide acid**

Poly(lactide acid) (PLA) is one of the most used biopolymeric materials in the world in terms of consumption volume. It can also be considered as the first biodegradable polymer used in biomedical applications because of its non-solubility in water and its biocompatibility and biodegradability. It is derived from various sources, such as corn starch, tapioca roots or sugarcane to name just a few. PLA exists under two different forms: poly-L-lactide (PLLA) which is a polymer made of L-lactide units only. And another form is poly(L-lactide-co-D,L-lactide) (PDLLA) which blends two units L-lactide and D,L-lactide. The two forms have different physico-chemical properties: for instance PLLA is a semi-crystalline polymer (crystallinity about 37 %) while PDLLA is amorphous. PLLA has a melting point of 180 °C while PDLLA has no melting point [159].

These differences lead to different mechanical properties but also to different applications: PLLA is widely used for its film-forming capabilities, in agricultural industry for example. Numerous companies are specialized in PLA based products such as Natureworks (Blair, NE, USA), Shimadzu (Kyoto, JPN), Treofan (Raunheim, GER). It also finds numerous applications in biomedicine: bone internal fixation devices, absorbable sutures, replacing ligaments and non-degradable fibers to name just a few [160]. Both PLLA, PDLLA or PLA are very promising in bone tissue engineering since they exhibit useful mechanical and biological properties, such as biocompatibility and biodegradability, and that is why PLA

based scaffolds that are biocompatible, biodegradable, and mechanically strong are already produced [161, 162].

The different forms of PLA, PLLA and PDLA have different mechanical properties. PLA or PLLA exhibit an elongation at break of 5 % and a tensile strength of 50-70 MPa [159, 163]. The modulus of the three forms varies from 0.35 to 2.8 GPa [159, 164]. More generally, the mechanical properties of these polymers vary in a large extent, from soft to stiff and strong materials, especially because the important effect of their molar mass and their degree of crystallinity on these properties [163].

### 3.2.11 Comparison of selected biopolymers

Table 3.1 summarizes the main properties for the biopolymers discussed above. From these preliminary findings, it appears that collagen and gelatin are among the strongest biopolymers.

<b>Polymer</b>	<b>Tensile strength (MPa)</b>	<b>Elongation at break (%)</b>	<b>Young's modulus (GPa)</b>	<b>FDA approved / biocompatible</b>
Cellulose	50-110	14-26	0.7-3.5	Yes
Chitosan	6.69-130	4.1-45	2.05-2.5	Yes
Starch	7.0-35	10-150	0.6-5	Yes
Glucomannan	76	31	0.98	Yes
Collagen - Gelatin	27.7-37.7	2.4-6.8	1.1	Yes
Shellac	5.7	1.7	0.46	No
Alginate	18-35	7-22	0.17	Yes
Pullulan	65	5	2.0	Yes
PHB	27-277	4-84	0.9-2	Yes
PLA	42-65	5-10	0.35-2.8	Yes

**Table 3.1: Comparison of previous biopolymers through their mechanical data [52, 94, 95, 99-101, 110, 120, 133, 136, 142, 151, 158, 159, 163].**

As described above, there are specific criteria for the selection of the. It is also important to take into account two important parameters in the choice of the materials: (i) the price of the material; (ii) the ease to work with the material, which simplifies the fabrication process and (iii) its biocompatibility, and whether it is FDA approved for use as implant in the human body. Table 3.1 summarizes the mechanical properties and biocompatibility/FDA approval of the different biopolymers selected here. It is clear that a wide range of properties is available through these different polymers, but when considering (i) and (ii), gelatin appears to be the best compromise in the choice of a weak interface in the multilayered bone graft. As previously mentioned, gelatin is easy to manipulate and to transform thanks to hydration – dehydration or heating - cooling cycles. It is also inexpensive and easy to obtain, while its mechanical properties are adapted to our purpose since gelatin is very weak when hydrated. Gelatin is also derived from collagen, which is the main protein in bone.

In the next chapter, an experimental study of the gelatin will take place. Again, different techniques can help to adjust the properties of the gelatin in case of they do not reach the target previously defined (toughness below 25% of the toughness of the mineral): crosslinking can increase the toughness of gelatin, or hydration can decrease it. The next chapter will also study the properties of the selected mineral (Suprastone) and the parameters that have an influence on these properties.

## **4. Chapter IV: Gelatin and Calcium Sulfate: Preparation Protocol and Mechanical Properties**

This chapter describes in more details the gelatin and CS which served as components for the proposed multilayered bone graft. The preparation protocols are given in details, and mechanical properties of each component are presented. The effects of preparation parameters on the mechanical properties are described, which led to the identification of optimum fabrication protocols for each of the components.

### **4.1 Gelatin**

Gelatin is usually extracted by boiling tissues containing collagen such as skin, tendons, ligaments, bones, etc. in water. The final product is then a granulated solid powder that can be dissolved in hot water which is almost the only solvent for this material [165]. Gelatin extracted from porcine skin was prepared from a porcine gelatin powder obtained from Sigma Aldrich (St. Louis, MO, USA). Following standard protocol [166] the gelatin powder was mixed with water following a mass ratio of 1:9 and heated to 70 °C with a hot plate so that the gelatin was completely dissolved. The obtained mixture was heterogeneous and made of high molecular weight molecules. At 70°C the mixture was liquid. When the mixture cooled down to room temperature (or at least below 35 °C), the collagen molecules crosslinked and the solution became a gel which is the hydrated form of gelatin at room temperature [167]. In this form, gelatin is very deformable, but weak. If the gel is allowed to dry at room temperature, the gelatin molecules completely crosslink and the dry material exhibits a completely different behavior: this dried form becomes very strong, stiff and brittle. This type of behavior is however not useful to make weak interfaces, and the dry conditions are not relevant because different from the in-vivo conditions. The drying-hydrating procedure is reversible: when re-hydrated dry gelatin reverts back into a soft gel. This reversible change of properties with water is useful for fabrication purposes.

#### **4.1.1 Tensile properties and effect of hydration**

The gelatin was first tested in tension to obtain an estimate of the behavior of the material in dry and hydrated conditions. 1 g of gelatin powder was mixed with 9 g of water and heated at

70 °C in order to turn the mixture into a liquid solution. The solution was then poured on a Teflon plate to produce a 1 mm thick film of gel. The gelatin turned into a gel almost immediately once in contact with the Teflon surface which was at room temperature. The film were then left to dry for 12 hours in ambient condition. Upon drying the 1mm thick film of gel became a 100  $\mu\text{m}$  thick layer of dried gelatin after evaporation of the water. Drying the film facilitated the precision laser cutting of the film into dog bone shaped samples as shown on figure 4.1a. Two batches of samples were tested: rehydrated samples and dry samples. Figure 4.1 shows typical curves of gelatin in tension, dry and hydrated. Dry gelatin (Figure 4.1b) is a stiff and strong material that does not deform more than 2.5 %. It also shows a brittle behavior because of the catastrophic failure. However, once hydrated, gelatin becomes very soft and the strength decreases by a factor 1000 as shown by figure 4.1c (strength of 26.7  $\pm$  6.11 KPa instead of 30.6  $\pm$  8.23 MPa for dry samples). At the same time, water brings high deformability to gelatin, since the elongation at strain becomes 35 %. The shape of the stress-strain curve also suggests a progressive failure in some hydrated cases instead of a brittle failure when dry. In the non-crosslinked hydrogel (hydrated gelatin), there are less bonds between the long molecular chains which facilitates the elongation of the material. When dry and thus more crosslinked, the material has more chemical connection between the long molecules and the material can resist better to the applied stress, and its molecules are less free to move which results in a lower strain at failure. The properties of the hydrated gelatin are those required for weak interface for a multilayered mineral composite.

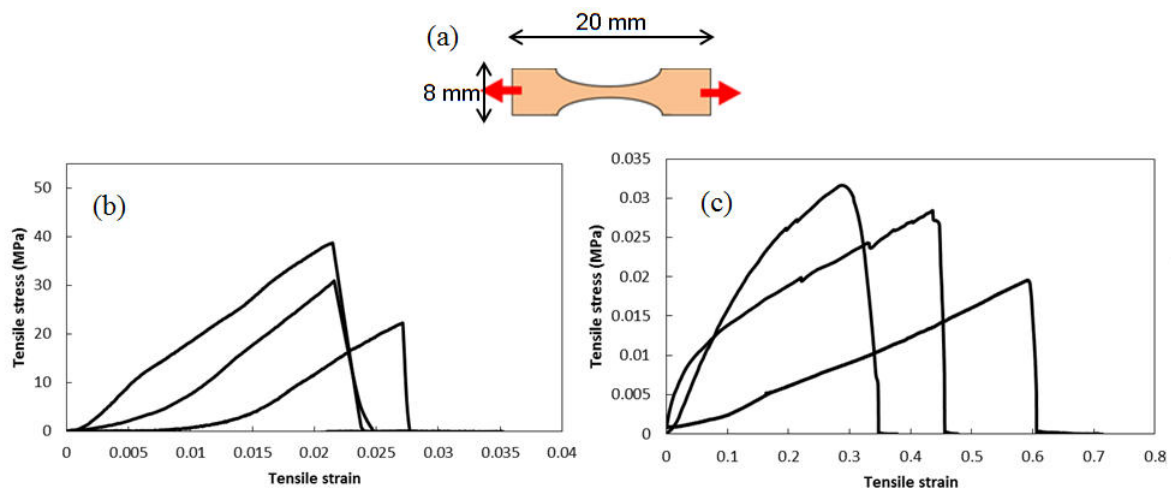


**Figure 4.1: (a) Dog bone shape obtained from a film of gelatin after laser cutting; (b) Typical stress-strain curve of dry gelatin in tension; (c) Typical stress-strain curve of hydrated gelatin in tension.**

These results suggest that hydrated gelatin could be a potential interface for multilayered bone graft material. However, since toughness is a more relevant parameter in the models described before, the next section will explore the fracture toughness of hydrated gelatin.

#### 4.1.2 Energy release rate

Fracture toughness is a material property which quantifies resistance to crack propagation. In the case of brittle materials, linear elastic fracture mechanics (LEFM) can be used and the fracture toughness ( $K_{IC}$ , in  $\text{Pa}\cdot\text{m}^{1/2}$ ) and energy release rate ( $G_{IC}$ , in  $\text{J}/\text{m}^2$ ) are related through:

$$G_{IC} = \frac{K_{IC}^2}{E} \quad (4.1)$$

Where  $E$  is the Young's modulus of the material that constitutes the sample, in Pa, or the dominant material (i.e. adherents when the fracture toughness of an adhesive is tested) [168]. This formula is valid for brittle materials such as Suprastone as it will be seen later, and ASTM empirical formulas [169] are used to compute  $K_{IC}$  and then formula (4.1) is used to compute  $G_{IC}$ . In the case of a soft and highly deformable material such as hydrated porcine gelatin, LEFM may not be valid. In that case, the energy dissipated by the material is directly computed from the area under the load ( $F$ , in N) - deflection ( $\delta$ , in m) curve of a flexural test, divided by the cross section area  $A$  in  $\text{m}^2$ :

$$G_{IC} = \frac{\int F d\delta}{A} \quad (4.2)$$

The two formulas above are valid for mode I deformation only. Figure 4.2 depicts the three different modes of fracture. In the case of mode I, the fracture toughness test mode I (double cantilever beam test, left on figure 4.2) gives mode I fracture toughness and energy release rate. In the case of interfaces, mode I (opening mode) is used to measure the toughness of adhesives using the geometry of the double cantilever beam in which the adhesive is sandwiched between two plates of known elastic properties. Multilayer materials subjected to flexure (three points bending test) present a different situation; the flexural deformation of the beam transmits a mode II deformation (sliding mode) to the interface. The energy release rate mode II  $G_{IIc}$  is hence more relevant. The measurement of this quantity requires a specific test called end notched flexure (ENF) test (middle on figure 4.2). The investigation of the properties of hydrated gelatin subjected to an ENF test is the purpose of this section.

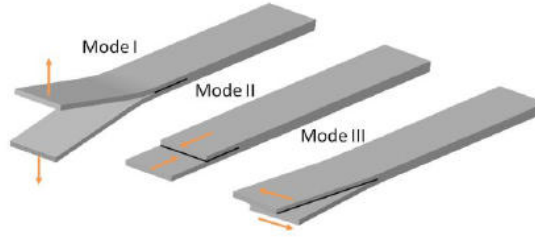


**Figure 4.2: Three different modes of fracture characterizes the failure of interfacial materials [170].**

### **1.2.1 End notched flexure test for mode II energy release rate**

As explained in the previous section, a crack can propagate only in mode II in the gelatin layer of a multilayered material. A mode II fracture toughness (also called ENF) test measurement of the gelatin is then required. The ENF test is a non-symmetrical test where the adhesive is sandwiched between two elastic beams with a pre-crack (notch) at one of the ends of the beam [171]. The configuration and geometrical parameters of the test are described on figure 4.3. In this part,  $a$  is the length of the pre-crack in m,  $L$  the pin-to-pin half-length in m,  $h$  the half thickness in m,  $b$  the width in m,  $P$  the load at failure in N and  $\delta$  the deflection of the sample at failure in m.

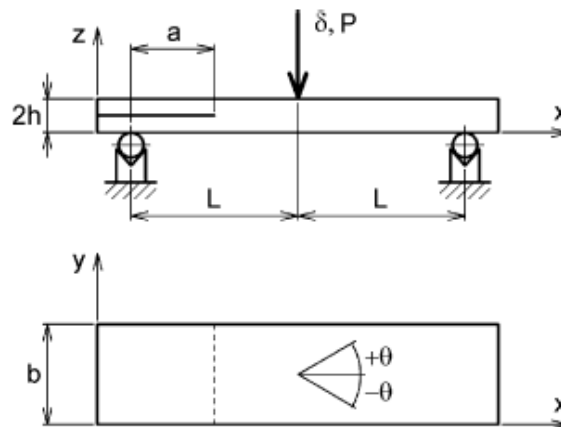


**Figure 4.3: Geometry of the ENF test which consists in a three points bending test of a beam ( $2L \times b \times 2h$ ) with a notch of length  $a$ . [171].**



Different theories are presented here to compute the energy release rate mode II of the interface. Depending on the formula considered, other properties can be used such as  $G$  (shear modulus of interface in Pa),  $E$  (Young's modulus of the mineral beams in Pa) or  $\mu$  (coefficient of friction, non-dimensional).

Morais [171] suggested a simple formula derived from beam theory for the calculation of the energy release rate mode II of the interface:

$$G_{IIc} = \frac{9a^2 P \delta}{2b(2L^2 + 3a^2)} \quad (4.3)$$

Meanwhile, the work of Both [170] revealed later that some corrections were required to take into account the effect of the “geometrical non linearities and the displacement of the load application point with reference to the delamination axis”. He thus improved the formula (4.3) with

$$G_{IIc} = \frac{9a^2 P \delta}{2b(2L^3 + 3a^2)} \frac{kF}{N} \quad (4.4)$$

by introducing three non-dimensional correction factors,  $k$ ,  $F$  and  $N$  defined as follow :

$$k = 1 + 0.2 \frac{Eh^2}{Ga^2} \quad (4.5)$$

$$F = 1 - 0.61 \left( \frac{\delta}{L} \right)^2 \quad (4.6)$$

$$N = 1 + 0.38 \left( \frac{\delta}{L} \right)^2 \quad (4.7)$$

Given that  $F$  and  $N$  were specific to the geometry of Both's samples and testing machine, Thouless [172] generalized this work: from the energy balance in the sample, he suggested that:

$$G_{IIc} = \frac{9P^2 a^2}{16Eb^2 h^3} \quad (4.8)$$

This formula is based on a simplified approach which neglects the influence of transverse shear and the influence of friction [173]. Thouless therefore augmented his model to the more general case by considering the corrected Timoshenko beam theory which led to:

$$G_{IIC} = \frac{9P^2 a^2}{16Eb^2 h^3} f_v \quad (4.9)$$

With  $f_v$  the transverse shear correction factor (non-dimensional) described as

$$f_v = 1 + 0.2 \frac{Eh^2}{Ga^2} \quad (4.10)$$

It is interesting to note that this formula is the most popular since Morais [171] also derived it and used it in his work. Moreover, it appears that the transverse shear correction factor is the same than the factor for geometrical non linearities previously calculated by Both in (4.5). To finish, in case of  $Ga^2 \gg Eh^2$ , (4.9) becomes (4.8). Carlsson et al. however reported that the factor  $f_v$  is never negligible and is often comprised between 1.05 and 1.18 [173] and demonstrated that the transverse shear must always be taken into account in the model. Carlsson et al. also extended the analysis to include friction and expressed the frictional work in order to use it in the Griffith crack growth criterion (“energy changes as the crack increases”):

$$f_v = 1 + 0.2 \frac{Eh^2}{Ga^2} - \frac{4\mu h}{3a} \quad (4.11)$$

The corrective term  $4\mu h/3a$  quantifies the effect of friction on the measure of  $G_{IIC}$ . Carlsson et al. nonetheless mentioned that this coefficient is negligible in most of the cases. Finally Thouless, through comparisons to numerical analysis of the ENF geometry, considered the following expression for the correction parameter as the most accurate:

$$f_v = (1 + 0.209 \frac{h}{a})^2 \quad (4.12)$$

The advantage of this final formula is double because even if the properties of the interface (shear modulus) are unknown, replacing equation (4.12) into equation (4.9) gives an accurate value for the energy release rate of the interface. The formula (4.9) and (4.12) will thus be used in the next sections.

### ***1.2.2 Measurements of mode II energy release rate of porcine gelatin***

Hydrated gelatin was tested using the ENF test geometry, testing protocol and analysis. The beams were made of CS type V (Suprastone) since this material was selected as the mineral

part of the composite, and the interface was made of gelatin. The thickness of the adhesive layer can have a significant impact on mechanical properties [174, 175]. We therefore tested two different thicknesses (10  $\mu\text{m}$  and 100  $\mu\text{m}$ ) of hydrated gelatin in mode II. To reach a thickness of 10  $\mu\text{m}$ , gelatin was compressed while still liquid. Sample with thickness of about 100  $\mu\text{m}$  were assembled without compression. The final thickness was then measured using optical microscopy. The two different samples are denoted as “thin” and “thick” gelatin samples in the next sections. Figure 4.4 displays the resulting energy release rates for the two different thicknesses. The value dramatically increases for smaller thickness (from 0.35 to 2.38  $\text{J/m}^2$ ), which could be due to effects of mechanical confinement of the polymer, or to a different degree of impregnation of the gelatin into the mineral substrate. According to the previous model, the energy release rate of the interface must be 4 times smaller than the energy release rate of the mineral to optimize crack deflections. The toughness of the mineral is therefore critical to select the optimum thickness for the gelatin layer.

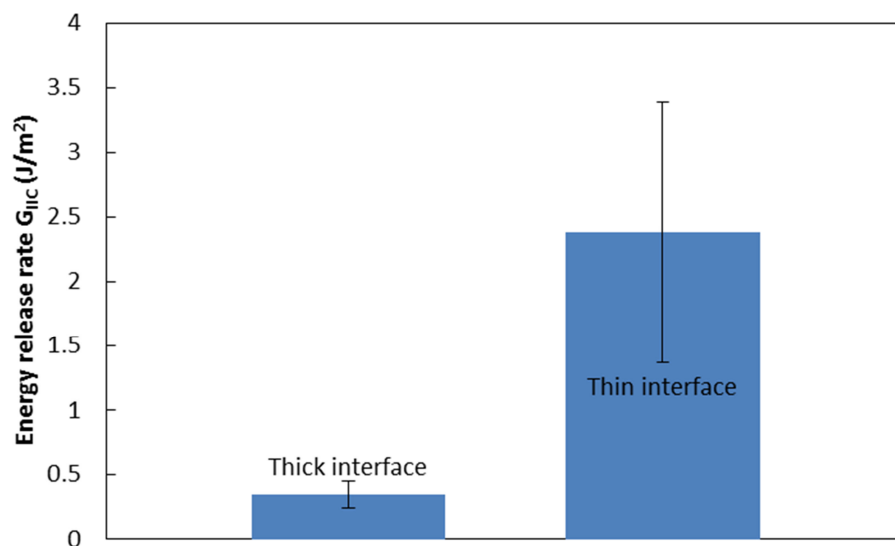


**Figure 4.4: Energy release rate in mode II of hydrated gelatin and effect of the thickness (100 and 10  $\mu\text{m}$ ).**

These values of energy release rates mode II for gelatin provide very useful guideline in what value of toughness is required for the mineral. The mechanical properties of the mineral are the topic of the next section.

## 4.2 Mechanical properties of Suprastone

The selected mineral is a CS cement type V, which is the strongest of the CS in terms of compressive strength as discussed in chapter III. The tensile and flexural strengths are more relevant for our purpose as described in chapter I. When a homogenous brittle sample is tested in flexural test, the rupture occurs at the side that is submitted to a tensile stress, and as a result tensile and flexural tests provide similar measures of strength. In this work flexural tests will be used to measure the mechanical properties of the mineral. Fracture toughness of the mineral is critical because this property governs whether cracks intersecting the interfaces will propagate through the mineral layers or be deflected. In particular, the toughness of the mineral must be maximized to promote crack deflection. In this section an optimized protocol for the fabrication of CS is presented.

### 4.2.1 Fabrication and testing protocol

The fabrication protocol was as follows: a scale was used to measure the exact amounts of powder (10 g) and water (various amounts depending on the desired ratio) and then the two products were poured together in a plastic cup. After mixing vigorously for 1 min, the paste was poured in a polycarbonate rectangular mold (25 mm x 12.5 mm x 1 mm) until complete drying (overnight). Once dried, beams (20 mm x 2 mm) were cut using a laser (Vitrolux H, Vitro, Minden, GER) which provided very accurate cutting while minimizing damage. The beams were then tested in three points bending using a miniature loading machine (Fullam Semtester, MTI instruments, Albany, NY, USA) which measured both displacement and force. Displacement (or deflection of the beam)  $D$  in m and force  $F$  in N were used to compute the flexural strain  $\epsilon$  (non-dimensional) and the flexural stress  $\sigma$  in Pa using the standard formulas [176]:

$$\epsilon = \frac{6Dd}{L^2} \quad (4.13)$$

$$\sigma = \frac{3FL}{2bd^2} \quad (4.14)$$

Where  $d$  is the thickness of the beam in m,  $b$  the width in m and  $L$  is the span for the three points bending test protocol in m (Figure 4.5). The dimensional of the mineral samples used here were  $d = 1$  mm,  $b = 2$  mm and  $L = 16$  mm. Thickness and width were measured on each

sample with a 1 micron precision. The flexural strength was the maximal point of the stress-strain curve.

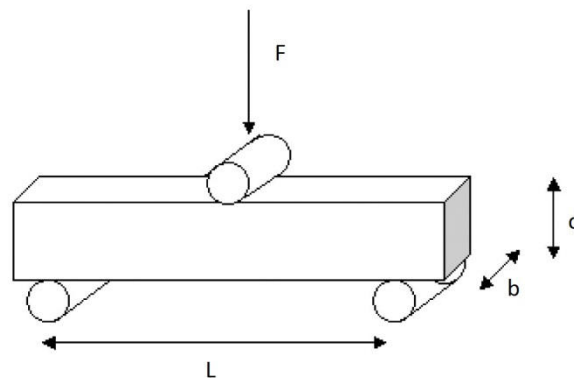


**Figure 4.5: Three points bending tests and its geometrical parameters: a force  $F$  is applied on the center of a beam (width  $b$ , thickness  $d$ ) supported by two points separated by a distance  $L$ .**

#### 4.2.2 Properties of Suprastone

This section investigates on the flexural properties of Suprastone, its toughness, and the parameters that have an influence on these properties.

##### 4.2.2.1 Effect of water – powder ratio the strength

According to the manufacturer (Kerr), the mineral powder must be mixed with water following a ratio 100 g – 19 mL. The highly purified and regular crystals of CS hemihydrate ( $\text{CaSO}_4 \cdot \frac{1}{2}\text{H}_2\text{O}$ ) then react with the molecules of water to give solid gypsum (CS dihydrate,  $\text{CaSO}_4 \cdot 2\text{H}_2\text{O}$ ). The viscous paste obtained after mixing has a work time of about 8 minutes, after which solidification starts. The recommended ratio is optimal for the original use of Suprastone, which is making imprints of teeth in dentistry. However, this protocol may not be optimal for strength, and we therefore improved and optimized the recommended preparation steps.

Several samples were prepared from 10 g of Suprastone powder, mixed with various amounts of water. Powder-water ratios of 10 g-1.5 mL, 10-1.7, 10-1.9 (recommended by the manufacturer) and 10-2.5 were tested (higher amounts of mineral could not be mixed and

molded properly). As summarized by figure 4.6, it appeared the ratio had a significant effect on the mineral properties since the best flexural strength was 2.5 times higher than the worst.

The 10-1.9 powder-water ratio recommended by the manufacturers appeared to be optimal for strength. Adding excess water resulted in added porosity and thus weaknesses once the water evaporated. Moreover, since CS dissolves in water, any excess of water dissolved the material and hence decreased its properties. In contrast, excess of powder left pockets of unreacted powder within the mineral, which weakened the material.

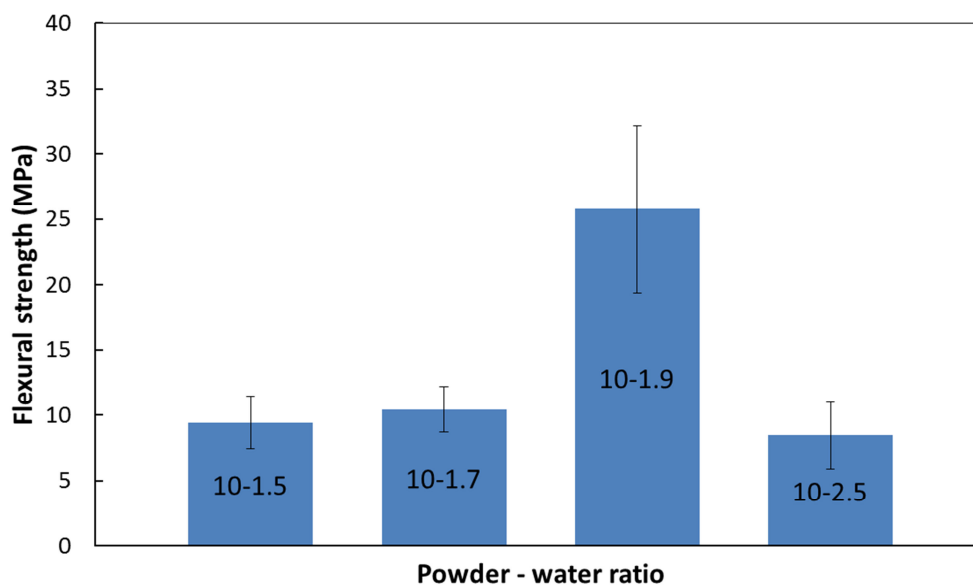


**Figure 4.6: Effect of powder – water ratio on the flexural strength of the Suprastone.**

The ratio 10-1.9 is therefore the optimal in terms of flexural strength and will be the ratio to follow in the making of the bone graft. In this part, some hypotheses have been made on the relationship between porosity and strength. Such hypotheses are the results of the scanning electron microscopy (SEM) study that takes place in the next section. In effect, not only the powder-water ratio affects the strength, but also the pressure applied during drying.

#### ***4.2.2.2 Effect of pressure on the strength***

In this section, three different protocols were tested: standard Suprastone was prepared from the optimal ratio and the polycarbonate mold. A group of samples was prepared using a doctor blading technique. This technique, notably used to manufacture thin ceramic films [177], consists in spreading the Suprastone paste with a blade. Two tapes on each side were

used as guides for the thickness. This technique is very effective to make accurate and thin films, but it requires a liquid paste to ensure smooth flow of the paste under the blade. After experimenting, it appeared that the standard 10-1.9 powder-water ratio produced a paste which was too viscous for doctor blading. A ratio of 10 g – 2.2 mL had therefore to be used for proper doctor blading. The porosity was thus higher than the porosity of standard Suprastone and the resulting strength lower than the one of standard Suprastone. Figures 4.7a and 22b compare scanning electron micrographs (SEM) taken for these two samples, showing the difference in porosity. Figure 4.7d also shows the results of density calculation made from microscale measurements and micrometer measurements (for the volume). These calculations showed that doctor bladed samples were 35 % less dense than standard Suprastone. By dividing the density of the samples by density of the dry powder, relative density was computed and gave 53.9% (porosity 46.1%) for the standard Suprastone, and 83.8% (porosity 16.2%) for doctor bladed samples which agrees with the microstructure observed on the SEM pictures. As described in the previous part, the flexural strength of the doctor bladed sample was decreased by 20% in comparison to standard Suprastone, as expected by the powder – water ratio which was not optimal.

The third type of samples called here “compressed” Suprastone exhibited different properties. For these samples, after being poured in the polycarbonate mold, the wet Suprastone paste was sandwiched between the mold and another polycarbonate plate, and compressed through a vise. The force applied by the vice was estimated to be 26.4 kN, which corresponds to a pressure of 37.7 MPa and the sample was left submitted to this pressure until complete drying. The resulting mineral was a Suprastone with a density higher by 21% (figure 4.7d) which corresponds to a relative density of 98.2% (porosity 1.8%). Figure 4.7c also confirms a very low porosity. Clearly flexural strength was better since it increased by 61% thanks to the compression of the sample during the drying as displayed by figure 4.7e.

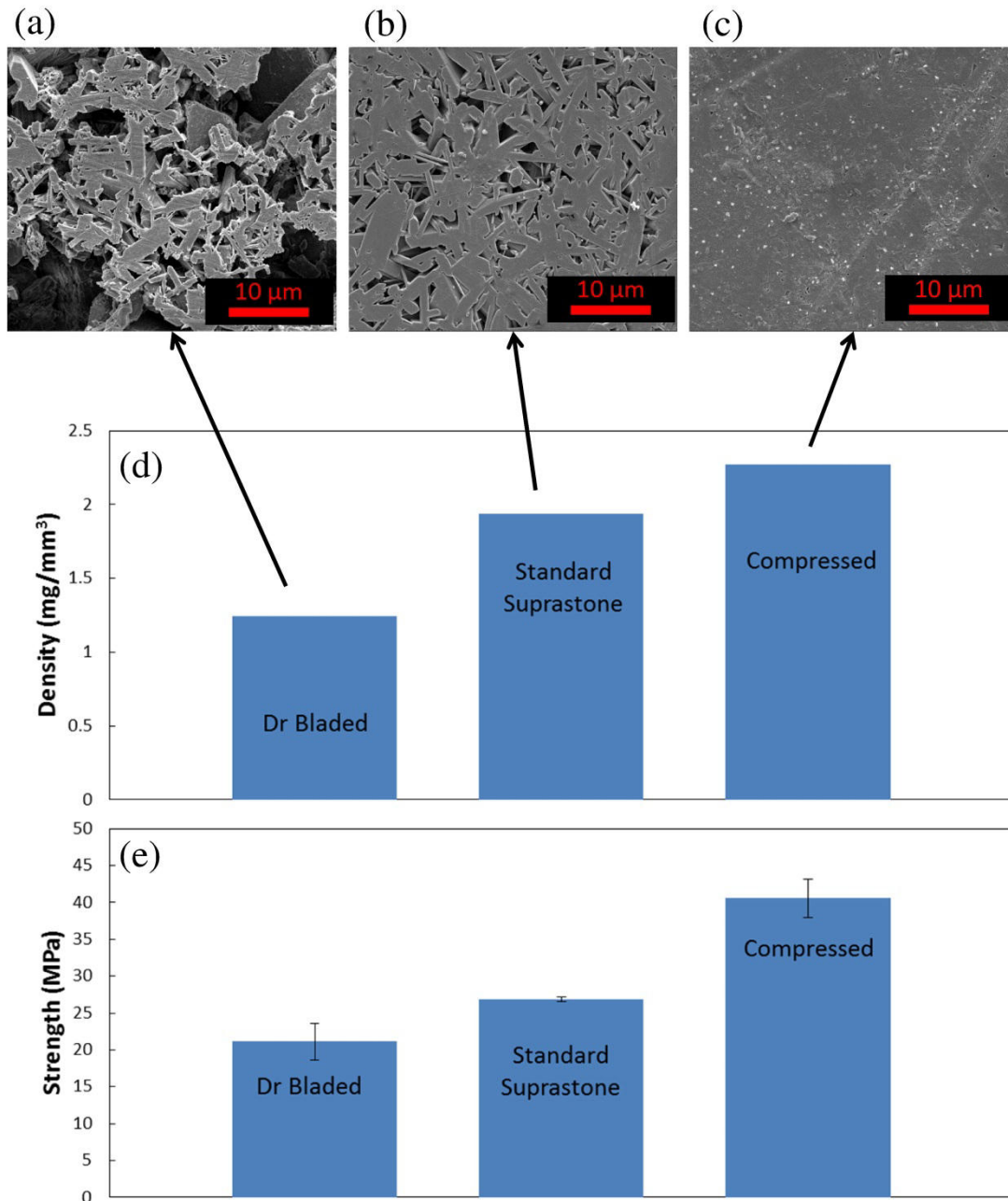


**Figure 4.7: (a) SEM view of doctor bladed Suprastone; (b) SEM view of standard Suprastone; (c) SEM view of compressed Suprastone; (d) density measured for the three different samples of Suprastone; (e) flexural strength measured for the three different samples of Suprastone.**

A simple experiment demonstrated the open porosity of Suprastone: a droplet of color dye was applied on a Suprastone plate and after seconds, the color appeared at the opposite side. This experiment revealed the open porosity of the mineral but also showed that all the surfaces of the mineral are in contact with water once the sample is submerged. The consequences of this open porosity are further discussed in the next part.



Compressing the fresh mineral paste during the setting phase is hence a method to increase the mechanical properties of the mineral, as well as adjusting the powder – water ratio helps to decrease the strength. These methods can be helpful to adjust the mineral properties and make them optimal for the multilayered bone graft.

Figure 4.8 displays the different flexural stress-strain curves obtained for the different processed Suprastone samples. All stress strain curves are characteristic of a brittle material, in other words the material is linear elastic until catastrophic failure. As previously described, the curves show that the strength increases as the density of the mineral is increased by the fabrication process. The Young's modulus is also increased when comparing the compressed mineral to the doctor bladed one.

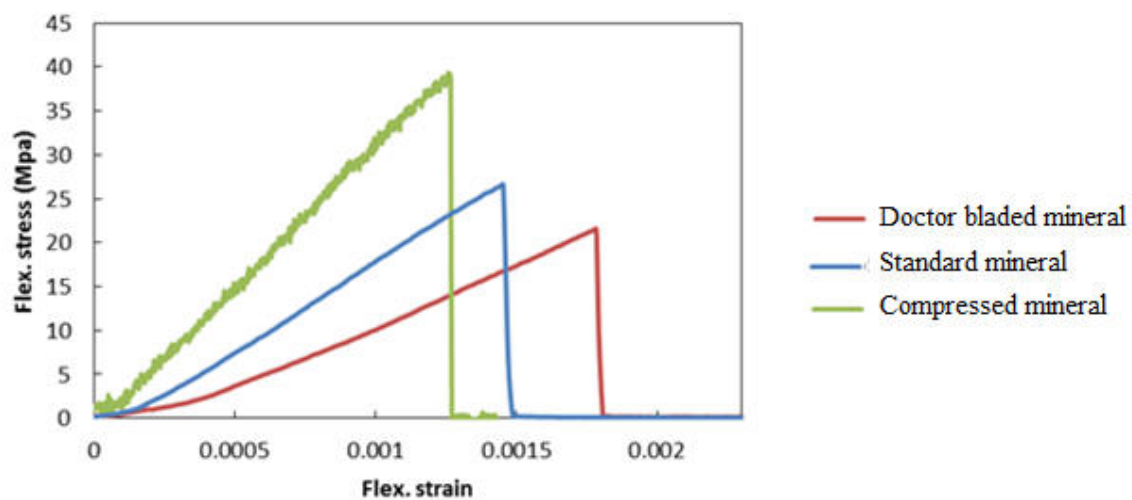


**Figure 4.8: Typical stress-strain curves for the three different processed Suprastone.**

#### ***4.2.2.3 Solubility of Suprastone in water***

In the human body, biological fluids such as blood are mainly composed of water, which can impact the properties of any material in contact with it. Biological materials that are permanently in contact with water (like nacre or bone) have better mechanical performances when hydrated. As described in previous sections in this thesis, hydrated gelatin has a completely different behavior than dry gelatin. It is also important to assess the effect of hydration on the mineral to better optimize the multilayered materials for conditions which reflect the conditions found in the human body.

CS like Suprastone dissolves overtime in water which could affect its mechanical properties. The effect of hydration is discussed in the next section. In this section, a measure of the solubility of Suprastone is presented. Solubility is a property of solid materials to dissolve in a liquid and is expressed in unit of mass of the solid per unit of mass or volume of the liquid (usually g/100 mL) [178]. If the solvent is water as it is the case for Suprastone, the solubility can be expressed in percentage. To measure the solubility of Suprastone, a rectangular sample of Suprastone was immersed in 600 mL of deionized water overnight in order to saturate the water. The sample was then removed from the water and dried. By comparing its weight after and before the immersion, it was found that 0.179 g dissolved and saturated the solution: the measured solubility was then 0.029 %.

Solid	Solubility (%)
HA	0.0014
Suprastone	0.029
Sugar	179

**Table 4.1: Solubility of Suprastone, sugar and HA at 20°C in water [178, 179].**

The solubility is a property that depends on temperature and the previous experimented was made at 20 °C. Table 4.1 compares the solubility of different solids in water at 20 °C. Sugar dissolves very fast in water and is an example of a material with a high solubility. For comparison, Suprastone is 6000 times less soluble than sugar. However, when compared to HA which is also widely used in bone graft substitutes, Suprastone is 20 times more soluble than HA. Both of these minerals are below the threshold of solids categorized as insoluble (0.1 g/100mL) [178]. HA has also a wide range of solubility constants reported in literature and all the factors affecting its solubility are still unknown [180]. This table thus shows that despite Suprastone dissolves in water, its solubility is relatively low.

#### **4.2.2.4 Effect of hydration on the strength**

Two types of samples (standard and compressed) were tested in dry and hydrated conditions. The samples were immersed in 100 mL of deionized water for 1 h. The flexural strength was then measured following the protocol previously described. Figure 4.9 shows the results for these tests: standard Suprastone exhibited a strength of 26.8 MPa while standard hydrated

Suprastone samples had a strength of only 13.3 MPa (50.4 % loss). The same experiment was repeated on compressed Suprastone sample. In that case the mineral lost only 40 % of its initial strength, dropping from 40.6 MPa to 24.1 MPa. Due to the high initial strength (thanks to the compression during mineral setting), the reduced hydrated strength was in the same range than the dry standard Suprastone. Therefore, the compression method described in the previous part successfully compensated the loss of strength provoked by hydration.

The dissolution of the mineral samples resulted in an increase of the porosity and hence a decrease of the strength. The previous section demonstrated the open porosity of the mineral, which implies that the surface area exposed to the water is larger for high porosity. This explains why the strength of the Suprastone decreases by 50.4 % immediately after being hydrated; the exchange of mineral molecules with water is more efficient and fast because of the large surface of contact. If a larger amount of water is used, larger volumes of samples can be dissolved and would result in a weaker strength. In fact samples left several days in the same amount (100 mL) of water exhibited the same loss of strength. This second result shows that the saturation of the water occurs fast and that the hydration time is not a factor.

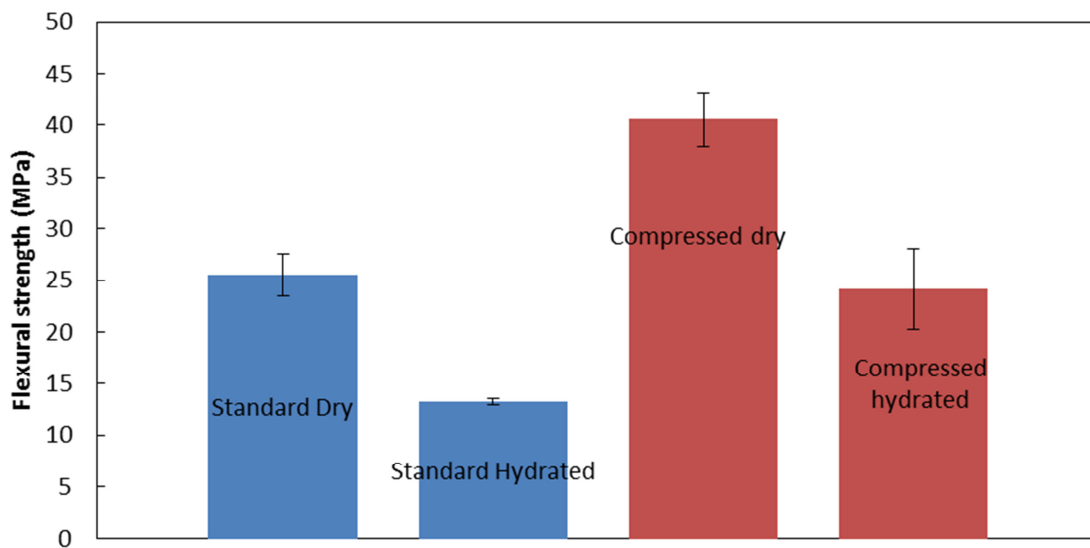


**Figure 4.9: Effect of hydration on standard and compressed Suprastone.**

There are techniques to limit the dissolution or degradation. For instance, CP is less dissoluble in water and mixing Suprastone with this mineral could help to modify its dissolution rate [181] and the presence of collagen in CS is also known to decrease the degradation rate [182]. Moreover, once implanted, the fluids around the bone graft are not renewed quickly and we

can suppose that the dissolution of the bone graft will be limited and the values presented in figure 4.9 are representative of what occurs in reality.

#### *4.2.2.5 Effect of ion content*

We previously explored a mechanical technique to increase the properties of Suprastone (compressing the fresh paste to decrease the porosity) but various studies in literature reported chemical methods that have various effects on the mechanical properties of calcium sulfate. Shen [55] showed that mixing the fresh paste with  $K_2SO_4$  improved the strength of the stone by 1 %. Better results were demonstrated with calcium and sodium lignosulfates by Combe and Smith [183] (strength improved by 30%) and then with Arabic gum, CaO and CaOH by Pietrzak [40], Ridge [184] or Sanad [56] (strength improved by 100%). The reason for these improvements is the increase of the optimal powder – water ratio: the different chemicals mixed with the CS fresh paste allowed decreasing considerably the needs in water of the CS powder for complete reaction. The resulting material was denser and thus stronger [56]. These results suggest that there are two effects of the water on the CS powder which are in competition: water reacts with the powder (reaction of solidification) and also dissolves the mineral. Hence, if the required amount of water for complete reaction with the powder is decreased, less dissolution occurs during the setting of the mineral, resulting in a stronger material. To eradicate this competing process of the water reacting and dissolving the mineral, Shen [55] replaced the water by a solution of water saturated with calcium ions and mixed it with CS powder. The saturated solution was unable to dissolve the mineral and the resulting mineral had a strength improved by 100%. Shen also mentioned that the presence of calcium ions could modify the shape and the size of the mineral crystals which could be an additional explanation for the strength improvement.

In this section, we repeated the experiment described by Shen and saturated 500 mL of water with calcium ions by introducing 10 g of solidified Suprastone thus following the protocol described by Shen. The solution was then left several days and was mixed with Suprastone powder to prepare samples. Samples were prepared in a mold compressed, then tested in hydrated conditions and compared with hydrated Suprastone samples compressed during the setting but prepared from pure water. Figure 4.10 shows the results of the two types of samples. The flexural strength of the compressed Suprastone was improved from 24.13 MPa

to 37.83 MPa which represents an improvement of 56.8 %. This last result demonstrated that chemical and mechanical techniques can significantly increase the strength of hydrated CS.

The properties of pure Suprastone are therefore influenced by four parameters: powder – water ratio and hydration that reduces the strength; compression and ion content that have the opposite effect.

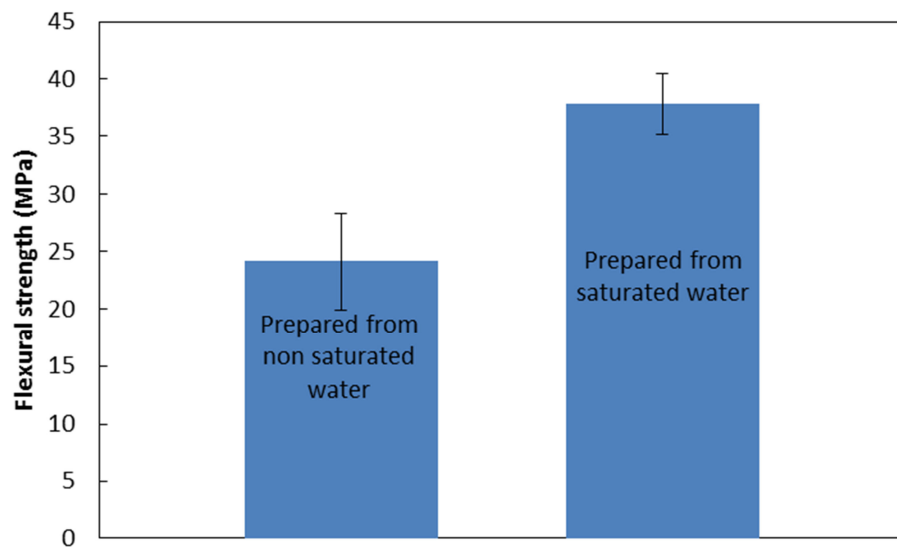


**Figure 4.10: Effect of calcium ion content on compressed Suprastone.**

#### **4.2.2.6 Fracture toughness of Suprastone**

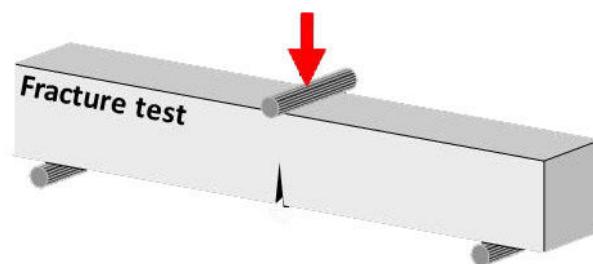


**Figure 4.11: Mode I fracture toughness testing for a 20 mm Suprastone beam.**

As mentioned for the case of gelatin, fracture toughness is a measure of resistance to crack propagation. Brittle materials have low fracture toughness and cracks in brittle materials tend to be unstable. In contrast, deformable materials tend to have more stable cracks and higher

fracture toughness. Because of the brittle behavior of the mineral, low fracture toughness is expected.

In the case of the gelatin, it was explained that the material was submitted to mode II crack propagation. In the case of the mineral, the crack propagates perpendicular to the layer of Suprastone, in mode I. Therefore, mode I fracture toughness tests were performed on Suprastone beams as described on figure 4.11. As the figure shows, the difference with the three points bending test is that an initial notch was added by laser cutting. According to American Society for Testing and Material (ASTM) standards [169], the notch must be between 45 and 55 % of the thickness of the beam. Knowing the size of the initial crack  $a$  in m, the geometry of the sample (width  $W$  in m and thickness  $t$  in m) and the force  $F$  in N required to break the sample, various theories allow to compute the mode I toughness  $K_{IC}$  [168] in  $\text{Pa}\cdot\text{m}^{1/2}$  but the most suitable is the formula given by the ASTM E1290-08 [169]:

$$K_{IC} = \frac{6F}{Wt} \sqrt{a} f\left(\frac{a}{t}\right) \quad (4.15)$$

Where  $f$  is an empirically determined parameter (non-dimensional) which can be expressed in function of  $a$  and  $t$  only:

$$f\left(\frac{a}{t}\right) = \frac{1.99 - \frac{a}{t}(1 - \frac{a}{t})(2.15 - 3.93\frac{a}{t} + 2.7(\frac{a}{t})^2)}{\left(1 + 2\frac{a}{t}\right)\left(1 - \frac{a}{t}\right)^{\frac{3}{2}}} \quad (4.16)$$

Samples were prepared with precise laser cutting (including initial notch). Optical microscopy on the broken samples was used to measure the length of the initial notch accurately.

Figure 4.12 compares the results for these two types of sample. Dry standard Suprastone showed a toughness of  $72 \text{ KPa}\cdot\text{m}^{1/2}$  while the toughness of hydrated Suprastone was 46 % lower. For comparison, the fracture toughness of concrete was displayed on the same plot ( $200 \text{ KPa}\cdot\text{m}^{1/2}$ ). Concrete is a material widely used in building construction and is a good example of a common material with low fracture toughness. Fracture toughness of concrete is 2.7 times higher than the one of Suprastone which means that it is 2.7 times easier for a crack to propagate in Suprastone than in concrete. This result on the toughness is important according to the criterion for crack deflection described in the previous chapter (the toughness of gelatin must be less than 25 % than the toughness of the mineral to optimize crack deflection).

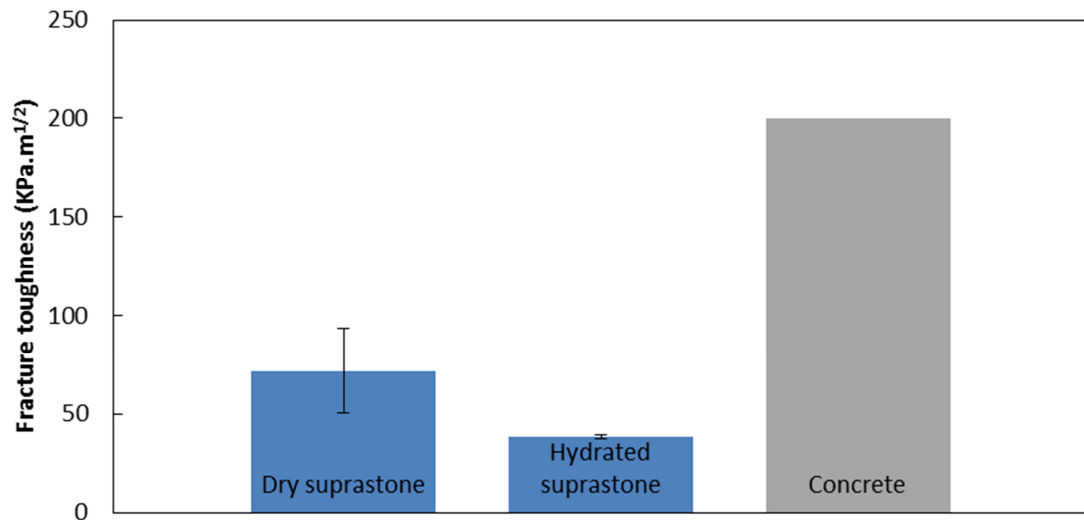


**Figure 4.12: Effect of hydration on the fracture toughness of Suprastone and comparison with concrete.**

This section concludes the study of the mechanical properties of Suprastone and gelatin. As expected, gelatin and Suprastone are dissimilar materials in terms of properties. On one side Suprastone is a hard and brittle mineral, and on the other side, gelatin is deformable with very low strength and modulus. This fact is critical and the next step is to assemble these two materials into a multilayered composite which requires certain techniques.

## 5. Chapter V: The Multilayered Bone Graft

Multilayered materials represent an architecture that is more efficient in term of energy than monolithic materials, and increases the mechanical performances. The previous sections of this thesis described that CS type V (Suprastone) and porcine gelatin are two potential components for a multilayered bone graft. The next step was to assemble them following the architecture of multilayered materials. In this chapter, a precise description of the fabrication protocol will be presented, as well as the mechanical results of the created bone graft.

### 5.1 Samples preparation and geometry of the bone graft

The fabrication protocol of the multilayered bone graft used the protocols developed for the preparation of gelatin samples and Suprastone samples. They take advantage from the fact that gelatin can go from its dry form to a gel when hydrated, and to a low viscosity fluid if heated at 70 °C and from the fact that these states are reversible. Concerning the geometry of the sample, only one constrain was presented in chapter II section 2.4 through the formula:

$$\delta_m = \frac{6E_c G_{IIc}}{\sigma_c^2} \quad (5.1)$$

Where  $\delta_m$  is the critical thickness of the interface in m (gelatin),  $E_c$  is the Young's modulus of the mineral in Pa,  $\sigma_c$  its strength in Pa and  $G_{IIc}$  the interfacial critical strain energy release rate in J.m<sup>-2</sup>. In the multilayered gelatin – Suprastone material, the thickness of the interface must be less than  $\delta_m$  in order to optimize the performances of the multilayered material. Applied to our case with the experimentally calculated values, it appears that the maximal thickness is 147 μm which will therefore be the upper limit in the multilayered bone graft. However, Nature teaches us that the smaller the interface the better the performances. Smaller interfaces allows reducing the volume fraction of interface, and increasing the fraction of the material that contributes the most to the strength and the modulus; for instance nacre from seashells contains a volume fraction of only 5 % polymeric materials [70]. Clegg [72] and Kovar [76] showed that the higher the number of layer, the more the deflection and the higher the energy dissipated. Thus a particular attention was made during the fabrication to get the thinnest possible mineral layers, in order to get as many bilayers of gelatin – mineral through a given thickness of 1-2 mm. The thickness of the interface had then to be even lower so that a low volume fraction of gelatin is preserved. Following these guidelines, a thickness of 200 μm



was achieved for the mineral. Thinner mineral layers could not be achieved without breaking them during their manipulation. Concerning the thickness of the gelatin layers, the target was around 50  $\mu\text{m}$  which below the upper limit of 147  $\mu\text{m}$  previously calculated. The next section will show that crack deflection is better at this thickness which is the thickness of the “thick” gelatin samples tested in ENF. Then the thickness of the composite material was determined by the number of bilayers (5-8 bilayers). For the rest of the geometry, laser cutting was used to get the same length and width than the previous samples of pure mineral.

Figure 5.1 shows the fabrication steps for the multilayered bone graft material. First, a thin layer of mineral was obtained by doctor blading a mineral paste in a polycarbonate mold (figure 5.1a). The thickness of the guides for the doctor blade was decreased to 0.5 mm (instead of 1 mm as for pure mineral samples) to reach the targeted thickness for the mineral layer. After the compressing step, the fresh mineral paste with a thickness of 0.5 mm became a solid mineral layer of approximately 200  $\mu\text{m}$ . The mineral layer was compressed using a high capacity vise during this step (figure 5.1b). This process was also highly efficient at making the density (and strength) higher. After 12 h of drying a layer of liquid gelatin was doctor bladed on the top surface of the mineral layer. This liquid gelatin was prepared from gelatin powder that has been hydrated and heated at 70 °C. The bilayer was then dried for another 12 h (figure 5.1c). The next step was to release the bilayer (figure 5.1d) and to cut it in 5 to 8 squares of equal size (3 cm by 3 cm). At this point, the gelatin was dry and the cutting was easy with scissors. Then the squares were superposed together and hydrated to turn the gelatin into a sticky gel. The sample was then placed onto a polycarbonate substrate and heated on a hot plate (70 °C) in order to melt the gelatin and finish the bonding of the different layers (figure 5.1e). At this point, the thickness of the gelatin was controlled by adding pressure on the sample (figure 5.1f). The order of magnitude for this pressure was not *MPa* as for the mineral but *KPa* in order to avoid damaging the mineral layers. Various pressures from 100 to 2000 KPa were tested; the multilayered samples that exhibited the best crack deflection were those prepared with a pressure of 800 KPa at the step (f). 800 KPa optimized the mechanical performances and was then called the optimal pressure; it was also the pressure that allowed reaching the desired thickness of interface stated in the previous paragraph. This pressure was a perfect compromise between reducing the thickness of the gelatin layer sufficiently to make a strong sample, but not too much since too thin gelatin layer does not allow crack deflection as it will be seen later. The pressure was applied while the gelatin was heated at 70 °C and still liquid, and the temperature then decreased to room

temperature in order to let the gelatin solidify. As a final step, the sample dried for 12 h in order to be cut with the laser (figure 5.1g). The cut beams were then re-hydrated for 1 h prior to be tested while respecting the hydrated conditions.

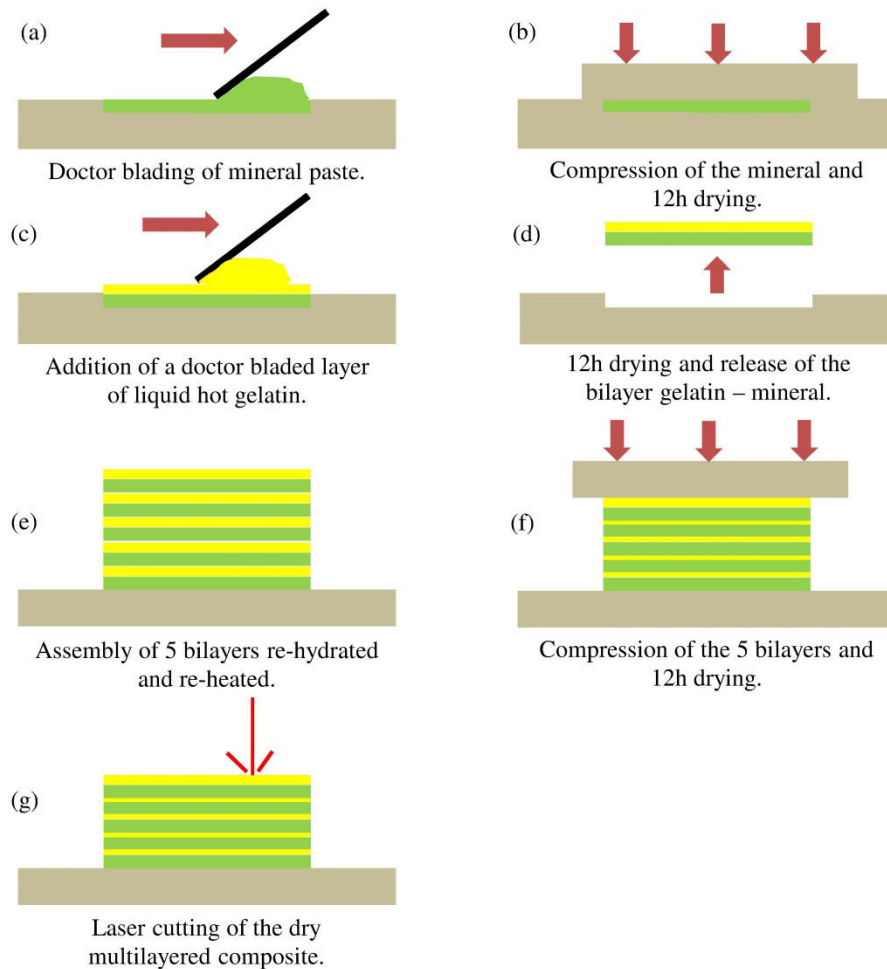


**Figure 5.1: Fabrication steps of the multilayered samples.**

Figure 5.2 shows two images of the final multilayered samples obtained (optical microscopy). The different components are clearly visible (gelatin in white, Suprastone in grey) or figure 5.2a where the material is dry. These pictures also show that the final thickness of the mineral is 200-300  $\mu\text{m}$ . The thickness of the mineral did not change during hydration of the sample, but gelatin multiplied its volume by ten after hydration. The thickness of the interface was then ten times smaller on dry samples than on hydrated samples. On figure 5.2a, the sample was imaged directly after cutting and while it is still dry to maximize image quality. After

hydration, the “holes” or “air bubbles” between the mineral layers were filled by the gelatin that multiplied its volume by ten and became transparent as shown on figure 5.2b.

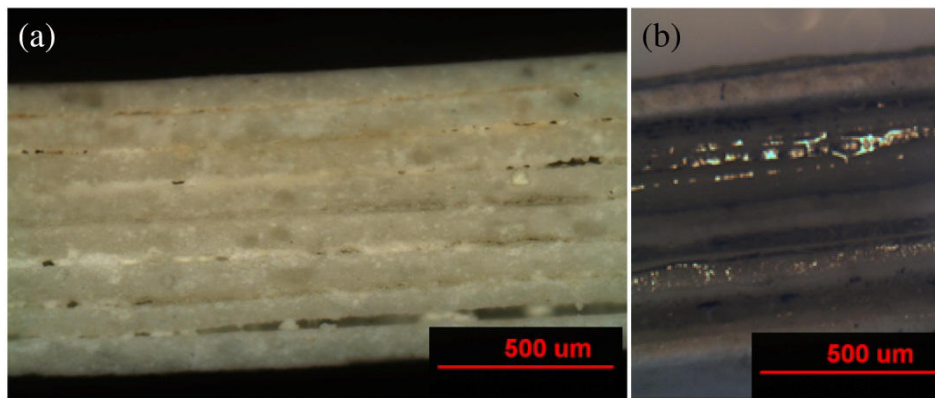


**Figure 5.2: Two optical microscopic views of: (a) dry multilayered sample; (b) hydrated multilayered sample.**

The samples were re-hydrated and tested to assess whether their mechanical performances were equivalent to those described in studies on multilayered materials [72, 73, 76]. The results are presented in the next sections.

## **5.2 Crack deflection in a multilayered sample**

Crack deflection is critical in multilayered material in order to increase toughness. This phenomenon is dominated by two parameters, the fracture toughness mode II of gelatin, and the fracture toughness mode I of Suprastone, and more precisely by the ratio of these toughnesses. The purpose of this section is to establish whether the criterion for optimal crack deflection is reached and to explore how the thickness of the interface affects the crack deflection.

### **5.2.1 Crack deflection in the case of calcium sulfate and gelatin**

A simple criterion for optimal crack deflection was described in chapter II section 2.3. This criterion was expressed in formula (2.1) and took into account the fracture toughnesses of the interface of the mineral. In chapter IV, section 4.1.2, it was explained that the crack

propagates in mode II in the interface, and in mode I in the mineral. Using the fracture toughness mode II of the gelatin  $K_{IIC}^{gel}$  in  $\text{Pa.m}^{1/2}$  and fracture toughness mode I of Suprastone  $K_{IC}^{sup}$  in  $\text{Pa.m}^{1/2}$ , (2.1) becomes:

$$K_{IIC}^{gel} < \frac{1}{4} K_{IC}^{sup} \quad (5.2)$$

Then, equation (4.1) seen in chapter IV, section 4.1.2 links energy release rate and fracture toughness. Formula (4.1) injected in (5.2) gives:

$$G_{IIC}^{gel} < \frac{1}{16} G_{IC}^{sup} \quad (5.3)$$

Where  $G_{IIC}^{gel}$  is the energy release rate mode II of the gelatin in  $\text{J.m}^{-2}$ , and  $G_{IC}^{sup}$  is the energy release rate mode I of Suprastone in  $\text{J.m}^{-2}$ . Formulas (5.2) and (5.3) are hence the same criterion for crack deflection expressed in terms of fracture toughness or in terms of energy release rate. Both of the criteria can be applied to the case of the gelatin – Suprastone multilayer.

Using formula (4.1) requires measuring the Young's modulus of the mineral. This measurement was made during the flexural testing of Suprastone and gave 14.73 GPa for the modulus of the hydrated Suprastone. Therefore the fracture toughness of the hydrated gelatin was computed from the energy release rate previously presented in chapter IV, section 4.1.2, where two different gelatin thicknesses were explored giving two different toughnesses. The energy release rate was higher for the “thin” gelatin (10  $\mu\text{m}$ ) layer than for the “thick” one (100  $\mu\text{m}$ ). Figure 5.3 summarizes the results of fracture toughnesses of hydrated Suprastone and thick and thin gelatin. A first observation is that the criterion of formula (5.2) is not reached, which means that the crack deflection was not optimal. The fracture toughnesses of thick or thin gelatin were higher than 25 % of the fracture toughness of the mineral. In any cases of interface thickness, the crack deflection should not be optimal according to the model. However thick gelatin exhibited a toughness closer to the optimal value than thin gelatin. More crack deflection is thus supposed to occur in a multilayer with thick interfaces. The purpose of the next section is to experimentally verify this hypothesis.

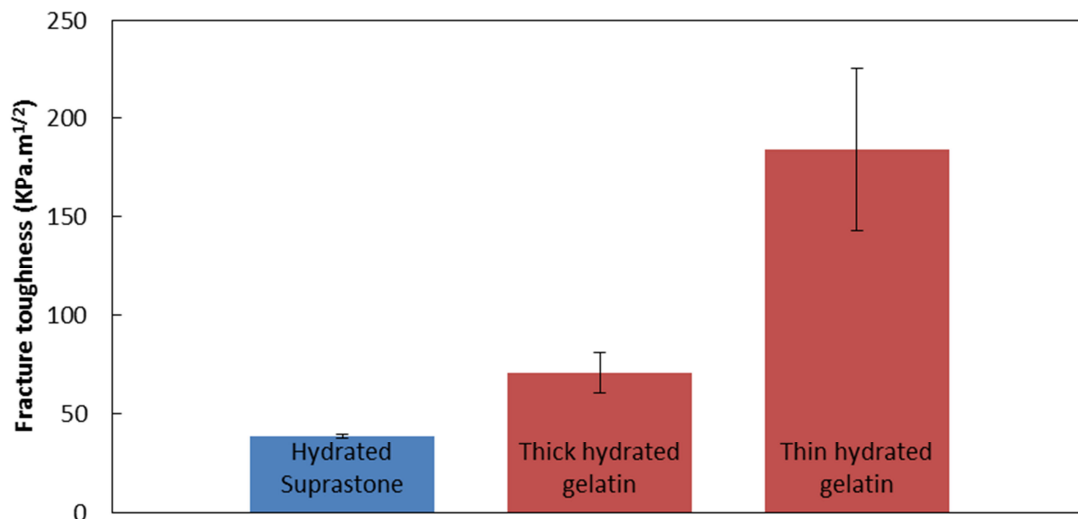


**Figure 5.3: Comparison of the fracture toughnesses of Suprastone and gelatin for two different thicknesses.**

### 5.2.2 Crack deflection observations

Two types of multilayered samples were prepared; one with “thick” gelatin layers (50  $\mu\text{m}$ ) and another one with “thin” gelatin layers (10  $\mu\text{m}$ ). “Thick” gelatin layers were achieved by applying the optimal pressure during the fabrication steps (800 KPa, see section 5.1 of this chapter). “Thin” gelatin layers were achieved by applying 2000 KPa during the fabrication steps. These two types of samples were fractured in three points bending test before imaging.

Optical microscopy observations were made on the fracture regions of the samples and are shown on figure 5.4. These observations revealed that multilayered samples made of thin gelatin (figure 5.4a) were able to deflect the propagating crack to a much lesser extent than the multilayered samples made of thick gelatin (figure 5.4b).

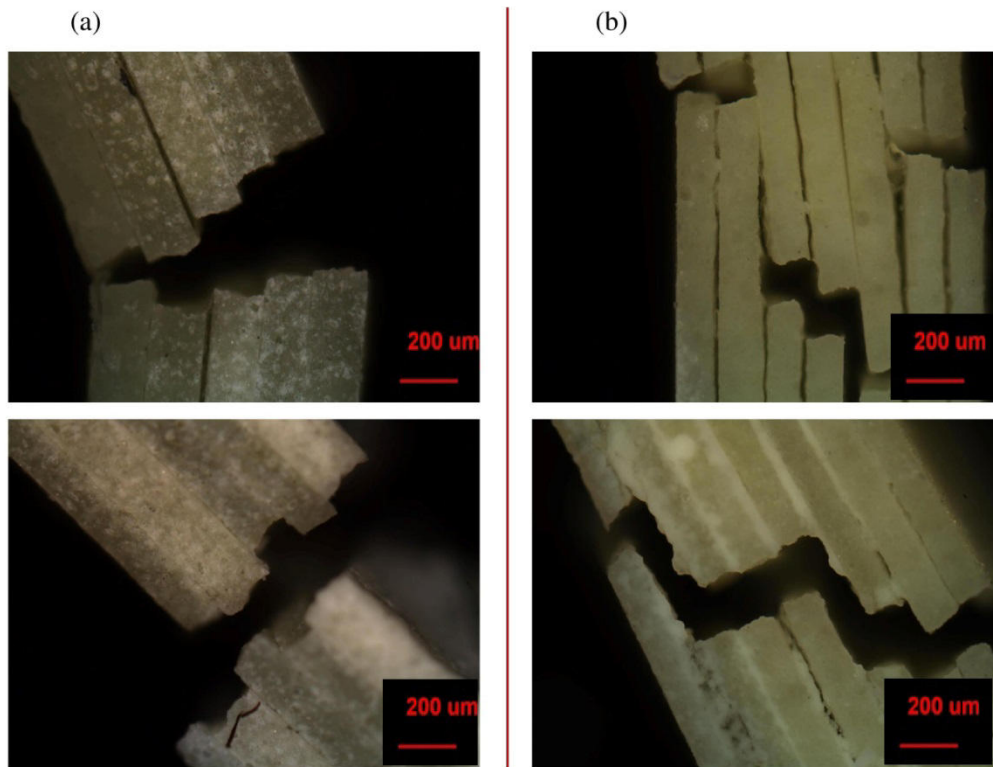


**Figure 5.4: (a) Microscopy of the failure of the thin gelatin multilayered samples; (b) microscopy of the failure of the thick gelatin multilayered samples.**

These pictures combined with figure 5.4 of the previous section confirm that the lower the fracture toughness of the interface, the better the crack deflection. Therefore, even if the toughness of gelatin was not optimized (formula (5.2) is not verified), significantly different behaviors are observed depending on the toughness of the interface. According to previous studies [72-74, 76], the samples with more deflected cracks should dissipate more energy. This hypothesis will be verified in the analysis of the mechanical performances of the next sections.

### 5.2.3 Stress – strain curves

Flexural stress and strain were computed using formulas (4.13) and (4.14). Figure 5.5 is the stress- strain curve of a sample with thick gelatin interfaces. In this type of samples, the most crack deflections were observed.

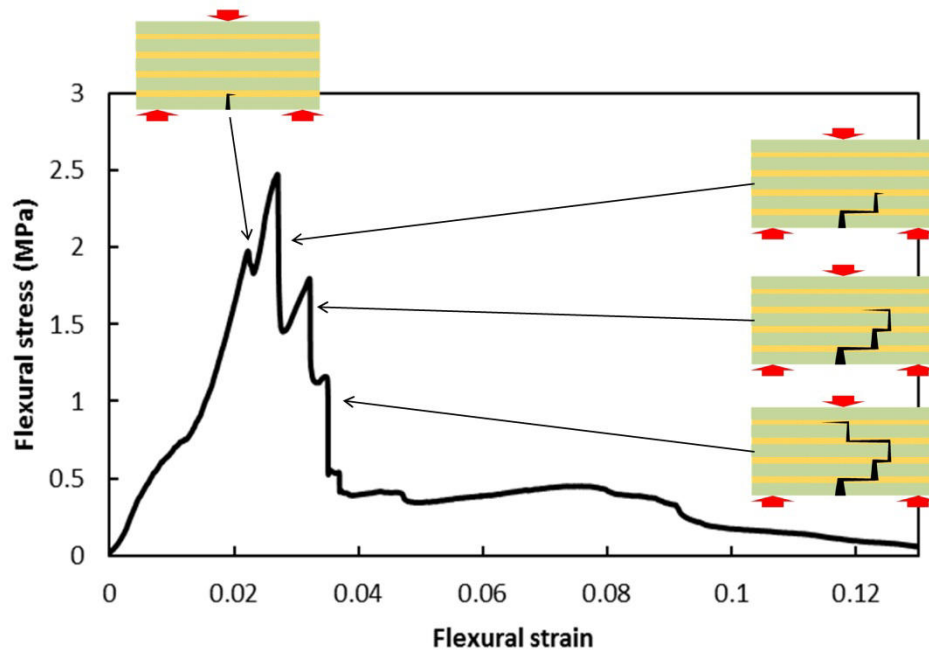


**Figure 5.5: Stress – strain curve of a multilayered gelatin – Suprastone composite.**

The first part of the curve exhibited a linear elastic behavior, as expected by the elasticity of the components. Brittle failure occurred at around 2.0 % of strain but was not catastrophic, since the stress reached a small plateau. The sudden drop of stress which followed corresponds to the failure of the first mineral layer located at the opposite side of the contact with the pin of the testing machine. The new load increasing (or plateau in some cases) corresponds to the propagation of the crack through the interfacial gelatin. Then, three successive non-catastrophic failures and small load increases (or plateaus) occurred which correspond to the successive breaks of the mineral outer layers that supported more stress at each failure step, and thus broke faster. Finally, even if the strength is between those of the mineral and the gelatin, the overall strain is much higher than for the brittle mineral because of these successive failures. Since the energy absorbed by the material is a product of the strength and the strain, the composite dissipates much more energy as discussed in the next sections.

### 5.3 Flexural strength results

Multilayered samples with thick gelatin interface were tested and the strength of the material was measured. The previous results showed that samples with thick gelatin interface

improved crack deflection. When compared to a multilayer with thin interfaces, the energy dissipated in a multilayer with thick interfaces should be improved while the strength should be decreased because of the higher volume fraction of gelatin. The choice of thick interfaces is justified by the goal of this study which is the optimization of the energy absorption of the new bone graft material as stated in chapter I. The protocol to prepare these samples is described in section 5.1 of this chapter. The geometry of the multilayered samples was the same than the pure Suprastone samples which made the comparison between the multilayered samples and the pure Suprastone samples straightforward and easy. The results are reported on figure 5.6. The tensile strength of pure gelatin is also displayed for a complete comparison. All these results were performed on hydrated samples to simulate the contact with body fluids.

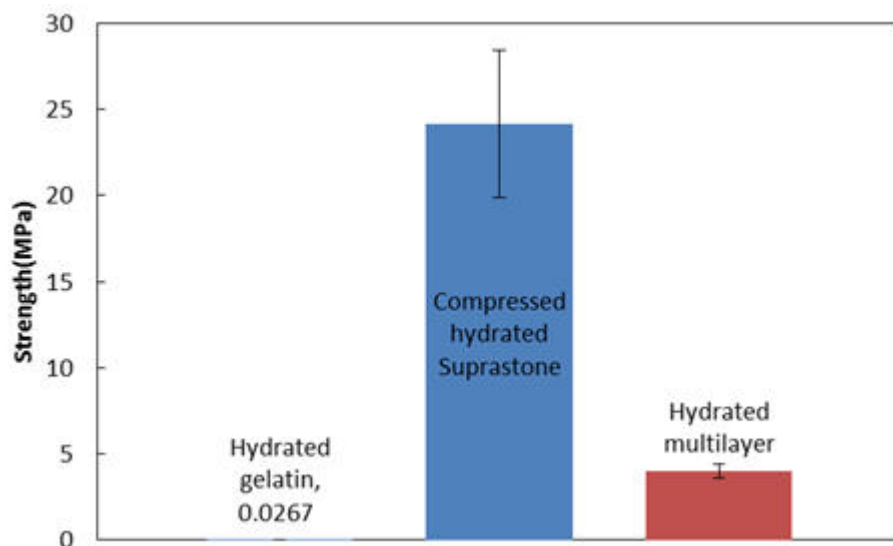


**Figure 5.6: Flexural strength of the multilayered gelatin – Suprastone composite, compared to the flexural strength of pure compressed Suprastone, and tensile strength of pure gelatin, in hydrated conditions.**

Figure 5.6 shows that the strength of the multilayered sample falls between the strength of Suprastone and gelatin. While the weakness of the gelatin is efficient to deflect cracks, it also limits the strength of the material. In the final chapter (Chapter VI, Conclusion), some strategies to increase the strength are discussed and could be used in a future work. The next section investigates the mechanical performance of the multilayered bone graft in terms of energy and fracture toughness.



#### 5.4 Toughness and energy results

The same fabrication protocol was followed for the fracture toughness testing of the multilayered samples. The same type of multilayered samples were fabricated, this time with an initial notch on the middle made with laser cutting, and then the samples were tested in flexure (three points bending test). All the results here are for samples in hydrated conditions. The toughness was then computed following the ASTM formula described in section 4.2.2.6 of chapter IV, and the results are displayed in figure 5.7a and compared to the toughness of gelatin and Suprastone. The computed fracture toughness was lower than the fracture toughness of its components. This result means that a crack, once it appears, has less difficulty to propagate in the multilayered composite than in pure gelatin or pure Suprastone. However, the crack is deflected more in the composite and its path is thus longer which has consequences in terms of energy. Moreover the composite is less stiff than Suprastone, but stiffer than gelatin. Thus, a bit of energy is dissipated during crack propagation, but large amounts of energy are also dissipated before the crack appears. This phenomenon was not taken into account in the fracture toughness measurement, but it can be seen in terms of energy.

The energy dissipated by the composite is showed on figure 5.7b and compared to the energy dissipated by the mineral and the gelatin. This time, the energy dissipated clearly showed that for a given area, the multilayered sample is much more efficient. It was able to dissipate  $6.09 \text{ J.m}^{-2}$  which represents 60 times more energy per unit area than the energy dissipated by the mineral, and  $17.10^6$  times more energy than the gelatin can dissipate. Such mechanical performance in terms of energy was expected from the stress-strain curve presented in the last section. Energy is a product of the strength and the strain. The strain at failure of the composite is lower than the strain at failure of gelatin, but the strength is much higher. The strength of the composite is lower than the strength of the mineral, but the strain is much higher. Finally, in terms of energy, the composite is much more efficient than the pure gelatin or the pure mineral. Crack deflection is consequently an efficient and powerful toughening mechanism, and the rule of mixture does not apply here since a multilayered material can dissipated much more energy than its components alone.

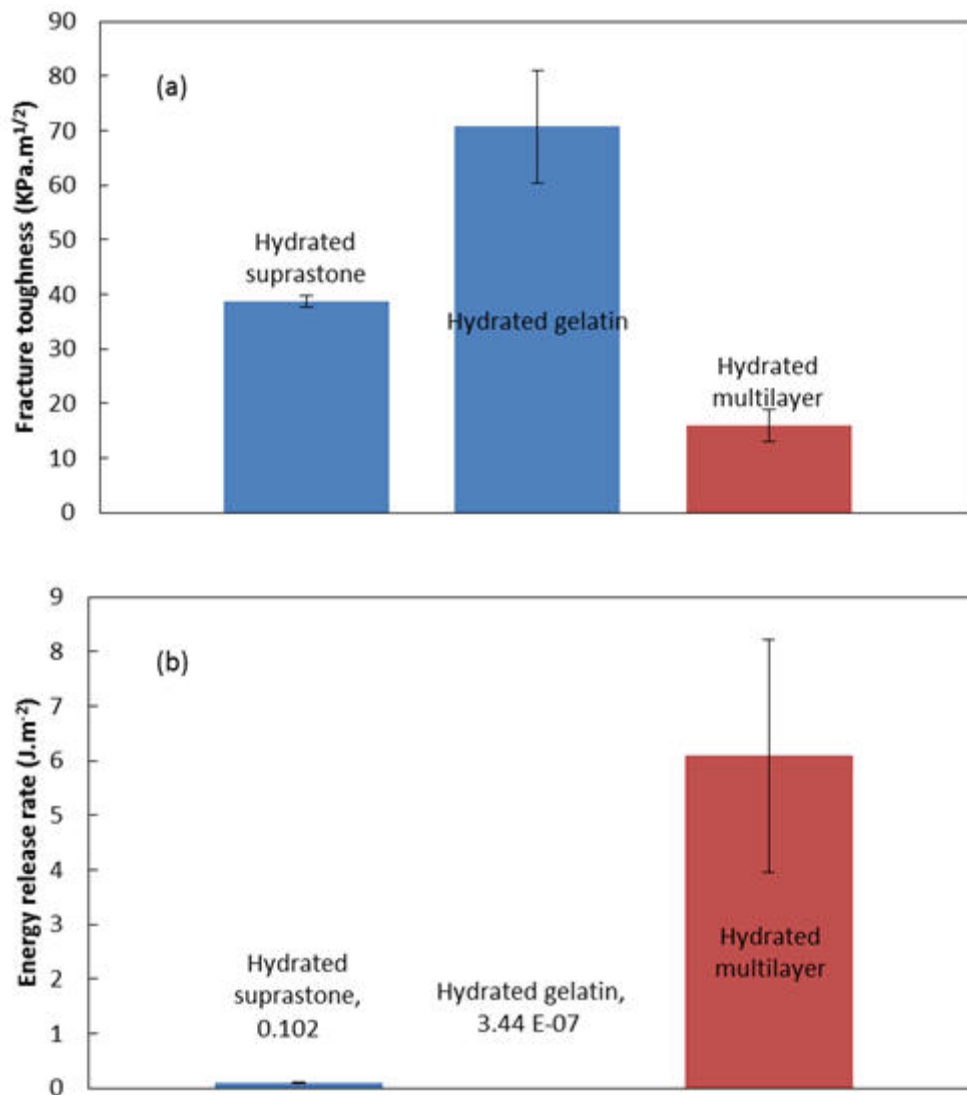


**Figure 5.7: (a) Fracture toughness of the multilayered gelatin – Suprastone composite, compared to the fracture toughness of pure Suprastone, and fracture toughness of pure gelatin, in hydrated conditions; (b) energy release rate of the multilayered gelatin – Suprastone composite, compared to the energy release rate of pure Suprastone, and energy release rate of pure gelatin, in hydrated conditions.**

These results demonstrate that some of the results seen in the literature for engineering ceramics can be repeated using materials suitable for bone graft and biomedical purposes. Many parameters are still far from the performances of bones, such as strength, but the present study focused on the most important mechanical parameter which is the dissipated energy, as well as the fabrication methods which have important impacts on the energy.

Figure 5.7b shows promising preliminary results for such materials, structure, and fabrication techniques, and might make multilayered gelatin – CS samples as the future of bone graft materials.

## **6. Chapter VI: Conclusion**

Many improvements can be done thanks to recent technologies. Doctor blading machines can help to produce multilayered bone grafts at a larger scale, or 3D printing machines can produce complex molds to develop bone grafts to implant in a specific region of the body. Then the bone graft itself can be improved. It was demonstrated in this report that it is not only the performances of the interfacial gelatin, but also those of the mineral that have to be enhanced to maximize the overall performance of the composite. More especially the fracture toughness of the mineral must be higher for better behavior, and strategies exist for such purpose.

It was the first time that a multilayered structure was used to create a bone graft material, and it is important to highlight what major contributions were brought in this project.

### **6.1 Accomplishments**

#### **6.1.1 An efficient design in terms of energy**

In the first chapter, it was explained how important the energy dissipated is for a biological material. In Nature, materials are submitted to various types of impacts and deformations, and a material with a high strength but that is brittle is not reliable. Likewise, a material that can deform a lot but with a low strength is not attractive as a skeletal material. Fracture toughness and energy absorption are two key properties which should be optimized in the ideal bone graft material. Energy absorption is roughly the product of deformation and strength. More specifically, a bone that is submitted to an impact must dissipate the energy of the shock without breaking to be efficient. The main goal was thus to design a structure which is efficient in terms of energy. In this perspective, the behavior of the composite was successful: even if the material was weaker than monolithic calcium sulfate, it demonstrated its capability to dissipate energy several orders of magnitude higher than its components. Moreover, in order to fulfill the requirements of a bone graft material, the composite was made of biocompatible, osteoconductive and biodegradable components hence the importance of their selection. The biocompatibility, degradability and osteoconductivity of the composite has however to be tested since the properties of the constituents is not sufficient to ensure the properties of the composite.

In this work we have developed multilayered materials as a possible answer to this challenge. Previous studies showed that multilayered ceramics can dissipate 160 times more energy than monolithic ceramics. Multilayered structures can be found everywhere in Nature: nacre is made of mineral micro-tablets embedded in an organic network or the bones themselves can be seen as a multilayered structure when looking at the structure of an osteon.

A critical aspect of multilayered materials is to manage the fracture toughness of the different layers: the toughness of the mineral must be four times higher than the toughness of the interface to optimize the crack deflection, complicate and make longer the crack propagation and thus absorb energy. The multilayered bone graft was not optimized for crack deflection, but this guideline helped to increase the crack deflection in the multilayered material. In the best material produced in this project, crack deflection is evident and energy dissipation is 60 times higher than in the pure mineral and six orders of magnitude higher than in gelatin. The multilayered structure thus successfully reproduced the observations done in other types of engineering ceramics [72-74, 76, 78]. The theory of multilayered ceramics also predicts that if the toughness of the mineral is increased again, more deflection could occur and more energy could be dissipated. Previous studies were able to dissipate much more energy than in this work [72] meaning that the current bone graft is not completely optimized and can be improved. The perspective of an improved bone graft demonstrates the interest that may grow in future designs for bone graft materials. In this point of view, the present multilayered bone graft represents a very encouraging result.

### **6.1.2 A bone graft at reduced cost**

One of the requirements when choosing the components of the bone graft material was the cost. Some costs will be related to the use of machines used to create the material, and some costs will be related to the expertise of the people manipulating the material. It was an objective to develop a material which is affordable. Being accessible to everybody and not only a class of people is a part of the goals that the material had to overcome. The goal of this section is to focus on the cost of the materials only and to demonstrate that Suprastone and gelatin allow producing affordable multilayered materials.

To prepare a typical batch of samples in this study, 10 g of Suprastone were used from a 15 kg box ordered at Kerr company for 51 US\$. 1 g of gelatin was used from a 100 g box

ordered at Sigma Aldrich company for 34 US\$. The cost was then 3 cents for the mineral and 34 cents for the gelatin, and the produced samples had a total volume of  $1.5 \text{ cm}^3$ . We can thus estimate a cost per volume of 25 cents/ $\text{cm}^3$ . Therefore, the cost of a typical large bone defect that has to be replaced with our bone graft (for instance a cylinder with a length of 10 cm and a radius of 1 cm, which corresponds to a volume of  $31.4 \text{ cm}^3$ ) is estimated at 7.85 US\$. The components of the bone graft will not be the limitation in term of price. From this point of view, the bone graft also successfully reached the requirement to stay affordable and in the same time, mechanically efficient. However, when thinking about large scale production, or thinking about replacing one of the complex shapes of our skeleton, some expensive machines could be involved (doctor blading machine, 3D printing machine, manual press) and could affect the final cost of the bone graft. These machines could be essential as it will be explained in the final part of this thesis, where future opportunities to develop this project are presented.

### 6.1.3 Limitations

The present thesis described the final protocol fabrication of the multilayered material but this protocol had to overcome several challenges before being functional. First of all, the mold in which the mineral is composed is made of polycarbonate: numerous other materials were tested as mold, but these tests were unfruitful since the calcium sulfate has a strong adherence to many materials, even Teflon. Using lubricant to detach the mineral from the mold would not guarantee the biocompatibility of the product. Polycarbonate mold was then fabricated from boards that are extremely flat and smooth. The disadvantage of such boards is that they are not resistant to scratches which appear easily during normal use of the mold. Scratches in the mold can create defects in the material, and mold must be replaced regularly.

Electrical tape is also used to fabricate the walls of the mold. The thickness of the tape is 0.2 mm which is the theoretical lower limit of the thickness of the mineral layers. However, it was never possible to prepare calcium sulfate with such thickness and with the same properties than thicker mineral samples. The capacity of the press might limit the possibility to create mineral samples with uniform porosity: because of the viscosity of the fresh mineral paste, a thin film of this paste cannot be properly squeezed under pressure as easily as thicker films. A press with higher capacity would help to decrease the thickness of the layers, and

thus to introduce more layers for a given overall thickness of the multilayered composite, which could improve the chances to deflect cracks during fracture propagation.

Gelatin has a very low strength that clearly limits the overall strength of the composite. Its toughness is however in an interesting range for this study since it allowed to deflect crack. A better interface would be a biopolymer with the same toughness, but stronger. It is not impossible that the other polymers described in chapter 3, even if they do not have the same advantages than gelatin, could be more adapted for this composite material. The lack of knowledge concerning the fracture toughness of the cited biopolymers, especially concerning the fracture toughness mode II, was a limiting factor in the choice of the polymeric interface.

## **6.2 Future work**

Making new types of bone graft materials is a long and multidisciplinary task that involves the expertise and the know-how of various fields. Chemistry is an important base to determine the best composition for the bone graft which, once created, will require concepts from mechanical engineering to identify the mechanisms that happen during fracture tests, and quantify many different parameters that measure the performance of the bone graft. Once the material is satisfactory in terms of mechanical properties, it must go through in vivo testing, on rabbits and then human. That is why, in this project, a surgeon from the Montreal General Hospital will take care of the in vivo testing. It is thus important to describe the future work of this project that will make the bone graft suitable for human.

Since this report focus on the very first steps of fabrication of a new type of bone graft material, it is important to situate the bone a graft in its entire project. This section explains what is the future studies that will make the composite graft accepted by the scientific community. Improvements can be done in the composition of the bone graft itself, but also in the fabrication process thanks to cutting edge technologies.

### **6.2.1 Improvement of the mechanical performances of the mineral**

In this thesis, a critical factor for crack deflection was the mechanical properties of the mineral used in the composite. A technique was developed to enhance these properties so has to almost double the strength of the mineral, and in the same time increase the fracture

toughness which is very important for crack deflection. These techniques were the compression of the mineral paste into a polycarbonate mold in order to significantly decrease the porosity of the material, and the use of a saturated solution. These methods brought interesting results but the post analysis showed that increasing again the fracture toughness of the mineral could deflect cracks better and improve the energetic performances of the multilayered composite.

In a review article on fiber reinforced CP cements, Kruger [57] related that fibers reinforcement is a well-known method to increase the toughness of brittle materials. This method was already used firstly in CP bone grafts [49, 50, 185], and strength, stiffness and matrix toughness were improved. Later, the same technique was experimented on HA [57] and CS [51] with improvements on the mechanical behavior too. The mechanisms responsible of these improvements are related to crack bridging: while an incoming crack propagates in the material, fibers are bridging the gap. Energy is dissipated through the elastic and plastic dissipation of the fibers in tension, pull out and frictional sliding of these fibers, or crack deflection at the interface of the fibers.

To be used in a bone grafts, the fibers must comply with the same requirements stated before: good mechanical performances, biocompatibility, osteoconductivity and degradability. A natural choice for the fibers is collagen since this type of fibers is already present in our bones. In fact, bones are a hierarchical composite material, and at a certain scale, bones can be seen as a composite made of mineralized collagen fibers [3]. Various biocompatible fibers can also be used to reinforce a mineral [57]. Fiber reinforcement theory reveals that fibers must agree two critical parameters to optimize the properties of the composite; the fiber content and fiber length.

Li [186] described the formula for the optimized fiber content  $V_f$  (non dimensional):

$$V_f = \frac{6K_{IC}E_f D_f^2}{g\tau^2 L_f^3} \quad (6.1)$$

Where  $K_{IC}$  is the composite fracture toughness in  $\text{Pa}\cdot\text{m}^{1/2}$ ,  $D_f$  the fiber diameter in m,  $L_f$  the fiber length in m,  $E_f$  the fiber modulus in Pa,  $g$  a factor computed experimentally (snubbing factor, in  $\text{m}^{-1/2}$ ) and  $\tau$  the interface frictional bond strength in Pa.

The second parameter, the critical fiber length  $L_{fc}$ , in m, was first expressed by Kelly and Tyson [187] in 1965 as :



$$L_{fc} = \frac{D_f \sigma_f}{\tau} \quad (6.2)$$

Where  $\sigma_f$  is the tensile strength of the fibers in Pa.

The theory of fiber reinforced materials is well documented and contains many other parameters to be optimized and used as guidelines [188]. In the case of collagen fibers, they can be extracted directly from natural sources such as sea cucumber. Trotter [189] described a precise protocol to extract them, but other sources can be used. For instance, collagen fibers are already used in catgut sutures in biomedical industry. Extracting collagen fibers from multifilament catgut sutures allow skipping purification steps. In our case, such sutures were ordered from Havel's (Cincinnati, OH, USA) and a preliminary study showed that it was possible to extract collagen particles. However AFM (atomic force microscopy) showed that the particles were not optimized in shapes of fibers of length  $L_{fc}$  yet.

Future work on the reinforcement of the mineral part of our bone graft material could lead to increase the fracture toughness of the mineral, and consequently the crack deflection of the composite and its energetic performance. Such study could follow the steps below:

- (i) Selection of a type of fibers.
- (ii) Experimental evaluation of the relevant parameters (mechanical tests for  $\sigma_f$ ,  $\tau$ ,  $E_f$ ..., microscopy observation for  $D_f$ ...).
- (iii) Calculation of the critical parameters ( $L_{fc}$ ,  $V_f$ ...).
- (iv) AFM observations of different samples of catgut sutures centrifuged at different speeds so as to identify which speed allow extracting fibers of length  $L_{fc}$ .
- (v) Finally, mixing the Suprastone with a percentage  $V_f$  of fibers of length  $L_{fc}$  and testing the resulting samples to measure the improvement in fracture toughness.

This section concludes the future work to be done on mechanical properties improvement. In the same time, improvements in the fabrication process can be investigated, such as large scale sample preparation or complexly shaped samples in the last steps of the bone graft development. The next sections present a quick overview of what the challenges and their solutions could be.

### 6.2.2 Large scale production

The samples presented in this report were made of six bilayers mineral – gelatin for a total thickness of a few millimeters. The other dimensions were also in the order of magnitude of millimeter or centimeter. This was sufficient to measure the effect of crack deflection, but a real bone can have a thickness of a few centimeters and a length around 10 cm. To optimize the fabrication time, the use of industrial equipment such as a doctor blading machine could help to make a large and thin mineral layer that can be then cut into several large bilayers. Once assembled, these bilayers form a larger bone graft. This technique saves a considerable amount of time, and moreover such machine allows increasing the uniformity in the thickness of the different layers. It could also help to decrease the thickness of the different layers and thus to be closer to what is observed in nature. Figure 6.1 is a view of an example of doctor blading machine (MSK-AFA-L800, MTI Corporation, Richmond, CA, USA) used in the preparation of large thin films in industry.

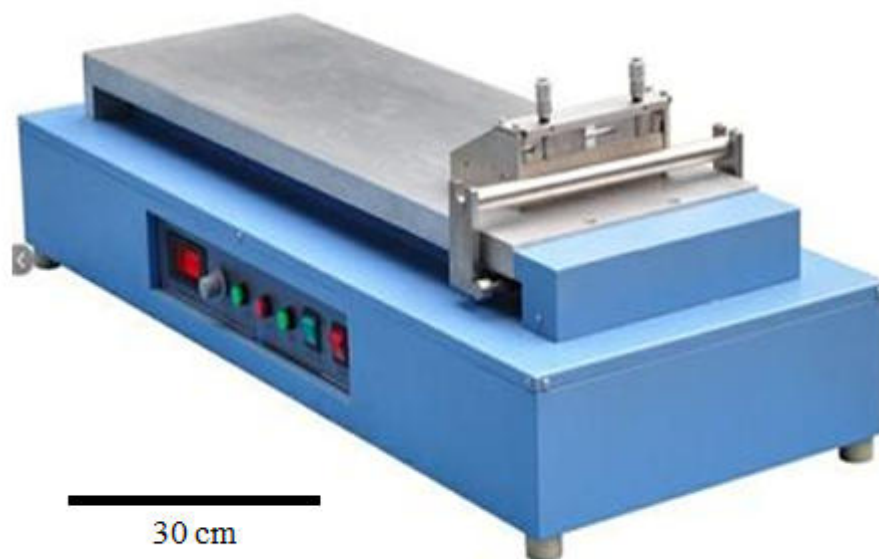


**Figure 6.1: Example of doctor blading machine (MSK-AFA-L800, MTI Corporation, Richmond, CA, USA) for large scale doctor bladed film production and high accuracy [190].**

### 6.2.3 Complex shapes

The success of an implant strongly relies on its capability to duplicate the geometry of the missing bone region so the repaired skeletal region can recover its functionality. The advantage of the multilayered composite fabrication method is that it provides flexibility in terms of geometry. We tested our method on a flat polycarbonate substrate but the same fabrication protocol is also possible on a very different substrate. The proposed protocol consists in reconstructing the shape of the missing bone numerically and in three dimensions and then converting it in a numerical file that can be used by a 3D printing machine. The 3D printing machine can then create a polymeric template that will be used to fabricate the complexly shaped bone graft material with exactly the same geometry than the missing bone. Such process is summarized in figure 6.2. 3D printing is a powerful tool that could help to solve many issues; for instance, to compress the complexly shaped initial mineral layer, a negative template could be also printed in order to sandwich the mineral layer between the two templates and make it denser and stronger after it dries.

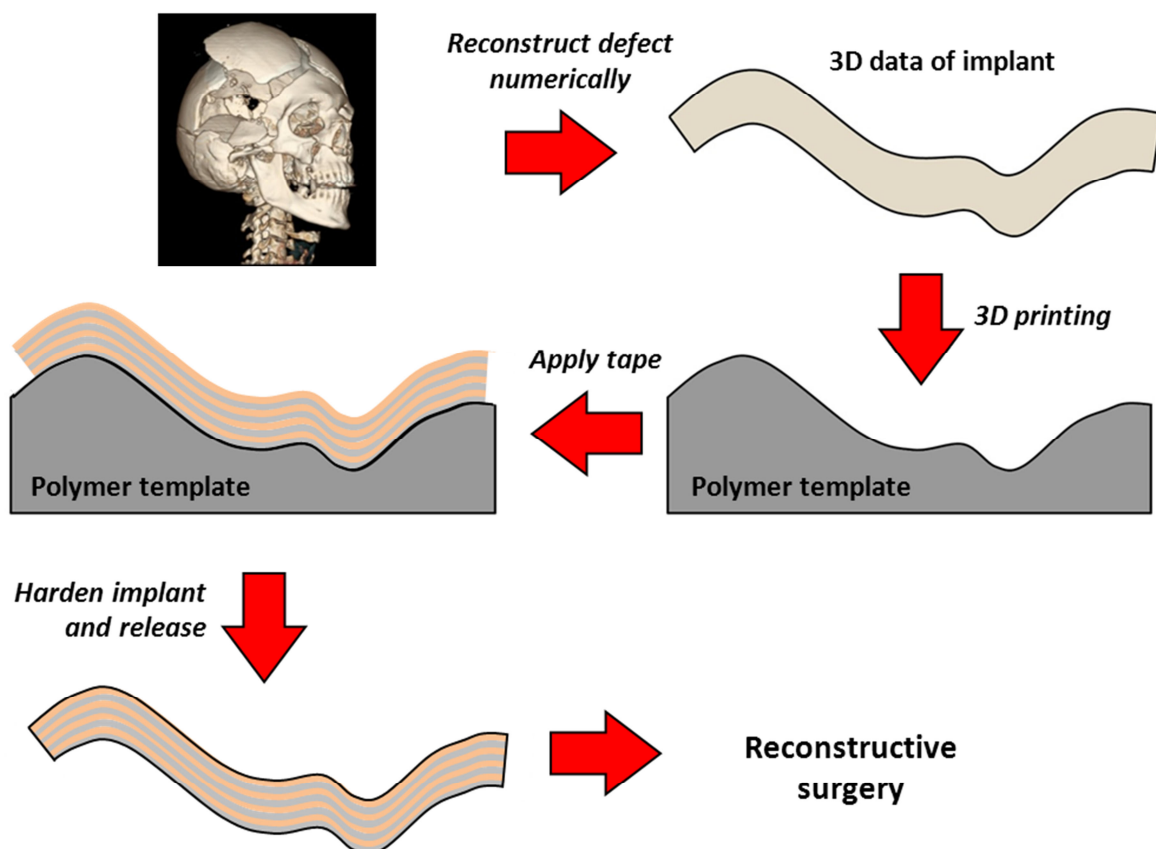


Figure 6.2: Step by step fabrication of a complexly shaped multilayered bone graft.

A high resolution printing machine (Perfactory® Micro 3D Printer Family, EnvisionTec, Dearborn, MI, USA) was used to validate the printing of the bone graft template. As a preliminary study, rectangular molds were printed and Suprastone samples were fabricated from these polymeric molds. The samples exhibited the same mechanical properties than the samples prepared from the polycarbonate mold. The polymer used by the 3D printing machine presented more adhesion to the mineral than polycarbonate, but not sufficiently to make the removal of the layer impossible. Complexly shaped bone grafts could therefore be fabricated in a future work.

#### **6.2.4 Cylindrical implants**

Although they are very common in the human skeleton, cylindrical shapes represent a challenge for our fabrication method. The fabrication protocol could be modified to create complex shapes. A solution could be to roll a bilayer of gelatin and mineral while the components are still fresh. The sample would then be let overnight at room temperature for proper drying and the resulting piece would be a bone graft mimicking the structure of an osteon but at a macro-scale. The advantage of such structure is that the properties are the same in any direction. Figure 6.3 displays a view of this type of bone graft material as well as a bony defect in a rabbit radius that will receive the graft. The figure also exhibits the aimed geometry of the artificial osteon. A diameter of 4 mm for a length of 16 mm is the classic model used for segmental defect studies, especially with rabbits. This geometry could be easily changed if necessary, for example with the dimensions of cylindrical human bone defect.

Such technique raises new questions. It has to be verified that it is possible to roll a fresh bilayer without damaging the mineral and creating new flaws and weaknesses. Another important step is also the compression of the mineral layer during its drying that could be solve in using heat shrinking tubes. These polymeric tubes decrease their diameter by two when they are submitted to heat. They could be the solution to harden an artificial osteon and the feasibility of this method deserves to be investigated.

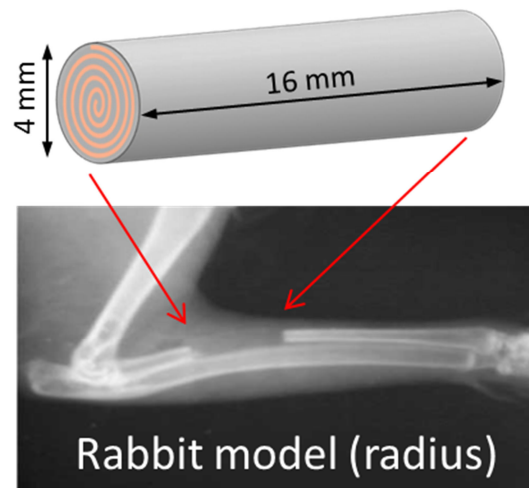


**Figure 6.3: Osteon-like multilayered bone graft for cylindrical bone replacement on rabbits.**

## References

- [1] Rho JY, Kuhn-Spearing L, Zioupos P. Mechanical properties and the hierarchical structure of bone. *Med Eng Phys* 1998;20:92-102.
- [2] Ritchie RO, Buehler MJ, Hansma P. Plasticity and toughness in bone. *Phys Today* 2009;62:41-7.
- [3] Weiner S, Wagner HD. The material bone: Structure-mechanical function relations. *Annual Review of Materials Research* 1998;28:271-98.
- [4] Taylor BL, Andric T, Freeman JW. Recent advances in bone graft technologies. *Recent Patents on Biomedical Engineering* 2013;6:40-6.
- [5] SEER. bone\_tissue.jpg. In: U.S. National Cancer Institute's Surveillance EaERSP, editor. 2013. p. Compact bone & spongy bone.
- [6] Meyers MA, Chen PY, Lin AYM, Seki Y. Biological materials: Structure and mechanical properties. *Prog Mater Sci* 2008;53:1-206.
- [7] Wegst UGK, Ashby MF. The mechanical efficiency of natural materials. *Philosophical Magazine* 2004;84:2167- 81.
- [8] Pneumaticos SG, Triantafyllopoulos GK, Basdra EK, Papavassiliou AG. Segmental bone defects: from cellular and molecular pathways to the development of novel biological treatments. *Journal of Cellular and Molecular Medicine* 2010;14:2561-9.
- [9] Gugala Z, Lindsey RW, Gogolewski S. New approaches in the treatment of critical-size segmental defects in long bones. *Macromolecular Symposia* 2007;253:147-61.
- [10] DeCoster TA, Gehlert R, Mikola EA, Pirela-Cruz MA. Management of posttraumatic segmental bone defects. *Journal of the American Academy of Orthopaedic Surgeons* 2004;12:28-38.
- [11] Huntington TW. Case of bone transference. Use of a segment of fibula to supply a defect in the tibia. *Annals of Surgery* 1905;41:249-51.
- [12] Agiza A. Treatment of tibial osteomyelitic defects and infected pseudarthroses by the Huntington fibular transference operation. *Journal of Bone and Joint Surgery-American Volume* 1981;63:814-9.
- [13] Watson JT, Anders M, Moed BR. Management strategies for bone loss in tibial shaft fractures. *Clinical Orthopaedics and Related Research* 1995:138-52.
- [14] Goldstrohm GL, Mears DC, Swartz WM. The results of 39 fractures complicated by major segmental bone loss and/or leg length discrepancy. *Journal of Trauma-Injury Infection and Critical Care* 1984;24:50-8.
- [15] Laurencin C, Khan Y, El-Amin SF. Bone graft substitutes. *Expert Review of Medical Devices* 2006;3:49-57.
- [16] Mumford JE, Simpson AHRW. Management of bone defects: A review of available techniques. *Iowa Orthopaedic Journal* 1992; 12:42-9.
- [17] Drezner MK. Hypophosphatemic rickets. *Endocrine development* 2003;6:126-55.
- [18] Böhner M, Galea L, Doebelin N. Calcium phosphate bone graft substitutes: Failures and hopes. *Journal of the European Ceramic Society* 2012;32:2663-71.
- [19] Kinaci A, Neuhaus V, Ring DC. Trends in bone graft use in the United States. *Orthopedics* 2014;37:783-8.
- [20] Maurer RC, Dillin L. Multistaged surgical management of posttraumatic segmental tibial bone loss. *Clinical Orthopaedics and Related Research* 1987;216:162-70.
- [21] Malkawi H, Shannak A, Sunna P. Active treatment of segmental defects of long bones with established infection - a prospective study. *Clinical Orthopaedics and Related Research* 1984:241-8.
- [22] Green SA, Dlabal TA. The open bone graft for septic non-union. *Clinical Orthopaedics and Related Research* 1983:117-24.
- [23] Mankin HJ, Doppelt S, Tomford W. Clinical experience with allograft implantation: The first ten years. *Clinical Orthopaedics and Related Research* 1983:69-86.
- [24] Johnston JO. Limb sparing technology in the management of primary bone sarcomas of the extremities. *Iowa Orthopaedic Journal* 1990;10:44-6.
- [25] May JJ, Jupiter J, Weiland A, Byrd H. Clinical classification of post-traumatic tibial osteomyelitis. *Journal of Bone and Joint Surgery - American Volume* 1989;71:1422-8.

- [26] Heiple KG, Kendrick RE, Herndon CH, Chase SW. A critical evaluation of processed calf bone. *Journal of Bone and Joint Surgery-American Volume* 1967;A 49:1119-&.
- [27] Cierny G, Zorn KE. Segmental tibial defects: comparing conventional and Ilizarov methodologies. *Clinical Orthopaedics and Related Research* 1994:118-23.
- [28] Niinomi M. Mechanical properties of biomedical titanium alloys. *Materials Science and Engineering* 1998;243:231-6.
- [29] Emsley J. Titanium. In: Press OU, editor. *Nature's building blocks: An A-Z guide to the elements*. Oxford, England, UK2001.
- [30] Torres Y, Trueba P, Pavon J, Montealegre I, Rodriguez-Ortiz JA. Designing, processing and characterisation of titanium cylinders with graded porosity: An alternative to stress-shielding solutions. *Materials & Design* 2014;63:316-24.
- [31] Hahn H, Palich W. Preliminary evaluation of porous metal surfaced titanium for orthopedic implants. *Journal of biomedical materials research* 1970;4:571-7.
- [32] Sim FH, Chao E, Galante JO. Segmental replacement of long bones using fiber titanium composites. *Clinical Orthopaedics and Related Research* 1983:108-14.
- [33] Leopold SS. Minimally invasive total knee arthroplasty for osteoarthritis. *New England Journal of Medicine* 2009;360:1749-58.
- [34] Vince KG. Total joint arthroplasty: hip, knee, and shoulder. *Current opinion in rheumatology* 1991;3:71-80.
- [35] Turner TM, Urban RM, Gitelis S, Haggard WO, Richelsoph K. Resorption evaluation of a large bolus of calcium sulfate in a canine medullary defect. *Orthopedics* 2003;26:S577-S9.
- [36] Maeda ST, Bramante CM, Taga R, Garcia RB, de Moraes IG, Bernadineli N. Evaluation of surgical cavities filled with three types of calcium sulfate. *Journal of Applied Oral Science* 2007;15:416-9.
- [37] Ducheyne P, Degroot K. In vivo surface activity of a hydroxyapatite alveolar bone substitute. *Journal of biomedical materials research* 1981;15:441-5.
- [38] Nasr HF, Aichelmann-Reidy ME, Yukna RA. Bone and bone substitutes. *Periodontol* 2000 1999;19:74-86.
- [39] Linhart W, Briem D, Amling M, Rueger JM, Windolf J. Mechanical failure of a porous hydroxyapatite ceramic 7.5 years after treatment of a fracture of the proximal tibia. *Unfallchirurg* 2004;107:154-7.
- [40] Pietrzak WS, Ronk R. Calcium sulfate bone void filler: A review and a look ahead. *J Craniofac Surg* 2000;11:327-33.
- [41] Vekinis G, Ashby M, Beaumont P. Plaster of Paris as a model material for brittle porous solids. *Journal of materials science* 1993;28:3221-7.
- [42] Coetzee AS. Regeneration of bone in the presence of calcium sulfate. *Archives of Otolaryngology-Head & Neck Surgery* 1980;106:405-9.
- [43] McKee JC, Bailey BJ. Calcium sulfate as a mandibular implant. *Otolaryngology-Head and Neck Surgery* 1984;92:277-86.
- [44] Kanatani M, Sugimoto T, Fukase M, Fujita T. Effect of elevated extracellular calcium on the proliferation of osteoblastic MC3T3-E1 cells:its direct and indirect effects via monocytes. *Biochemical and Biophysical Research Communications* 1991;181:1425-30.
- [45] Goel SC, Singh D, Rastogi A, Kumaraswamy V, Gupta A, Sharma N. Role of tricalcium phosphate implant in bridging the large osteoperiosteal gaps in rabbits. *Indian Journal of Experimental Biology* 2013;51:375-80.
- [46] Gerhart TN, Miller RL, Kleshinski SJ, Hayes WC. In vitro characterization and biomechanical optimization of a biodegradable particulate composite bone cement. *Journal of biomedical materials research* 1988;22:1071-82.
- [47] Xu HHK, Quinn JB. Calcium phosphate cement containing resorbable fibers for short-term reinforcement and macroporosity. *Biomaterials* 2002;23:193-202.
- [48] Moreau JL, Weir MD, Xu HHK. Self-setting collagen-calcium phosphate bone cement: Mechanical and cellular properties. *Journal of Biomedical Materials Research Part A* 2009;91A:605-13.
- [49] Muller FA, Gbureck U, Kasuga T, Mizutani Y, Barralet JE, Lohbauer U. Whisker-reinforced calcium phosphate cements. *Journal of the American Ceramic Society* 2007;90:3694-7.

- [50] Pan ZH, Jiang PP, Fan QY, Ma B, Cai HP. Mechanical and biocompatible influences of chitosan fiber and gelatin on calcium phosphate cement. *Journal of Biomedical Materials Research Part B-Applied Biomaterials* 2007;82B:246-52.
- [51] Coutts RSP. Wood-fibre reinforced plaster. *Journal of materials science* 1986;21:2959-64.
- [52] Gao CJ, Huo SJ, Li XL, You XD, Zhang Y, Gao JP. Characteristics of calcium sulfate/gelatin composite biomaterials for bone repair. *Journal of Biomaterials Science-Polymer Edition* 2007;18:799-824.
- [53] Park L. Composites as biomaterials. *Biomaterials* 2007. p. 207-24.
- [54] Thomas DF. Reinforcing plaster of Paris. *The lancet - Letters to the editor* 1955:205.
- [55] Shen C, Mohammed H, Kamar A. Effect of K<sub>2</sub>SO<sub>4</sub> and CaSO<sub>4</sub> dihydrate solutions on crystallization and strength of gypsum. *Journal of Dental Research* 1981;60:1410-7.
- [56] Sanad MEE, Combe EC, Grant AA. The use of additives to improve the mechanical properties of gypsum products. *Journal of Dental Research* 1982;61:808-10.
- [57] Kruger R, Groll J. Fiber reinforced calcium phosphate cements - On the way to degradable load bearing bone substitutes? *Biomaterials* 2012;33:5887-900.
- [58] Ducheyne P, Qiu Q. Bioactive ceramics: the effect of surface reactivity on bone formation and bone cell function. *Biomaterials* 1999;20:2287-303.
- [59] Rahaman MN, Day DE, Bal S, Fu Q, Jung SB, Bonewald LF, et al. Bioactive glass in tissue engineering. *Acta Biomaterialia* 2011;7:2355-73.
- [60] Oonishi H, Hench LL, Wilson J, Sugihara F, Tsuji E, Kushitani S, et al. Comparative bone growth behavior in granules of bioceramic materials of various sizes. *Journal of biomedical materials research* 1999;44:31-43.
- [61] Wheeler DL, Stokes KE, Park HM, Hollinger JO. Evaluation of particulate bioglass(R) in a rabbit radius ostectomy model. *Journal of biomedical materials research* 1997;35:249-54.
- [62] Fu Q, Rahaman MN, Fu H, Liu X. Silicate, borosilicate, and borate bioactive glass scaffolds with controllable degradation rate for bone tissue engineering applications. I. Preparation and in vitro degradation. *Journal of Biomedical Materials Research Part A* 2010;95A:164-71.
- [63] Ciccone WJ, Motz C, Bentley C, Tasto JP. Bioabsorbable implants in orthopaedics: new developments and clinical applications. *The Journal of the American Academy of Orthopaedic Surgeons* 2001;9:280-8.
- [64] Kasuga T, Maeda H, Kato K, Nogami M, Hata K, Ueda M. Preparation of poly(lactic acid) composites containing calcium carbonate (vaterite). *Biomaterials* 2003;24:3247-53.
- [65] Yukna RA. Synthetic bone grafts in periodontics. *Periodontol* 2000 1993;1:92-9.
- [66] Duplat D, Chabadel A, Gallet M, Berland S, Bedouet L, Rousseau M, et al. The in vitro osteoclastic degradation of nacre. *Biomaterials* 2007;28:2155-62.
- [67] Lopez V, Berland, Camprasse, Silve. Demonstration of the capacity of nacre to induce bone formation by human osteoblasts maintained in vitro. *Tissue and Cell* 1992;24:667-79.
- [68] Böhner M. Design of ceramic-based cements and putties for bone graft substitution. *European cells and materials* 2010;20:1-12.
- [69] Barthelat F, Rabiei R. Toughness amplification in natural composites. *J Mech Phys Solids* 2011;59:829-40.
- [70] Barthelat F, Tang H, Zavattieri PD, Li CM, Espinosa HD. On the mechanics of mother-of-pearl: A key feature in the material hierarchical structure. *Journal of the Mechanics and Physics of Solids* 2007;55:306-37.
- [71] Bekah S, Rabiei R, Barthelat F. The micromechanics of biological and biomimetic staggered composites. *Journal of Bionic Engineering* 2012;9:446-56.
- [72] Clegg WJ, Kendall K, Alford NM, Button TW, Birchall JD. A simple way to make tough ceramics. *Letters to Nature* 1990;347.
- [73] Clegg WJ. The fabrication and failure of laminar ceramic composites. *Acta Metallurgica et Materialia* 1992;40:3085-93.
- [74] Philipps AJ, Clegg WJ, Clyne TW. Fracture behavior of ceramic laminates in bending-I. modelling of crack propagation. *Acta Metallurgica et Materialia* 1993;41:805-17.
- [75] Livanov K, Jelitto H, Bar-On B, Schulte K, Schneider GA, Wagner DH. Tough alumina/polymer layered composites with high ceramic content. *Journal of the American Ceramic Society* 2015;98:1285-91.



- [76] Kovar D, Thouless MD, Halloran JW. Crack deflection and propagation in layered silicon nitride/boron nitride ceramics. *Journal of American ceramic society* 1998;81:1004-12.
- [77] Folsom CA, Zok FW, Lange FF. Flexural properties of brittle multilayer materials: I, modeling. *Journal of American ceramic society* 1994;77:689-96.
- [78] He M-Y, Hutchinson JW. Crack deflection at an interface between dissimilar materials. *Journal of solid structures* 1989;25:1053-67.
- [79] Lewis KN, Thomas MV, Puleo DA. Mechanical and degradation behavior of polymer-calcium sulfate composites. *Journal of Materials Science-Materials in Medicine* 2006;17:531-7.
- [80] Singh NB, Middendorf B. Calcium sulphate hemihydrate hydration leading to gypsum crystallization. *Progress in Crystal Growth and Characterization of Materials* 2007;53:57-77.
- [81] Anusavice K. Phillips' science of dental materials. 11th ed: Saunders; 2003.
- [82] Earnshaw R. The compressive strength of gypsum-bonded investments at high temperatures *Australian Dental Journal* 1969;14:264-8.
- [83] Shereen S, Azer REK, Lisa A. Knobloch. Effect of mixing methods on the physical properties of dental stones. *Journal of dentistry* 2008;36:736-44.
- [84] Craig RG PJ, Sakaguchi RL. Craig's restorative dental materials. 12th ed: Mosby Elsevier; 2006.
- [85] Gao C, Huo S, Li X, You X, Zhang Y, Gao J. Characteristics of calcium sulfate/gelatin composite biomaterials for bone repair. *Journal of Biomaterials Science, Polymer Edition* 2012;18:7999-824.
- [86] CO Ge. Plaster of Paris reinforced with magnesium sulfate. In: CO Ge, editor. USA1973.
- [87] LTD NcC. Fibre-reinforced plaster of Paris panels. Japan1974.
- [88] Tada H, Paris P, Irwin G. The stress analysis of cracks handbook: Wiley; 2000.
- [89] Klemm D, Heublein B, Fink H, Bohn A. Cellulose: fascinating biopolymer and sustainable raw material. *Organic chemistry* 2005;36.
- [90] Pranger L, Tannenbaum R. Biobased nanocomposites prepared by in situ polymerization of furfuryl alcohol with cellulose whiskers or montmorillonite clay. *Macromolecules* 2008;41:8682-7.
- [91] Ach A. Biodegradable plastics based on cellulose acetate. *Journal of Macromolecular Science, Part A: Pure and Applied Chemistry* 1993;30:733-40.
- [92] Isken T, Alagoz SM, Onyedi M, Izmirli H. Use of diced bone grafts wrapped in surgicel in the augmentation of maxillofacial area. *J Craniofac Surg* 2008;19:1440-5.
- [93] Ioannis GD, Athanasios K, Aggelos PN, Charalambos M, Khaled AQ, Nikolaos BA, et al. Bone graft wrapping with cellulose polymer sheet in posterior spinal fusion. A technical note. *Journal of Spine* 2011;1.
- [94] Stark A, Hoydonckx H. Biopolymer matrix materials. *Biocomp*; 2008.
- [95] Sun S. Comparison of the mechanical properties of cellulose and starch films. *Biomacromolecules* 2010;11:126-32.
- [96] Islam M, Masum S, Rahman M, Molla M, Shaikh A. Preparation of chitosan from shrimp shell and investigation of its properties. *International Journal of Basic & Applied Sciences* 2011;11:77-80.
- [97] Berger J, Reist M, Mayer J, Felt O, Peppas N, Gurny R. Structure and interactions in covalently and ionically crosslinked chitosan hydrogels for biomedical applications. *European Journal of Pharmaceutics and Biopharmaceutics* 2004;57:19-34.
- [98] Croisier F, Jérôme C. Chitosan-based biomaterials for tissue engineering. *European Polymer Journal* 2013;49:780-92.
- [99] Arvanitoyannisa I, Nakayamab A, Aibab S. Chitosan and gelatin based edible films: state diagrams, mechanical and permeation properties. *Carbohydrate Polymers* 1998;37:371-82.
- [100] Caner C, Vergano P, Wiles J. Chitosan film mechanical and permeation properties as affected by acid, plasticizer, and storage. *Journal of food science* 1998;63:1049-63.
- [101] Bonderer L, Studart A, Woltersdorf J, Pippel E, Gauckler L. Strong and ductile platelet-reinforced polymer films inspired by nature: Microstructure and mechanical properties. *Journal of Materials Research* 2009;24:2741-54.
- [102] Kumar M. A review of chitin and chitosan applications. *Reactive & Functional Polymers* 2000;46:1-27.
- [103] Ghosh B, Urban M. Self-repairing oxetane-substituted chitosan polyurethane networks. *Science* 2009;323:1458-60.
- [104] Venkatesan J, Kim S-K. Chitosan composites for bone tissue engineering - an overview. *Marine Drugs* 2010;8:2252-66.

- [105] Chen R, Hwa H-D. Effect of molecular weight of chitosan with the same degree of deacetylation on the thermal, mechanical, and permeability properties of the prepared membrane. *Carbohydrate Polymers* 1996;29:353–8.
- [106] Tomka I. Thermoplastically processable starch and a method of making it. In: I S, editor. Switzerland 1994.
- [107] Hardin B. Stuck on starch: A new wood adhesive. In: Service AR, editor.: US Department of Agriculture; 2000.
- [108] Salgado AJ, Coutinho OP, Reis RL. Novel starch-based scaffolds for bone tissue engineering: Cytotoxicity, cell culture, and protein expression. *Tissue Engineering* 2004;10:465-74.
- [109] Salgado AJ, Coutinho OP, Reis RL, Davies JE. In vivo response to starch-based scaffolds designed for bone tissue engineering applications. *Journal of Biomedical Materials Research Part A* 2007;80A:983-9.
- [110] Piyada K, Waranyou S, Thawien W. Mechanical, thermal and structural properties of rice starch films reinforced with rice starch nanocrystals. *International Food Research Journal* 2013;20:439-49.
- [111] Katsuraya K, Okuyama K, Hatanaka K, Oshima R, Sato T, Matsuzaki K. Constitution of konjac glucomannan: chemical analysis and <sup>13</sup>C NMR spectroscopy. *Carbohydrate Polymers* 2003;53:183-9.
- [112] Chen Y, Zhang L, Lu Y, Ye C, Du L. Preparation and properties of water-resistant soy dreg/benzyl konjac glucomannan composite plastics. *Journal of Applied Polymer Science* 2003;90:3790-6.
- [113] Zhang Y, Xie B, Gan X. Advance in the applications of konjac glucomannan and its derivatives. *Carbohydrate Polymers* 2005;60:27-31.
- [114] Tokiwa Y, Tsuchiya A. Biodegradable resin compositions. USA: National Institute Of Advanced Industrial Science And Technology; 2000.
- [115] Huang J, Ma T, Tang H, Fan X, Xu Y. Vancomycin cationic liposome combined with nano-hydroxyapatite/chitosan/konjac glucomannan scaffold for treatment of infected bone defects in rabbits. *Chinese journal of reparative and reconstructive surgery* 2012;26:190-5.
- [116] Nie HR, Shen XX, Zhou ZH, Jiang QS, Chen YW, Xie A, et al. Electrospinning and characterization of konjac glucomannan/chitosan nanofibrous scaffolds favoring the growth of bone mesenchymal stem cells. *Carbohydrate Polymers* 2011;85:681-6.
- [117] Pan LZ, He HW, Yao ZW, Chen ZQ, Liu JS, Zhang HL, et al. Preparation and characterization of nano-hydroxy apatitekonjac glucomannan composite scaffolds. *J Wuhan Univ Technol-Mat Sci Edit* 2010;25:484-6.
- [118] Lee C. Glucomannan scaffolding for three-dimensional tissue culture and engineering. In: California Trotuo, editor. USA 2013.
- [119] Xiao C, Gao S, Wang H, Zhang L. Blend films from chitosan and konjac glucomannan solutions. *Journal of Applied Polymer Science* 2000;76:509–15.
- [120] Enomoto-Rogers Y, Ohmomo Y, Iwata T. Syntheses and characterization of konjac glucomannan acetate and their thermal and mechanical properties. *Carbohydrate Polymers* 2013;92:1827-34.
- [121] Gautieri A, Buehler M, Redaelli A. Deformation rate controls elasticity and unfolding pathway of single tropocollagen molecules. *Journal of the Mechanical Behavior of Biomedical Materials* 2009;2:130-7.
- [122] Hulmes DJS. Building collagen molecules, fibrils, and suprafibrillar structures. *Journal of Structural Biology* 2002;137:2-10.
- [123] MSPOT. general\_tendonitis\_anatomy01.jpg. 2012.
- [124] Hansen E, Lee S, Sobel H. The effects of relative humidity on some physical properties of modern vellum: implications for the optimum relative humidity for the display and storage of parchment. In: Conservation TAlf, editor. Book and Paper specialty group session, AIC 19th Annual Meeting. Albuquerque, New Mexico, USA 1991.
- [125] Hunter L. The C-F bond as a conformational tool in organic and biological chemistry. *Beilstein Journal of Organic Chemistry* 2010;6.
- [126] Cunniffe G, O'Brien F. Collagen scaffolds for orthopedic regenerative medicine. *The Journal of The Minerals, Metals & Materials Society* 2011;63:66-73.

- [127] Rodrigues CVM, Serricella P, Linhares ABR, Guerdes RM, Borojevic R, Rossi MA, et al. Characterization of a bovine collagen-hydroxyapatite composite scaffold for bone tissue engineering. *Biomaterials* 2003;24:4987-97.
- [128] Yang XBB, Bhatnagar RS, Li S, Oreffo ROC. Biomimetic collagen scaffolds for human bone cell growth and differentiation. *Tissue Engineering* 2004;10:1148-59.
- [129] Liao SS, Cui FZ, Zhang W, Feng QL. Hierarchically biomimetic bone scaffold materials: Nano-HA/collagen/PLA composite. *J Biomed Mater Res Part B* 2004;69B:158-65.
- [130] Grant G, Koktysh D, Yun B, Matts R, Kotov N. Layer-by-layer assembly of collagen thin films: controlled thickness and biocompatibility. *Biomedical Microdevices* 2001;3:301-6.
- [131] Hahna S, Hoffman A. Preparation and characterization of biocompatible polyelectrolyte complex multilayer of hyaluronic acid and poly-L-lysine. *International Journal of Biological Macromolecules* 2005;37:227-31.
- [132] Kuijper A, Engbers G, Krijgsveld J, Zaat S, Dankert J, Feijen J. Cross-linking and characterisation of gelatin matrices for biomedical applications. *Journal of Biomaterials Science, Polymer Edition* 2000;11:225-43.
- [133] Koide T, Daito M. Effects of various collagen crosslinking techniques on mechanical properties of collagen film. *Dental Materials Journal* 1997;16:1-9.
- [134] Liu X, Smith LA, Hu J, Ma PX. Biomimetic nanofibrous gelatin/apatite composite scaffolds for bone tissue engineering. *Biomaterials* 2009;30:2252-8.
- [135] Rehm B, Valla S. Bacterial alginates: biosynthesis and applications. *Applied Microbiology and Biotechnology* 1997;48:281-8.
- [136] Mollah M, Khan M. Mechanical properties development of sodium alginate films with additives by UV-radiation processing. *Journal of Applied Polymer Science* 2012;124:275-81.
- [137] Rowe R, Sheskey P, Quinn M. Handbook of pharmaceutical excipients. 6 ed: Pharmaceutical Press; 2009.
- [138] Li ZS, Ramay HR, Hauch KD, Xiao DM, Zhang MQ. Chitosan-alginate hybrid scaffolds for bone tissue engineering. *Biomaterials* 2005;26:3919-28.
- [139] Valente JFA, Valente TAM, Alves P, Ferreira P, Silva A, Correia IJ. Alginate based scaffolds for bone tissue engineering. *Materials Science & Engineering C-Materials for Biological Applications* 2012;32:2596-603.
- [140] Barnes C. Chemical nature of shellac. *Industrial & Engineering Chemistry* 1938;30:449-51.
- [141] Farag Y. Characterization of different shellac types and development of shellac-coated dosage Forms. Hamburg: University of Hamburg; 2010.
- [142] Arnautov A, Korhov V, Faitelson E. Physicomechanical properties of shellac films grafted by using ultraviolet irradiation. *Mechanics of Composite Materials* 2013;49:163-70.
- [143] Soradech S, Limatvapirat S, Luangtana-anan M. Stability enhancement of shellac by formation of composite film: Effect of gelatin and plasticizers. *Journal of Food Engineering* 2013;116:572-80.
- [144] Leathers TD. Biotechnological production and applications of pullulan. *Applied Microbiology and Biotechnology* 2003;62.
- [145] Hijiya H, Shiosaka M. Shaped bodies of pullulan esters and their use. USA: Hayashibara Biochem Lab; 1972.
- [146] Fujimoto M, Fujita F, Fukami K. Pullulan aminoalkyl ether. USA: Hayashibara Biochemical Laboratories, Inc., Sumitomo Chemical Company, Limited; 1979.
- [147] Fujimoto M, Masuko F, Nagase T, Tsuji K. Cross-linked pullulan. USA: Hayashibara Biochemical Laboratories, Inc., Sumitomo Chemical Company, Ltd.; 1979.
- [148] Diab T, Biliaderis C, Gerasopoulos D, Sfakiotakis E. Physicochemical properties and application of pullulan edible films and coatings in fruit preservation. *Journal of the Science of Food and Agriculture* 2001;81:988-1000.
- [149] Amrita, Arora A, Sharma P, Katti D. Pullulan-based composite scaffolds for bone tissue engineering: Improved osteoconductivity by pore wall mineralization. *Carbohydrate Polymers* 2015;123:180-9.
- [150] Yuen S. Pullulan and its applications. *Process Biochemistry* 1974;9:7-9.
- [151] Kawahara M, Mizutani K, Suzuki S, Kitamura S, Fukada H, Yui T, et al. Dependence of the mechanical properties of a pullulan film on the preparation temperature. *Bioscience, Biotechnology, and Biochemistry* 2003;67: 893-5.

- [152] Bekkum HV, Röper H, Voragen F. Carbohydrates as organic raw materials III: Wiley-VCH Verlag GmbH & Co. KGaA, Weinheim; 2007.
- [153] Hankermeyer C, Tjeerdema R. Polyhydroxybutyrate: plastic made and degraded by microorganisms. *Reviews of Environmental Contamination and Toxicology* 1999;159:1-24.
- [154] Sabir MI, Xu X, Li L. A review on biodegradable polymeric materials for bone tissue engineering applications. *Journal of materials science* 2009;44:5713-24.
- [155] Khorasani M, Mirmohammadi S, Irani S. Polyhydroxybutyrate (PHB) scaffolds as a model for nerve tissue engineering application: fabrication and in vitro assay. *International Journal of Polymeric Materials and Polymeric Biomaterials* 2011;60:562-75.
- [156] Ray SS, Okamoto M. Polymer/layered silicate nanocomposites: a review from preparation to processing. *Progress in Polymer Science* 2003;28:1539-641.
- [157] Chen GQ, Wu Q. The application of polyhydroxyalkanoates as tissue engineering materials. *Biomaterials* 2005;26:6565-78.
- [158] Aoyagi Y, Doi Y, Iwata T. Mechanical properties and highly ordered structure of ultra-high-molecular-weight poly (R)-3-hydroxybutyrate films: Effects of annealing and two-step drawing. *Polym Degrad Stabil* 2003;79:209-16.
- [159] Middleton JC, Tipton AJ. Synthetic biodegradable polymers as orthopedic devices. *Biomaterials* 2000;21:2335-46.
- [160] Lopesa MS, Jardini AL, Filhoa RM. Poly (lactic acid) production for tissue engineering applications. *Procedia Engineering* 2012;42:1402-13.
- [161] Hutmacher DW. Scaffolds in tissue engineering bone and cartilage. *Biomaterials* 2000;21:2529-43.
- [162] Burg K, Porter S, Kellam J. Biomaterial developments for bone tissue engineering. *Biomaterials* 2000;21:2347-59.
- [163] Sodergard A, Stolt M. Properties of lactic acid based polymers and their correlation with composition. *Progress in Polymer Science* 2002;27:1123-63.
- [164] Daniels C, Andriano. Mechanical properties of biodegradable polymers and composites proposed for internal fixation of bone. *Journal of Applied Biomaterials* 1990;1:57-78.
- [165] Sigma-Aldrich. St. Louis, MO, USA2015.
- [166] Oldershaw RA, Baxter MA, Lowe ET, Bates N, Grady LM, Soncin F, et al. Chondrocyte protocol. In: *Community TSCR*, editor.: StemBook; 2012.
- [167] Xing Q, Yates K, Vogt C, Qian Z, Frost MC, Zhao F. Increasing mechanical strength of gelatin hydrogels by divalent metal ion removal. *Scientific Reports* 2014;4.
- [168] Zhu X-K, Joyce JA. Review of fracture toughness (G, K, J, CTOD, CTOA) testing and standardization. *Engineering Fracture Mechanics* 2012;85.
- [169] ASTM. Standard test method for crack-tip opening displacement (CTOD) fracture toughness measurement (withdrawn 2013). ASTM E1290-08e1. West Conshohocken, PA2008.
- [170] Both J, Barfuß D, Baier H. Mode II delamination of CFRP-metal laminates at bolted joints. 18th international conference on composite materials2009.
- [171] deMoraes A. Analysis of mode II interlaminar fracture of multidirectional laminates. *Composites Part A: Applied Science and Manufacturing* 2004;35:51-7.
- [172] Thouless MD. The effects of transverse shear on the delamination of edge-notch flexure and 3-point bend geometries. *Composite part B* 2009;40:305-12.
- [173] Carlsson L, Gillespie J, Pipes J, Pipes R. Specimen for mode II testing on the analysis and design of the end notched flexure (ENF). *Journal of Composite Materials* 1986;20.
- [174] Page KA, Kusoglu A, Stafford CM, Kim S, Kline RJ, Weber AZ. Confinement-driven increase in ionomer thin-film modulus. *Nano Letters* 2014;14:2299-304.
- [175] Tvergaard V, Hutchinson JW. On the toughness of ductile adhesive joints. *Journal of the Mechanics and Physics of Solids* 1996;44:789-800.
- [176] ASTM. Standard test method for flexural strength of advanced ceramics at ambient temperature. ASTM C1161-02c(2008)e1. West Conshohocken, PA2008.
- [177] Walther A, Bjurhager I, Malho J-M, Pere J, Ruokolainen J, Berglund LA, et al. Large-area, lightweight and thick biomimetic composites with superior material properties via fast, economic, and green pathways. *Nano Letters* 2010;10:2742-8.

- [178] Rogers E, Stovall I. Fundamentals of chemistry: solubility. Department of Chemistry. University of Wisconsin2000.
- [179] Bell L, Mika H, Kruger B. Synthetic hydroxyapatite-solubility product and stoichiometry of dissolution. *Arch Oral Biol* 1978;23:329-36.
- [180] Larsen S. Solubility of hydroxyapatite. *Nature* 1966;212:605-&.
- [181] Fisher RD, Hanna JV, Rees GJ, Walton RI. Calcium sulfate-phosphate composites with enhanced water resistance. *Journal of Materials Chemistry* 2012;22:4837-46.
- [182] Chen Z, Kang L, Meng Q-Y, Liu H, Wang Z, Guo Z, et al. Degradability of injectable calcium sulfate/mineralized collagen-based bone repair material and its effect on bone tissue regeneration. *Materials Science & Engineering C-Materials for Biological Applications* 2014;45:94-102.
- [183] Combe EC, Smith DC. Improved stones for the construction of models and dies. *Journal of Dental Research* 1971;50:897-&.
- [184] Ridge M, Boell G. Water requirement of calcined gypsum. C.S.I.R.O. Division of Building Research; 1964.
- [185] Moreau JL, Weir MD, Xu HHK. Self-setting collagen-calcium phosphate bone cement: Mechanical and cellular properties. *Journal of Biomedical Materials Research Part A* 2009;91.
- [186] Li V. The effect of snubbing friction on the first crack strength of flexible fiber reinforced composite. In: D.Firrao, editor. *ECF 8 – Fracture Behaviour and Design of Materials and Structures*1990.
- [187] Kelly A, Tyson WT. Tensile properties of fibre-reinforced metals: copper/tungsten and copper/molybdenum. *Journal of the Mechanics and Physics of Solids* 1965;13:329–50.
- [188] Evans AG. Perspective on the development of high-toughness ceramics. *Journal of the American Ceramic Society* 1990;73:187-206.
- [189] Trotter JA, Lyons-Levy G, Thurmond FA, Koob TJ. Covalent composition of collagen fibrils from the dermis of the sea cucumber, *Cucumaria frondosa*, a tissue with mutable mechanical properties. *Comparative Biochemistry and Physiology Part A: Physiology* 1995;112:463–78.
- [190] MTI Corporation. Richmond, CA, USA2015.